

Copyright © 1992, by the author(s).  
All rights reserved.

Permission to make digital or hard copies of all or part of this work for personal or classroom use is granted without fee provided that copies are not made or distributed for profit or commercial advantage and that copies bear this notice and the full citation on the first page. To copy otherwise, to republish, to post on servers or to redistribute to lists, requires prior specific permission.

**CHUA'S CANONICAL CIRCUIT:  
A TUTORIAL**

by

Philippe Deregél

Memorandum No. UCB/ERL M92/99

1 September 1992

**CHUA'S CANONICAL CIRCUIT:  
A TUTORIAL**

by

Philippe Deregél

Memorandum No. UCB/ERL M92/99

1 September 1992

**ELECTRONICS RESEARCH LABORATORY**

College of Engineering  
University of California, Berkeley  
94720

**CHUA'S CANONICAL CIRCUIT:  
A TUTORIAL**

by

Philippe Deregél

Memorandum No. UCB/ERL M92/99

1 September 1992

**ELECTRONICS RESEARCH LABORATORY**

College of Engineering  
University of California, Berkeley  
94720

# CHUA'S CANONICAL CIRCUIT : A TUTORIAL

Philippe DEREGEL

Department of Electrical Engineering and Computer Sciences,  
University of California,  
Berkeley, CA 94720, USA

September 1, 1992

## Abstract

Chaos has been widely reported and studied in Chua's circuit family, which is characterized by a 21 parameter family of odd-symmetric piecewise-linear vector fields in  $R^3$ . In this tutorial paper, we shall prove that, up to a topological equivalence, all the dynamics of this family are subsumed within that of a single circuit : *Chua's canonical circuit*. We provide explicit formulas of the parameters of Chua's canonical circuit leading to a behavior qualitatively identical to that of any system belonging to Chua's circuit family. These formulas are then used to construct, in an almost trivial way, a gallery of (quasi-periodic and strange) attractors belonging to Chua's circuit family. A user-friendly program is available to allow a better understanding of the evolution of the dynamics as a function of the parameters of the canonical circuit, and to follow the trajectory in the eigenspaces.

## 1 Introduction

In this paper, we shall focus on a class of particularly simple three-dimensional chaotic systems : Chua's circuit family. This class of dynamical systems , henceforth denoted by  $\mathcal{C}$ , is characterized by a three-region, continuous, piecewise-linear vector field  $F$  with odd symmetry i.e.  $F(-x) = -F(x)$  where we assume that there is no plane or line parallel to the boundary planes  $B_+$  and  $B_-$  which is invariant under the action of  $F$  in the middle region (by continuity, this properties will also hold true for the outer regions). Since, as we shall

see, the origin is an equilibrium point, this last assumption is equivalent to assuming that the eigenspaces <sup>1</sup> through the origin are not parallel to the boundary plane. As shown in Fig.1, the Jacobian matrices of the vector field  $f$  in the inner region  $D_0$ , and in the outer regions  $D_1$  and  $D_{-1}$ , are denoted by  $M_0$  and  $M_1$ , respectively.  $\mathbf{b}$  is a vector of  $R^3$ , which ensures the continuity of  $F$  on the boundary planes  $B_+$  and  $B_-$ . We shall denote by  $\mu_1, \mu_2$  and  $\mu_3$  the eigenvalues of  $M_0$ , and by  $\nu_1, \nu_2$  and  $\nu_3$  the eigenvalues of  $M_1$ . In order to avoid complex numbers, we shall introduce the following notation:

$$\begin{cases} p_1 = \mu_1 + \mu_2 + \mu_3 & q_1 = \nu_1 + \nu_2 + \nu_3 \\ p_2 = \mu_1\mu_2 + \mu_2\mu_3 + \mu_3\mu_1 & q_2 = \nu_1\nu_2 + \nu_2\nu_3 + \nu_3\nu_1 \\ p_3 = \mu_1\mu_2\mu_3 & q_3 = \nu_1\nu_2\nu_3 \end{cases} \quad (1)$$

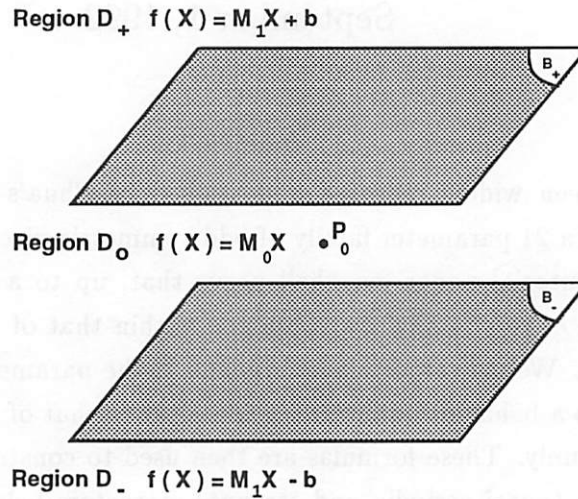


Figure 1: A three-region piecewise-linear system

The fact that the elements of  $\mathcal{C}$  can be considered as three affine systems, each of which having a well-known solution, glued together simplifies the theoretical study of these systems. These properties allow an in-depth study of the dynamics in  $\mathcal{C}$ . In particular, it has made it possible to give a rigorous proof of chaos in Chua's circuit [1]; an element of  $\mathcal{C}$  [2] [3] shown in Fig.2(a) and known as the simplest autonomous circuit which exhibits chaos.

From a physical point of view, the circuits which belong to  $\mathcal{C}$  are very simply built. They only have one nonlinear element : a Chua's diode [4], a five-region piecewise linear nonlinear resistor whose i-v characteristic is given in Fig.2(b). Note that from a physical

---

<sup>1</sup>eigenvector or eigenplane

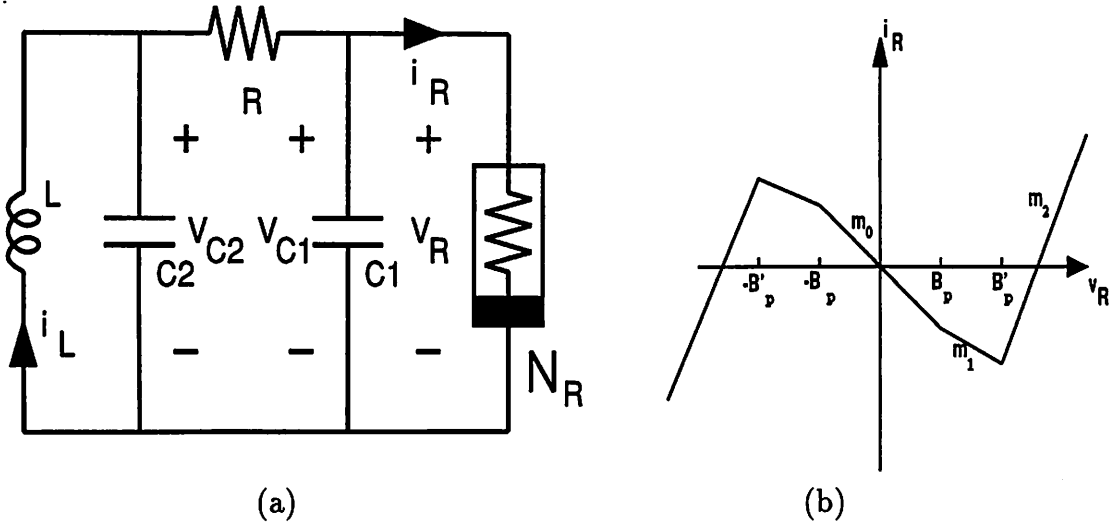


Figure 2: (a) Chua's circuit (b) characteristic of Chua's diode

point of view, in a real circuit, the two outer segments with a positive slope  $m_2$  are always present, otherwise the system could gain an infinite amount of energy which is physically impossible. However, these two segments do not play any interesting role in the chaotic dynamics. When a three-region system is simulated (without these outer segments), the trajectory might diverge, due to an improper choice of parameters or initial conditions. In this paper, we shall only include the inner segments of slope  $m_0$  and the two outer ones of slopes  $m_1$  as shown in Fig.3.

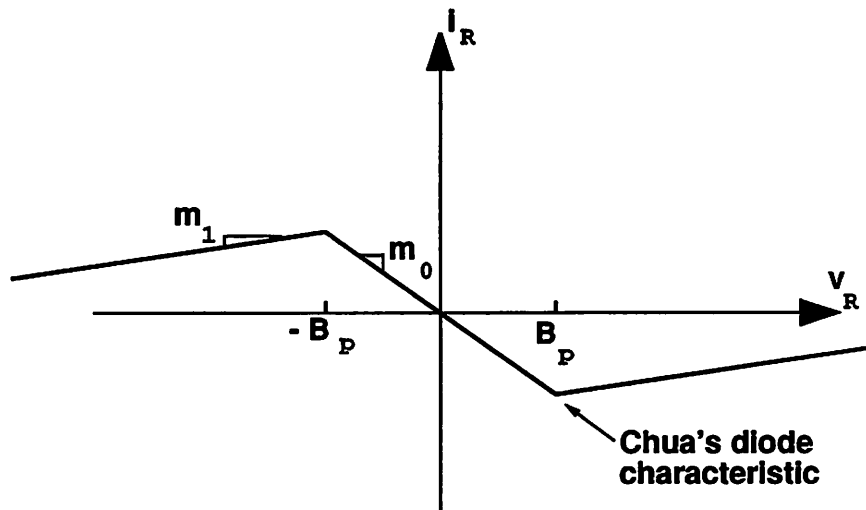


Figure 3: Three-region characteristic of Chua diode

The possibility of a simple and robust realization of the elements of  $\mathcal{C}$  is certainly an advantage for their study. This is all the more interesting since, as we shall see in this paper, there exists a single circuit which is imbued with all the complicated dynamics of  $\mathcal{C}$ . We shall introduce this circuit, Chua's canonical circuit [5], and its state equations from which we shall first derive a dimensionless form. Then we shall give values of the parameters of Chua's canonical circuit, as well as those of its dimensionless form (after a time rescaling), corresponding to any eigenvalue pattern <sup>2</sup>

$$(\mu; \nu) = (\mu_1, \mu_2, \mu_3; \nu_1, \nu_2, \nu_3) \quad \text{or} \quad (p; q) = (p_1, p_2, p_3; q_1, q_2, q_3) \quad (2)$$

If, as proven in section 6, two elements of  $\mathcal{C}$  having the same eigenvalues exhibit the same behavior, all the complicated dynamics of  $\mathcal{C}$  are subsumed within that of Chua's canonical circuit or its associated dimensionless form.

In section 3 we shall illustrate the properties of Chua's canonical circuit with some examples. We shall determine the parameters of Chua's canonical circuits and of its associated dimensionless form leading to some well-known attractors belonging to  $\mathcal{C}$ .

In section 4, we shall systematically determine them for all the attractors found so far in  $\mathcal{C}$ . For each attractor, we shall give the Lyapunov dimension, the eigenvalue pattern, the parameters of Chua's canonical circuit and of its dimensionless form, and a phase portrait.

In section 5 we shall present some basic concepts relative to the dynamics of  $\mathcal{C}$ . In this tutorial paper, written for the non-specialist, this section can be considered as both a short introduction to chaotic dynamics and a simple answer to questions that might arise in the reading of the four first sections. In the same spirit, we wait for the end of this paper to prove that two elements of  $\mathcal{C}$  having the same eigenvalues  $(\mu, \nu)$  exhibit the same dynamics. This is the basis of this paper and will be assumed in the five first sections.

## 2 Chua's canonical circuit

### 2.1 The circuit and its equations

Our aim in this section is to provide a circuit to realize any prescribed eigenvalue pattern associated with a vector field belonging to  $\mathcal{C}$ . First of all, since the system is of the third order, the circuit must have three-dynamic elements. In addition, since our objective is

---

<sup>2</sup>Note that  $(\mu; \nu)$  is obtained from  $(p; q)$  with (1). Conversely,  $\mu_i$  (resp.  $\nu_i$ ) are the roots of the polynomial :  $\mu^3 - p_1\mu^2 + p_2\mu - p_3 = 0$  (resp.  $\nu^3 - q_1\nu^2 + q_2\nu - q_3 = 0$ ) . We shall assume without any loss of generality that  $\mu_1$  (resp.  $\nu_1$ ) is real.



a three region symmetric piecewise-linear continuous vector field, we can allow only one nonlinear resistor, the *Chua's diode*, whose v-i characteristic shown in Fig.4 is odd-symmetric 3-segment piecewise linear. All other elements must be linear.

In an autonomous linear RC circuit which has two elements, there is only one natural frequency  $\nu = 1 / RC$ . Therefore, to produce a prescribed natural frequency R or C can be assigned an arbitrary value ( e.g., let  $C=1$  ) and then the value of the other parameters can be calculated. In other words, to synthesize a circuit having  $n$  arbitrarily prescribed eigenvalues, at least  $(n + 1)$  circuit parameters are necessary.

If we are given 6 eigenvalues, then we need at least 7 parameters. We already have 3 dynamic elements and 2 slopes for the nonlinear resistor; therefore, 2 more linear resistors are the minimum requirement. The chosen circuit is shown in Fig.3, its state equations, henceforth denoted by  $\Sigma_c$  are :

$$\begin{cases} \frac{dv_1}{dt} = \frac{1}{C_1}[-\hat{f}(v_1) + i_3] \\ \frac{dv_2}{dt} = \frac{1}{C_2}[-Gv_2 + i_3] \\ \frac{di_3}{dt} = \frac{-1}{L}[v_1 + v_2 + Ri_3] \end{cases} \quad (3)$$

where

$$\hat{f}(v) = G_b v + \frac{1}{2}(G_a - G_b)(|v + B_p| - |v - B_p|) \quad (4)$$

is the v-i characteristic of the Chua's diode shown in Fig.3.

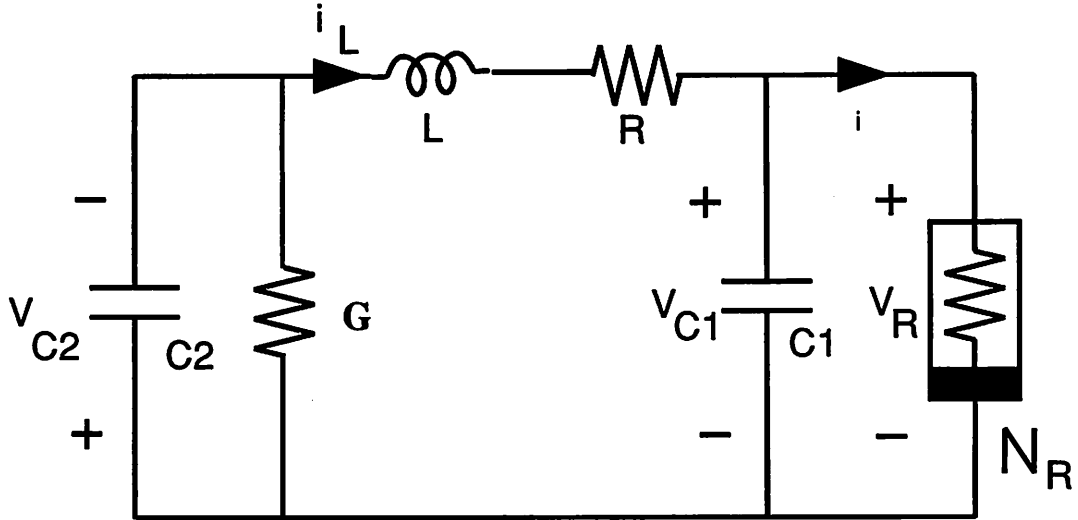


Figure 4: Chua's canonical circuit

We can transform the state equation  $\Sigma_c$  into a dimensionless form by defining :

$$\begin{aligned} x &\equiv v_1/B_p & y &\equiv v_2/B_p & z &\equiv Ri_3/B_p \\ \tau &\equiv t/RC_1 & m_0 &\equiv RG_a & m_1 &\equiv RG_b \\ \alpha &\equiv C_1RG/C_2 & \beta &\equiv C_1/C_2 & \gamma &\equiv C_1R^2/L \end{aligned} \quad (5)$$

The corresponding dimensionless state equation is given by :

$$\begin{cases} \dot{x} = -f(x) + z \\ \dot{y} = -\alpha y + \beta z \\ \dot{z} = -\gamma(x + y + z) \end{cases} \quad (6)$$

where :

$$f(x) = m_1x + \frac{1}{2}(m_0 - m_1)(|x + 1| - |x - 1|) \quad (7)$$

Note that in (6),  $\dot{x} = \frac{dx}{d\tau}$  and also that throughout the paper we shall assume that  $B_p = 1$  which does not affect the dynamics<sup>3</sup>. The system (6) has a *qualitatively* identical behavior to that obtained from (3), provided that  $RC_1 > 0$ . If  $RC_1 < 0$ , an attractor in (3) becomes a “repeller” in (6) because the dimensionless time  $\tau < 0$  when  $t > 0$ . We operate a negative *time rescaling* in (5). In this case, we can still use (6) to obtain an attractor of (3), by merely integrating (6) *backwards* in time. This is equivalent to integrating the following alternate dimensionless equation in forward time:

$$\begin{cases} \dot{x} = f(x) - z \\ \dot{y} = \alpha - \beta z \\ \dot{z} = \gamma(x + y + z) \end{cases} \quad (8)$$

where the parameters  $\alpha, \beta$  and  $\gamma$  and the function  $f$  are the same as in (6). Equations (6) and (8) can be combined into a single equation :

$$\begin{cases} \dot{x} = \theta(-f(x) + z) \\ \dot{y} = \theta(-\alpha y + \beta z) \\ \dot{z} = \theta(-\gamma(x + y + z)) \end{cases} \quad (9)$$

where  $\theta = 1$  if  $RC_1 > 0$  and  $\theta = -1$  if  $RC_1 < 0$ . Equations (9), henceforth denoted by  $\Sigma_d$  are known as the *Chua's canonical equations*. Observe that we only have five dimensionless parameters  $\alpha, \beta, \gamma, m_0$  and  $m_1$ , compared to the twenty one parameters required to completely define an element of  $\mathcal{C}$ , as shown in Fig.1.

---

<sup>3</sup>if  $B_p \neq 1$ , we would divide  $x, y$  and  $z$  by  $B_p$  to find the solution of  $\Sigma_c$

Let us first assume, as it will be proven in section 6, that the qualitative behavior of  $\mathcal{C}$  is determined by its six eigenvalues :  $\mu_1, \mu_2, \mu_3, \nu_1, \nu_2$  and  $\nu_3$ . As we shall see, in the outer regions, for all the examples presented in this paper, we shall always find one real and two complex conjugate eigenvalues that can be denoted by :

$$\nu_1 = \gamma_1 \quad \nu_2 = \sigma_1 + j\omega_1 \quad \nu_3 = \sigma_1 - j\omega_1 \quad (10)$$

Since we are only interested in preserving the qualitative behavior of the system, we can assume for convenience that  $\omega_1 = 1$  so that only five parameters need to be matched by those of  $\Sigma_d$ . This assumption is equivalent to a change in the time scale and hence involves no loss of generality. Note that if the eigenvalues in the outer regions were all real, we could impose to one eigenvalue, for example  $\nu_1$ , to have a norm equal to 1 and proceed as above.

## 2.2 Explicit formulas for calculating the parameters of Chua's canonical circuit

Given any prescribed set of eigenvalues, [5] gives the explicit formulas for calculating the circuit parameters  $C_1, C_2, L, R, G, G_a$  and  $G_b$  of the Chua's canonical circuit shown in Fig. As mentioned before, among the seven parameters, we can assign an arbitrary value to any one of them. In [5]  $C_1 = 1$ . The other circuit parameters are :

$$\left\{ \begin{array}{l} G_a = -p_1 + \frac{p_2 - q_2}{p_1 - q_1} \\ G_b = -q_1 + \frac{p_2 - q_2}{p_1 - q_1} \\ L = \frac{1}{p_2 + \left( \frac{p_2 - q_2}{p_1 - q_1} - p_1 \right) \left( \frac{p_2 - q_2}{p_1 - q_1} \right) - \frac{p_3 - q_3}{p_1 - q_1}} \\ R = -L \left( \frac{p_2 - q_2}{p_1 - q_1} + k \right) \\ C_2 = \frac{1}{L \left[ \frac{p_3 - q_3}{p_1 - q_1} + k \left( \frac{p_2 - q_2}{p_1 - q_1} + k \right) \right]} \\ G = kC_2 \end{array} \right. \quad (11)$$

where :

$$k = -L \left[ p_3 + \frac{G_a(p_3 - q_3)}{C_1(p_1 - q_1)} \right] \quad (12)$$

Observe that the parameters *cannot* be found whenever the numerator in one the equations (11) is equal to zero. This is the case when :

$$p_1 = q_1 \quad (13)$$

or

$$p_2 + \left( \frac{p_2 - q_2}{p_1 - q_1} - p_1 \right) \left( \frac{p_2 - q_2}{p_1 - q_1} \right) - \frac{p_3 - q_3}{p_1 - q_1} = 0 \quad (14)$$

or

$$\frac{p_3 - q_3}{p_1 - q_1} + k \left( \frac{p_2 - q_2}{p_1 - q_1} + k \right) = 0 \quad (15)$$

Each of these three equations (13)-(15) represents a 5-dimensional hyper-surface in the six-dimensional space  $(p_1, \dots, q_3)$ . The eigenvalue patterns that cannot be reached from Chua's canonical circuit belong to one of the three hyper-surfaces, and therefore constitute a set of measure zero, we shall denote it by  $S_c$ . Given an eigenvalue pattern  $(p; q)$ , we can always perturb it in order to obtain :

$$(p_1 + \delta p_1, p_2 + \delta p_2, p_3 + \delta p_3; q_1 + \delta q_1, q_2 + \delta q_2, q_3 + \delta q_3) \quad (16)$$

where  $\delta p_i$  and  $\delta q_i$  are arbitrarily small, so that the resulting eigenvalue pattern (16) does not belong to  $S_c$  and hence can be generated by Chua's canonical circuit. If  $\delta p_i$  and  $\delta q_i$  are chosen sufficiently small, which is always possible since  $S_c$  is a zero-measure set, it follows that by the continuity property of ODE with respect to parameters, that the qualitative behavior of the system will be preserved. We will illustrate this with examples in section 3.

### 2.3 Explicit formulas for calculating the parameters of Chua's canonical equations

Our aim is now to obtain the parameters of Chua's canonical equations as a function of the eigenvalues. Consider an eigenvalue pattern  $(\mu, \nu)$  and its corresponding circuit parameters obtained with (11). From these circuit parameters we can determine the dimensionless parameters with (5), assuming in the process of finding the parameters *and* the time rescaling, we do not encounter any numerator equal to zero, i.e. :  $C_2 \neq 0$ ,  $L \neq 0$  and  $RC_1 \neq 0$ .  $C_1$  is fixed at  $C_1 = 1$ , and from (11), it is obvious that  $L$ , and  $C_2$  cannot be equal to zero, but we can have  $R = 0$ . As (13)-(15),  $R = 0$  represents a hyperplane that is a zero-measure set; by slightly perturbing the eigenvalues we can find an eigenvalue pattern leading to the same qualitative behavior and  $R \neq 0$ . We shall denote by  $S_d$  the zero-measure set of eigenvalues for which we cannot find the dimensionless parameters, note that  $S_d \subset \{S_c \cup \{R = 0\}\}$ . Also note that (except for  $|R| = 1$ , which is a zero-measure set), when we find dimensionless parameters corresponding to  $(\mu, \nu)$ , this does not mean that the eigenvalues of  $\Sigma_d$  are  $(\mu; \nu)$ , *but* that there exists a system  $\Sigma_c$ , that has the eigenvalues  $(\mu, \nu)$  and whose dynamics is equivalent to that of  $\Sigma_d$  (up to a positive time rescaling). Therefore  $\Sigma_d$  has the same qualitative behavior as any element of  $\mathcal{C}$  having the eigenvalues  $(\mu, \nu)$ .

In order to obtain directly the parameters of Chua's canonical equations as a function of the eigenvalues, we can substitute (11) into (5). Another possibility consists of directly deriving these formulas from (9) as it is done in appendix A. In this appendix, we use Chua's canonical equations as an example, to show how to determine the parameters of a system as a function of the eigenvalues <sup>4</sup>. Fortunately, in both cases, substitution of (11) into (5) and direct derivation, we find the same result :

$$\begin{cases} \alpha = \frac{K_1 K_3}{(K_2)^2} \\ \beta = \frac{q_3 - p_3}{(q_1 - p_1) K_2} - \frac{K_1 K_3}{(K_2)^2} \\ \gamma = \frac{(K_3)^2}{K_2} \\ m_0 = \left( -p_1 - \frac{p_2 - q_2}{q_1 - p_1} \right) \frac{K_3}{K_2} \\ m_1 = \left( -q_1 - \frac{p_2 - q_2}{q_1 - p_1} \right) \frac{K_3}{K_2} \\ \theta = \text{sgn}(K_2 K_3) \end{cases} \quad (17)$$

where:

$$\begin{cases} K_1 = -p_3 + \frac{q_3 - p_3}{q_1 - p_1} \left( p_1 + \frac{p_2 - q_2}{q_1 - p_1} \right) \\ K_2 = p_2 - \frac{q_3 - p_3}{q_1 - p_1} + \frac{p_2 - q_2}{q_1 - p_1} \left( \frac{p_2 - q_2}{q_1 - p_1} + p_1 \right) \\ K_3 = \frac{p_2 - q_2}{q_1 - p_1} - \frac{k_1}{k_2} \end{cases} \quad (18)$$

The zero-measure set for which the parameters of Chua's canonical circuit *cannot* be determined is :

$$p_1 = q_1 \quad (19)$$

or

$$p_2 - \frac{q_3 - p_3}{q_1 - p_1} + \frac{p_2 - q_2}{q_1 - p_1} \left( \frac{p_2 - q_2}{q_1 - p_1} + p_1 \right) = 0 \quad (20)$$

or

$$\frac{p_2 - q_2}{q_1 - p_1} - \frac{-p_3 + \frac{q_3 - p_3}{q_1 - p_1} \left( p_1 + \frac{p_2 - q_2}{q_1 - p_1} \right)}{p_2 - \frac{q_3 - p_3}{q_1 - p_1} + \frac{p_2 - q_2}{q_1 - p_1} \left( \frac{p_2 - q_2}{q_1 - p_1} + p_1 \right)} = 0 \quad (21)$$

Note first that (19) and (20) are the same as (13) and (14), respectively. Second, (21) is not present in  $S_c$ . In fact, it represents a time rescaling that must not be equal to zero. We do not have this problem in  $\Sigma_c$ . In this case, although we can still find values for  $\alpha, \beta, \gamma, m_0$  and  $m_1$ , they are meaningless because the equation (5) is not valid. The reader can read appendix A for more details. Third, in (5), only  $1/C_2$  appears (not  $C_2$ ), and assuming that  $p_1 \neq q_1, 1/C_2$  always exists (see (11)). Therefore (15) is not present in  $S_d$ . Also note that

---

<sup>4</sup>Note that in general, for systems other than Chua's canonical equations, the set of eigenvalues for which the parameters does not exists is *not* a zero-measure set

Chua's canonical circuit generates some eigenvalue patterns that Chua's canonical equations cannot generate *and* vice-versa. These sets have both a zero measure zero.

## 2.4 Equilibrium points and eigenspaces

In this section we shall determine the equilibrium points and the eigenspaces corresponding to the Chua's canonical equations. These formulas constitute the basis of a user-friendly program, presented in Appendix B, that determines the equilibrium points and displays the trajectory in the eigenspaces, starting from any initial conditions. Let us first determine the equilibrium points <sup>5</sup> of Chua's canonical equations. Consider the equilibria:

$$\begin{cases} -f(x) + z &= 0 \\ -\alpha y + \beta z &= 0 \\ \gamma(x + y + z) &= 0 \end{cases} \quad (22)$$

From a physical point of view, (22) can be interpreted as the equations of the circuit at dc, when the capacitors are open-circuited and the inductor short-circuited. The equation of the load line is:

$$z = -\frac{\alpha}{\alpha + \beta}x \quad (23)$$

The only interesting case, which can lead to complicated dynamics, is when the circuit has three dc-operating points. The nonlinear function  $F(\cdot)$  and the load line are shown in Fig.5.

The load line intersects the outer segment if and only if the operating point I has an abscissa

$$x_I = -\frac{a - b}{-b - \frac{\alpha}{\alpha + \beta}} \quad (24)$$

greater than 1 as in Fig.5, leading to an equilibrium point in each of the three regions.

$$\begin{cases} P_+ &= (x_I, -\frac{\beta}{\alpha + \beta}x_I, -\frac{\alpha}{\alpha + \beta}x_I) \in D_+ \\ P_0 &= (0, 0, 0) \in D_0 \\ P_- &= (-x_I, \frac{\beta}{\alpha + \beta}x_I, \frac{\alpha}{\alpha + \beta}x_I) \in D_- \end{cases} \quad (25)$$

In the case of three equilibrium points, let us now study their stability i.e. the nature of eigen spaces present in the neighborhood of  $P_+, P_0$  and  $P_-$ . One of the advantages of a piecewise-linear vector field is that in each region these eigenvalues and the eigen spaces are constant, therefore we do not have to do any local approximation in order to determine the Jacobian

---

<sup>5</sup>In our case, the equilibrium points are the points where the vector field is equal to zero

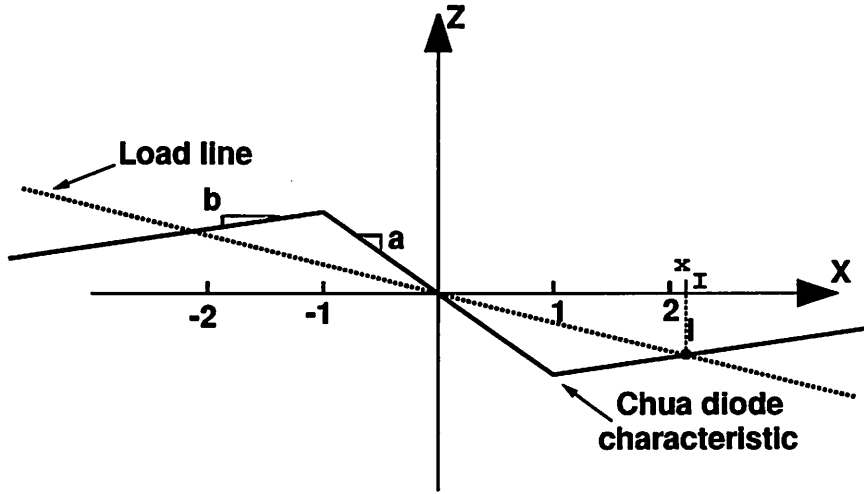


Figure 5: dc operating points of the Chua diode

matrices of the system. Let us first examine the stability of the origin  $P_0$ . In the region  $D_0$  the state equation is :

$$\dot{X} = M_0 X \quad (26)$$

where the Jacobian matrix is the constant matrix :

$$M_0 = \theta \begin{pmatrix} -m_0 & 0 & 1 \\ 0 & -\alpha & \beta \\ -\gamma & -\gamma & -\gamma \end{pmatrix} \quad (27)$$

and its chracteristic polynomial is :

$$\begin{aligned} |\lambda I - M_0| &= \lambda^3 + \theta\lambda^2(a + \alpha + \gamma) \\ &\quad + \lambda(\alpha a + \alpha\gamma + a\gamma + \beta\gamma + \gamma\epsilon) \\ &\quad + \theta(a\alpha\gamma + \gamma\alpha\epsilon + \beta\gamma a) = 0 \end{aligned} \quad (28)$$

The eigenvalues of the Chua's canonical equations are the roots of (28). In order to determine the type of the eigenvalue pattern associated with  $M_0$ , let us introduce  $\Gamma$  :

$$\begin{aligned} \Gamma &= \frac{1}{9} [3(\alpha a + \alpha\gamma + a\gamma + \beta\gamma + \gamma) - (a + \alpha + \gamma)^2]^2 \\ &\quad + \frac{1}{3^{1/2}} [2\theta(a + \alpha + \gamma)^3 - 9\theta(a + \alpha + \gamma)(\alpha a + \alpha\gamma + a\gamma + \beta\gamma + \gamma) \\ &\quad + 27\theta(a\alpha\gamma + \gamma\alpha\epsilon + \beta\gamma a)]^3 \end{aligned} \quad (29)$$

According to the value of  $\Gamma$ , there are three different cases:

(a) ( $\Gamma > 0$ ) : one real and two complex conjugate eigenvalues

(b) ( $\Gamma = 0$ ) : three real eigenvalues of which at least two are equal.

(c) ( $\Gamma < 0$ ) : three real and unequal eigenvalues.

If we have determined the canonical dimensionless parameters from an eigenvalue pattern  $(\mu; \nu)$ , we already know the type of eigenvalue pattern. However as we have already noticed, the eigenvalues of  $\Sigma_d$  are not  $(\mu; \nu)$  but  $\frac{|K_3|(\mu; \nu)}{|K_2|}$  where  $K_2$  and  $K_3$  are given in (18). This multiplication of the eigenvalues by a *positive* coefficient does not affect the qualitative behavior of the system. After having found the eigenvalues of  $\Sigma_d$ , in each of the three cases (a),(b) and (c), we shall determine the corresponding eigen spaces:

**case(a)** The eigenvector  $V_{\lambda_R}$ , corresponding to the real eigenvalue  $\lambda_R$ , is determined up to a multiplicative constant by:

$$M_0 V_{\lambda_R} = \lambda_R V_{\lambda_R} \quad (30)$$

and a solution of (26) is:

$$V_\lambda = \begin{pmatrix} 1 \\ -\frac{1}{\gamma} ((\theta\lambda + \gamma)(\theta\lambda + a) + \gamma) \\ (\theta\lambda + a) \end{pmatrix} \quad (31)$$

Note that if  $\gamma$  were equal to zero, (30) would imply that  $\lambda_R$  is also equal to zero. The eigenplane  $P_0$  corresponding to the complex conjugate eigenvalues :

$$\lambda_{C\pm} = u \pm iv \quad (32)$$

is determined as a linear combination of the two vectors U and V such that:

$$\begin{pmatrix} A - uI & vI \\ A - vI & -uI \end{pmatrix} \begin{pmatrix} U \\ V \end{pmatrix} = 0 \quad (33)$$

By definition of  $u$  and  $v$ , the determinant of the linear system (33) which has six unknowns and 6 equations is equal to zero. By giving an arbitrary value to one of the coordinates of U or V, we obtain a full rank i.e. (5) Cramer system that can be easily solved by classical methods. Note that  $\Gamma \neq 0$  implies that there exists such a fifth-order Cramer system of equations in (33).

**case(b)** This case corresponds to a measure-zero set of parameters. Therefore, as it has been explained in 2.2, it is possible to slightly perturb the paramaters without changing the behavior of the system and obtain a system that belongs to case (a) of in case (c). This case could also have been directly treated.



**case(c)** The coordinates of the three eigenvectors corresponding to the real eigenvalues  $\lambda_R$  can directly be determined by (31).

The study of the stability of the outer equilibrium points is very similar to that at  $P_0$ , except that the Jacobian matrix of the vector field is now:

$$M_1 = \theta \begin{pmatrix} -m_1 & 0 & 1 \\ 0 & -\alpha & \beta \\ -\gamma & -\gamma & -\gamma \end{pmatrix} \quad (34)$$

Therefore, we can determine the eigen elements in the outer regions by substituting  $m_1$  into  $m_0$  in the equations obtained in the inner region. In the next section, we shall examine examples of eigenvalue and eigenspace patterns in  $\mathcal{C}$

### 3 Example of the use of the explicit formulas to find the parameters of Chua's canonical systems

#### 3.1 introduction

In this section, we have two objectives. First we want to show with some well-known examples that it is easily possible to obtain the dynamics of any elements<sup>6</sup> of  $\mathcal{C}$  from Chua's canonical circuit and from its associated canonical system. In each case we shall verify that we find the same trajectory with Chua's canonical equations as with the original system (the trajectories are copied from the original paper). Second, we shall take advantage of these examples to present some aspects of the dynamics in  $\mathcal{C}$ , in particular the role of the eigenspace and the eigenvalues in the dynamics of an element of  $\mathcal{C}$ .

For each element of  $\mathcal{C}$  considered in this section, we shall give the expression of the vector field before giving the eigenvalue pattern corresponding to each attractor. To avoid any confusion with the notations, the parameters relative to the original system will have a tilde (i.e.  $\tilde{\alpha}, \tilde{\beta}, \dots$ ). All these systems belong to  $\mathcal{C}$ , therefore they have the same three-region piecewise linear nonlinearity:

$$\tilde{f}(x) = \tilde{m}_1 x + \frac{1}{2}(\tilde{m}_0 - \tilde{m}_1)(|x + 1| - |x - 1|) \quad (35)$$

When there are three real eigenvalues in the middle region  $D_0$ ,  $(\mu, \nu)$  is said of *type I*. If there is one real and two complex conjugate eigenvalues in  $D_0$ ,  $(\mu, \nu)$  is said of *type II*.

---

<sup>6</sup>Chua's circuit, Chua's torus circuit, Orgozalec ladder circuit, Brockett and Sparrow's systems

### 3.2 Three examples of attractors from Chua's circuit

The dimensionless form of Chua's circuit state equations [6] [7] [8] is :

$$\begin{cases} \dot{x} &= \tilde{\alpha}(y - \tilde{f}(x)) \\ \dot{y} &= x - y + z \\ \dot{z} &= -\tilde{\beta}y \end{cases} \quad (36)$$

#### 3.2.1 A Rossler-type attractor.

For  $\tilde{\alpha} = 8.5$ ;  $\tilde{\beta} = 14.28$ ;  $\tilde{m}_0 = -1/7$ ;  $\tilde{m}_1 = 2/7$ , (36) leads to a chaotic attractor [9] shown in Fig.6-a,. This corresponds to the following set of eigenvalues :

$$\begin{cases} \mu_1 = 0.677 & \mu_2 = -0.304 + j0.901 & \mu_3 = -0.304 - j0.901 \\ \nu_1 = -1.22 & \nu_2 = -0.304 + j & \nu_3 = -0.304 - j \end{cases} \quad (37)$$

which is equivalent to :

$$\begin{cases} p_1 = 0.07030 & p_2 = 0.4915 & p_3 = 0.6125 \\ q_1 = -1.125 & q_2 = 0.8837 & q_3 = -1.225 \end{cases} \quad (38)$$

With (11) (resp. (17)), we can determine the parameters of Chua's canonical circuit (resp. Chua's canonical equations ):

$$C_1 = 1 ; \quad C_2 = -0.5952 ; \quad G = -5.733 ; \quad G_a = -0.3984 ; \quad G_b = 0.7968 ; \quad L = -1.092 ; \quad R = -0.3586$$

$$(\text{resp. } \alpha = 0 ; \quad \beta = 1.680 ; \quad \gamma = 0.1176 ; \quad m_0 = -0.1428 ; \quad m_1 = 0.2857 ; \quad \theta = -1 )$$

The trajectory obtained from Chua's canonical equations is shown in Fig.6-b. One can compare it to that obtained from the original Chua's system in [9], shown in Fig.6-a. Suppose that starting from the initial conditions  $(x_{ini}, y_{ini}, z_{ini})$  we obtain the trajectory  $T_1$  shown in Fig. 6-b, if we change the initial conditions into  $(-x_{ini}, -y_{ini}, -z_{ini})$ , we obtain a trajectory which is the symmetric image of  $T_1$  with respect to the origin as shown in Fig.6-c. Provided that the vector field  $\Sigma_d$  is symmetric with respect to the origin, if we find a trajectory  $T$  from any element of  $\mathcal{C}$ , it is *always* possible to find its "twin" symmetric by choosing the odd-symmetric initial conditions. Note that the symmetric image of  $T$  can be  $T$  for all odd-symmetric *periodic* orbit. This will also appear to be the case in the next example, but it is only an illusion, since the double scroll presented below *cannot* be periodic. With sufficient computer precision, one can always find its symmetric twin, which will look almost identical to its twin.

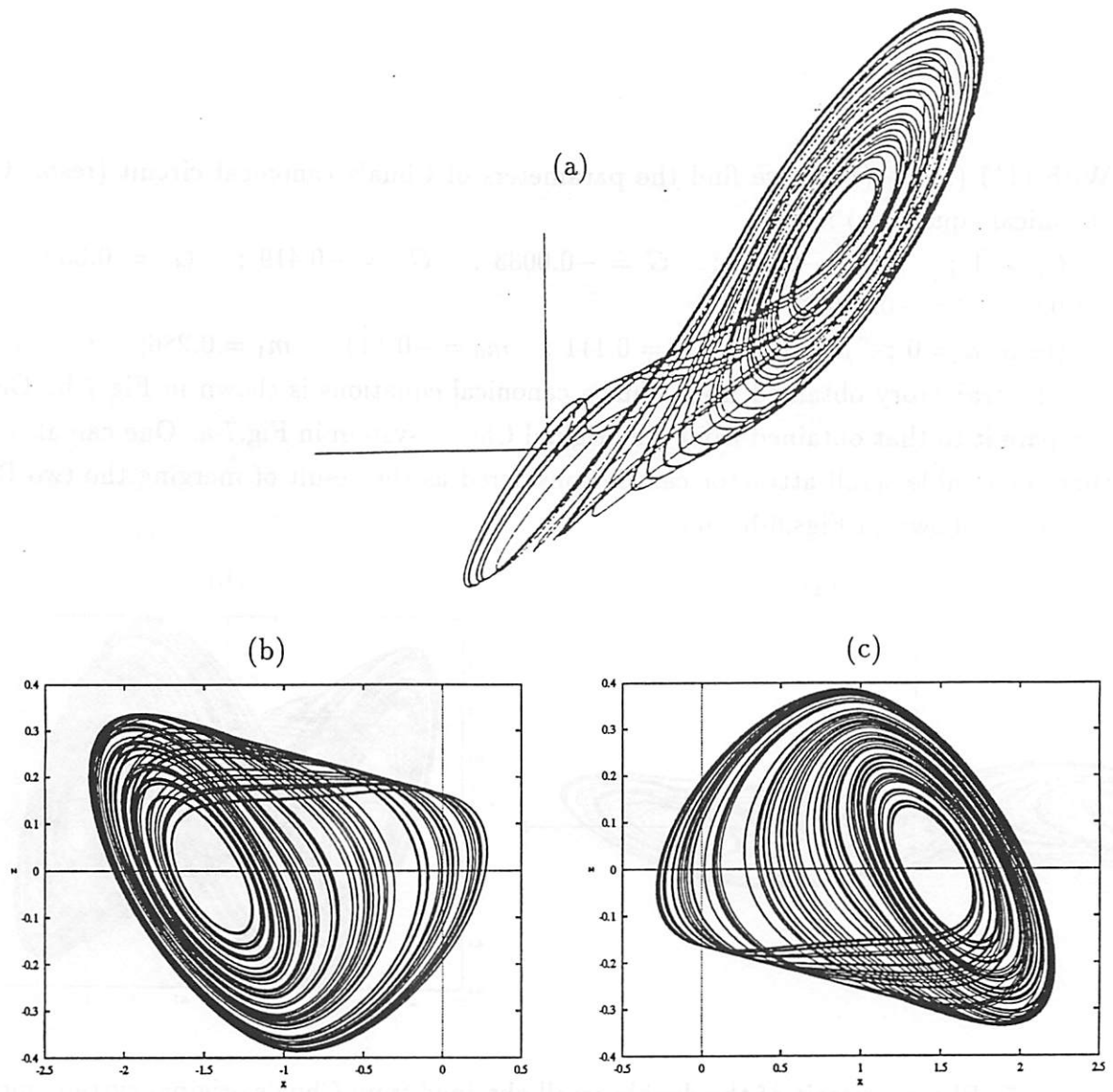


Figure 6: Comparison of a Rossler-type attractor and its odd-symmetric twin obtained from  $\Sigma_d$  with the attractor obtained from the original Chua's system

### 3.2.2 The Double Scroll

For :  $\tilde{\alpha} = 9; \tilde{\beta} = 14.28; \tilde{m}_0 = -1/7; \tilde{m}_1 = 2/7(36)$  leads to a chaotic attractor [10] [11] called the *double scroll*, shown in Fig. 7-a . This corresponds to the following set of eigenvalues :

$$\begin{cases} \mu_1 = 0.728 & \mu_2 = -0.317 + j0.889 & \mu_3 = -0.317 - j0.889 \\ \nu_1 = -1.29 & \nu_2 = 0.0608 + j & \nu_3 = 0.0608 - j \end{cases} \quad (39)$$

which is equivalent to :

$$\begin{cases} p_1 = 0.0937 & p_2 = 0.430 & p_3 = 0.649 \\ q_1 = -1.17 & q_2 = 0.846 & q_3 = -1.29 \end{cases} \quad (40)$$

With (11) (resp. (17)), we find the parameters of Chua's canonical circuit (resp. Chua's canonical equations) :

$$C_1 = 1 ; \quad C_2 = -0.632 ; \quad G = -0.0033 ; \quad G_a = -0.419 ; \quad G_b = 0.839 ; \quad L = -1.02 ; \quad R = -0.330$$

$$(\text{resp. } \alpha = 0 ; \quad \beta = 1.58 ; \quad \gamma = 0.111 ; \quad m_0 = -0.143 ; \quad m_1 = 0.286 ; \quad \theta = -1 )$$

The trajectory obtained from Chua's canonical equations is shown in Fig 7-b. One can compare it to that obtained from the original Chua's system in Fig.7-a. One can also notice that the double scroll attractor can be considered as the result of merging the two Rossler attractors shown in Figs.6-b - 6-c.

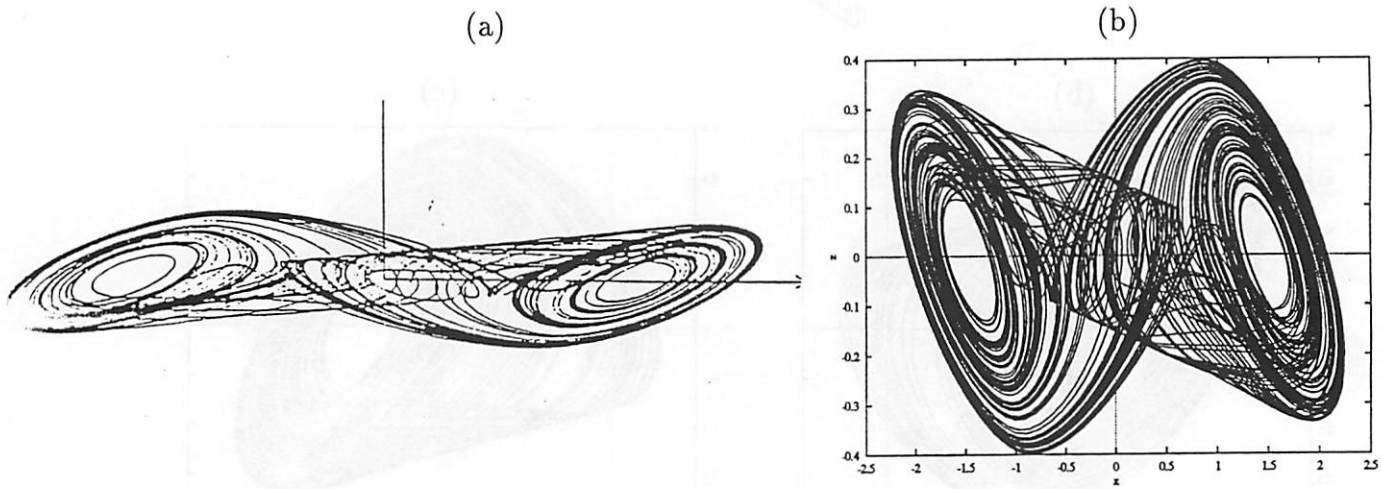


Figure 7: Phase portrait of the double scroll obtained from Chua's original system and from  $\Sigma_d$

A typical trajectory of the double scroll and its eigenspaces are shown in Fig.8. The eigenvalue pattern  $(\mu, \nu)$  is of type II; in each region, there is one eigenvector corresponding to the real eigenvalue and one eigenplane corresponding to the two complex conjugate eigenvalues. One can recognize in Fig.8 the middle region  $D_0$ , separated by the two boundary planes  $U_1$  and  $U_{-1}$ , the outer region  $D_1$  which is the half space above  $U_1$ , and  $D_{-1}$  which is the symmetric image of  $D_1$  with respect to the origin O. As we have said earlier, one the advantages of  $\mathcal{C}$  is that in each region  $(D_{-1}, D_0 \text{ and } D_1)$ , the system is affine, therefore it has a well-known behavior. Before going any further, let us recall the solution of a linear <sup>7</sup> system whose dynamics are determined by a state equation of the type:

$$\dot{X} = MX \tag{41}$$

<sup>7</sup>we assume that the origin of the basis B is located at an equilibrium point

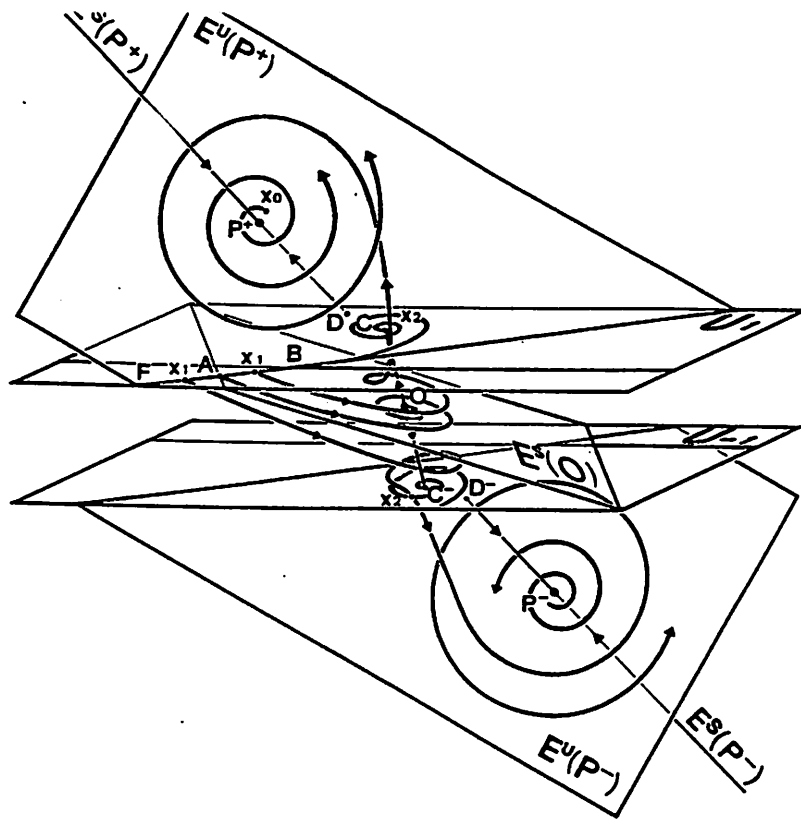


Figure 8: Typical trajectories and eigen spaces for the double scroll

If the matrix has one real eigenvalue  $\lambda_R$  and two complex conjugate eigenvalues  $\lambda_{C\pm} = \sigma \pm j\omega$ , there exists a basis  $B$  where the matrix  $M$  is in the form <sup>8</sup> :

$$\begin{pmatrix} \lambda_R & 0 & 0 \\ 0 & \sigma & -\omega \\ 0 & \omega & \sigma \end{pmatrix} \quad (42)$$

A solution of (41) is of the type :

$$\begin{cases} x = Ge^{\lambda_R t} \\ y = e^{\sigma t}(H \cos(\omega t) - K \sin(\omega t)) \\ z = e^{\sigma t}(H \sin(\omega t) + K \cos(\omega t)) \end{cases} \quad (43)$$

The behavior of the system crucially depends on the sign of  $\lambda_R$  and  $\sigma$ , this will determine the sign of the parameter located before  $t$  in the exponentials in the equations (43) . We have to consider four cases as shown in Fig.9. In the case (a), the system is stable, the trajectory is attracted along the eigenvector towards the eigenplane where it spirals inwards towards the equilibrium point. This cannot lead to any interesting dynamics, if we have such an eigenvalue pattern in a region  $D_i$ , as soon as the trajectory enters  $D$  it is attracted towards the corresponding equilibrium point. In the case (b), the trajectory is attracted towards

---

<sup>8</sup>Jordon form

the eigenplane while spiralling outwards. In the case (c), the trajectory spirals inwards and diverges along the eigenvector. In the last case (d), the trajectory spirals outwards and diverges along the eigenvector.

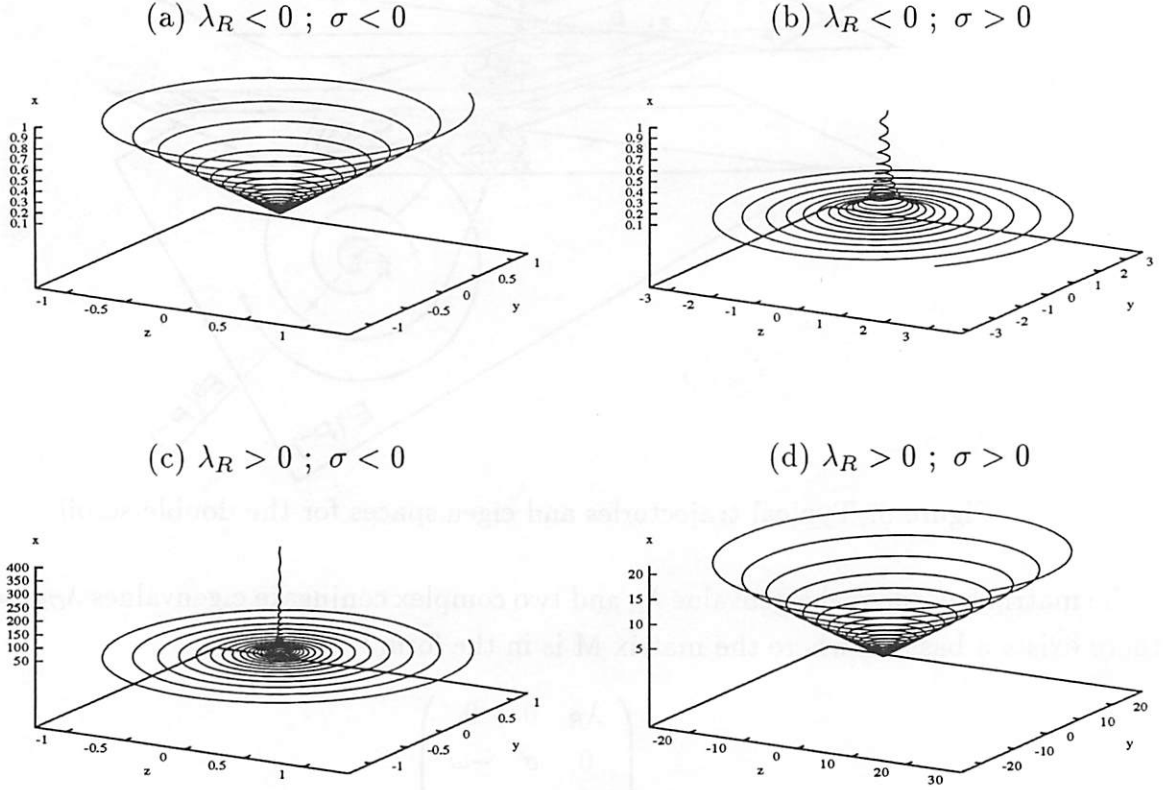


Figure 9: Four types of trajectory in an affine system with one real and two complex conjugate eigenvalues

For the double scroll, we are in case(c) in the middle region and in case (b) in the outer regions. Let us for example start from a point  $X_0$  in the region  $D_1$ . The trajectory is strongly ( $\nu_1 \ll 0$ ) attracted towards the eigenplane  $E^U(P^+)$  while it spirals outwards. We have assumed that in  $\mathcal{C}$  no eigenspace can be parallel to the boundary plane, therefore the trajectory will exit from  $D_1$ . In  $D_0$ , we are in the case (b), the trajectory spirals inwards in  $E^S(0)$ , and diverges along the eigenvector  $E^S(O)$ . Schematically, as shown in Fig.8, if the trajectory enters  $D_0$  above  $E^S(0)$  it will return to  $D_1$  and if it enters  $D_0$  below  $E^S(0)$  it will go to  $D_{-1}$ . Thus, one can easily understand the evolution of the trajectory. However, although deterministic, it cannot be predicted as it is chaotic. For us, this means that the system exhibits a sensitive dependence on the initial conditions. If instead of starting from

$x_0$ , we started from a point  $x'_0$  infinitely close to  $x_0$  (but different), we would find two different trajectories. If we integrate these two trajectories simultaneously, the distance between two corresponding points (one on each trajectory) does not remain infinitely small (it increases exponentially with time until the two trajectories are practically uncorrelated). For example, one of the two trajectories coming from the region  $D_0$  would go to  $D_1$  while the other one would go to  $D_{-1}$ . In Fig.10 we show the time series corresponding to the trajectories  $T_1$  and  $T_2$  (dash line) starting from  $(0.001, 0.001, 0.001)$  and  $(0.0015, 0.001, 0.001)$ , respectively. The two trajectories are close to each other until  $t = 280$  when  $T_1$  and  $T_2$  are both in the middle region  $D_0$ . Then  $T_1$  goes to the region  $D_1$  while  $T_2$  returns to  $D_{-1}$ . After this,  $T_1$  and  $T_2$  are completely uncorelated.

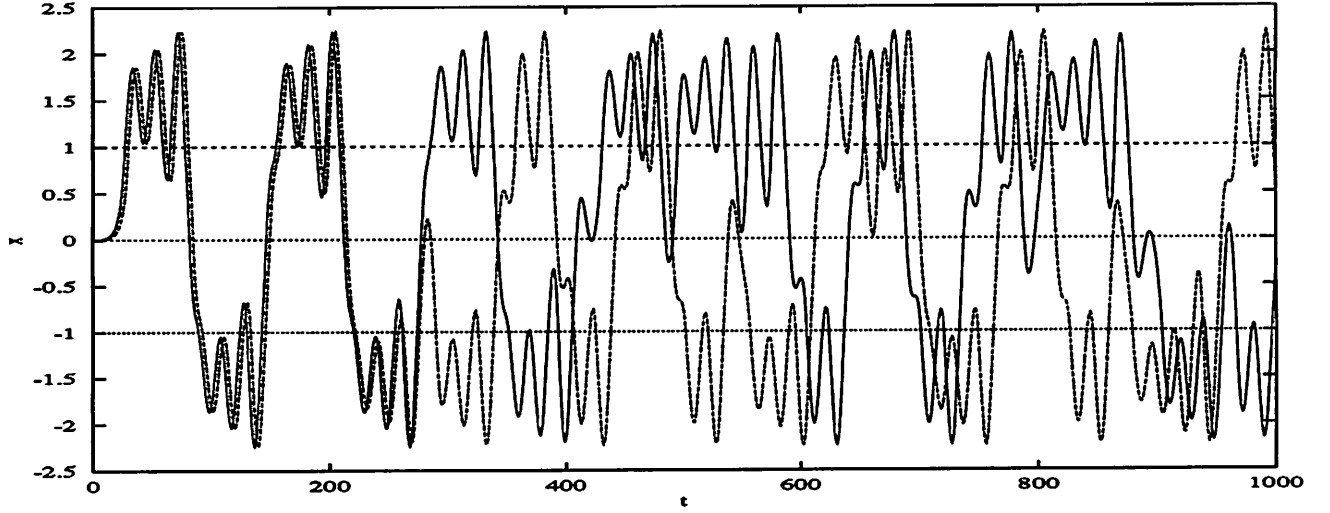


Figure 10: Time series of the double scroll obtained from  $\Sigma_d$ , starting from two different but close initial conditions

### 3.2.3 The double hook

For  $\tilde{\alpha} = 9; \tilde{\beta} = 14.28; \tilde{m}_0 = -1/7; \tilde{m}_1 = 2/7(36)$  leads to a chaotic attractor [12] shown in Fig 11-a . This corresponds to the following set of eigenvalues :

$$\begin{cases} \mu_1 = 1.15 & \mu_2 = -2.98 & \mu_3 = -5.70 \\ \nu_1 = -0.89 & \nu_2 = 0.15 + j & \nu_3 = 0.15 - j \end{cases} \quad (44)$$

which is equivalent to :

$$\begin{cases} p_1 = -7.53 & p_2 = 6.99 & p_3 = 19.60 \\ q_1 = -0.589 & q_2 = 0.753 & q_3 = -0.911 \end{cases} \quad (45)$$

This eigenvalue pattern is of *Type I*. In the middle region, instead of having one eigenvector and an eigenplane as it was the case so far, there are three eigenvectors. Two of them are stable and the third one is unstable. The Jordan form of the Jacobian matrix of the linear dynamical system present in  $D_0$  is a diagonal matrix with the eigenvalues on its diagonal. The associated dynamical system has a solution of the type :

$$\begin{cases} x = Ge^{\mu_1 t} \\ y = He^{\mu_2 t} \\ z = Ke^{\mu_3 t} \end{cases} \quad (46)$$

With (11) (resp. (17)), we find the parameters of Chua's canonical circuit (resp. Chua's canonical equations) :

$$C_1 = 1 ; \quad C_2 = -1.35 ; \quad G = 0.014 ; \quad G_a = 6.63 ; \quad G_b = -0.310 ; \quad L = 0.251 ; \quad R = 0.226$$

$$(\text{resp. } \alpha = 0 ; \quad \beta = -0.741 ; \quad \gamma = 0.2029 ; \quad m_0 = 1.492 ; \quad m_1 = 4.928 ; \quad \theta = 1)$$

The trajectory obtained from Chua's canonical equations is shown in Fig 11-b. One can compare it to that obtained from the original Chua's system in Fig.11-a.

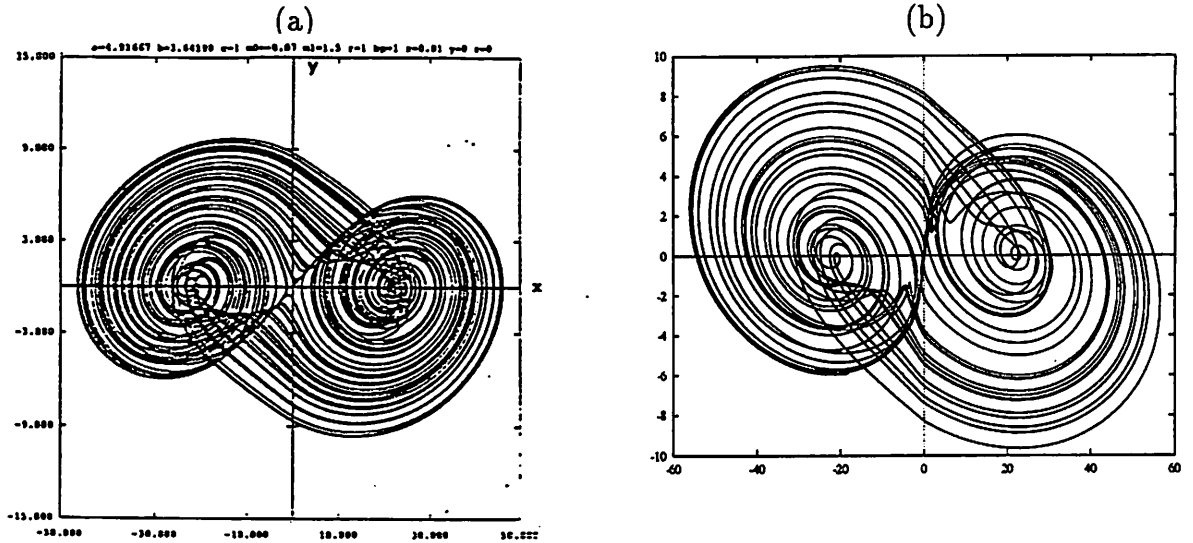


Figure 11: Phase portrait of the double hook obtained from Chua's original system in and from  $\Sigma_d$



### 3.3 Two examples of attractors from Chua's torus circuit

The dimensionless form of Chua's torus circuit [13] is

$$\begin{cases} \frac{dx}{dt} = -\alpha \hat{f}(y - x) \\ \frac{dy}{dt} = -\hat{f}(y - x) - z \\ \frac{dz}{dt} = \beta y \end{cases} \quad (47)$$

#### 3.3.1 A two-dimensional quasi-periodic torus

For :  $\tilde{\alpha} = 2; \tilde{\beta} = 1; \tilde{m}_0 = 0.1; \tilde{m}_1 = -0.07$ , (47) leads to a quasi-periodic 2-torus<sup>9</sup> [13] shown in Fig 11-a . It corresponds to the following set of eigenvalues :

$$\begin{cases} \mu_1 = 0.1955 & \mu_{2-3} = -0.04794 & \pm j1.004 \\ \gamma_1 = -0.1381 & \nu_2 = -0.03419 + j & \nu_2 = -0.03419 - j \end{cases} \quad (48)$$

Which is equivalent to :

$$\begin{cases} p_1 = 0.09958 & p_2 = 0.9917 & p_3 = 0.1975 \\ q_1 = -0.06970 & q_2 = 0.9917 & q_3 = -0.1382 \end{cases} \quad (49)$$

With (11) we can determine the parameters of Chua's canonical circuit :  $C_1 = 1$  ;  $C_2 = -0.5$  ;  $G = 0$  ;  $G_a = -0.09958$  ;  $G_b = 0.06970$  ;  $L = -1.008$  ;  $R = 0$

We have found  $R = 0$ , therefore we know that we shall have to perturb the eigenvalues in order to use Chua's canonical equations. As we have seen in 2.3,  $R = 0$  is equivalent to  $K_3 = 0$  which belongs to  $S_d$ . In order to have  $K_3 \neq 0$ , let us add for example  $10^{-6}$  to  $\mu_1$ . After this perturbation we find  $R = 1.77 \cdot 10^{-5} \neq 0$  and :

$$\alpha = 2.07 \cdot 10^{-10} ; \quad \beta = -2.000 ; \quad \gamma = -3.114 \cdot 10^{-10} ; \quad m_0 = -1.764 \cdot 10^{-6} ; \quad m_1 = 1.235 \cdot 10^{-6} ; \quad \theta = 1$$

Unfortunately, when we integrate the system  $\Sigma_d$ , with our program, we do not find the trajectory shown in Fig.11-a, because the calculations are not made with enough precision. To solve this problem, we can multiply the parameters by a coefficient  $K$ , e.g.  $K = 10^5$ , so that we avoid very small parameters. This leads us to a system with identical behavior. Note that if we choose  $K = \frac{1}{|R|}$ , the trajectory would be the same as that obtained directly with Chua's canonical circuit (in another basis). However, our aim is to find parameters to use Chua's canonical equations directly . In order to do so, we have to perturb the eigenvalues a little bit more. Let us add  $10^{-2}$  to  $\mu_1$ . In this case, we find :

---

<sup>9</sup>see 5.3 for a definition

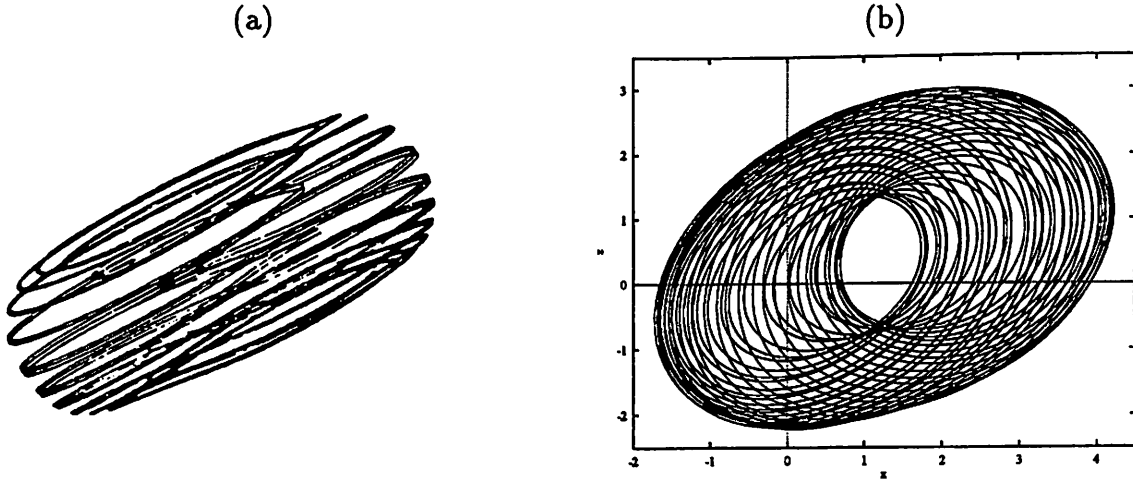


Figure 12: Two-dimensionnal quasi-periodic torus obtained from the original Chua's torus system and from  $\Sigma_d$

$\alpha = 0.0211$  ;  $\beta = -2.036$  ;  $\gamma = -0.03169$  ;  $m_0 = -7.35964 \cdot 10^{-3}$  ;  $m_1 = 0.02302$ ;  $\theta = 1$

With these parameters, using  $\Sigma_d$ , we obtain the trajectory shown in Fig.12-b. One can verify that it is identical to that obtained directly from the torus circuit shown in Fig.12-a.

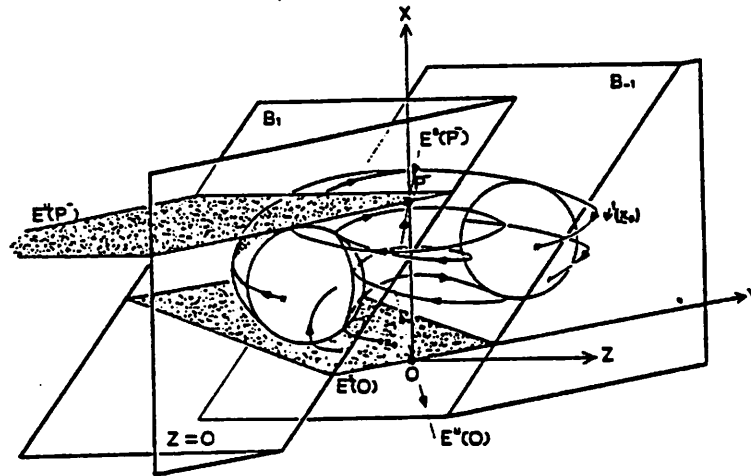


Figure 13: Typical trajectories and eigenspaces for the 2-torus

As we did for the double scroll, let us also examine the typical trajectories and the eigenspaces represented in Fig.11 . The eigenvalue pattern is also of type (c) in the middle region and of type (b) in the outer region. However there are two slight differences :

- The magnitude of  $|\gamma_1| = 0.14$  is not as large as for the double scroll (1.29) and therefore the “flattening” onto  $E^U(P^\pm)$  is relatively weak.
- $E^s(0)$  and  $E^U(P^\pm)$  are almost parallel.

The reader can verify that if we increase  $(\tilde{\alpha})$ , we would find a double scroll ( $\tilde{\alpha} = 30$ ). A time series of the quasiperiodic attractor is given in Fig.11. It is characteristic of a quasiperiodic system with two incommensurate frequencies.

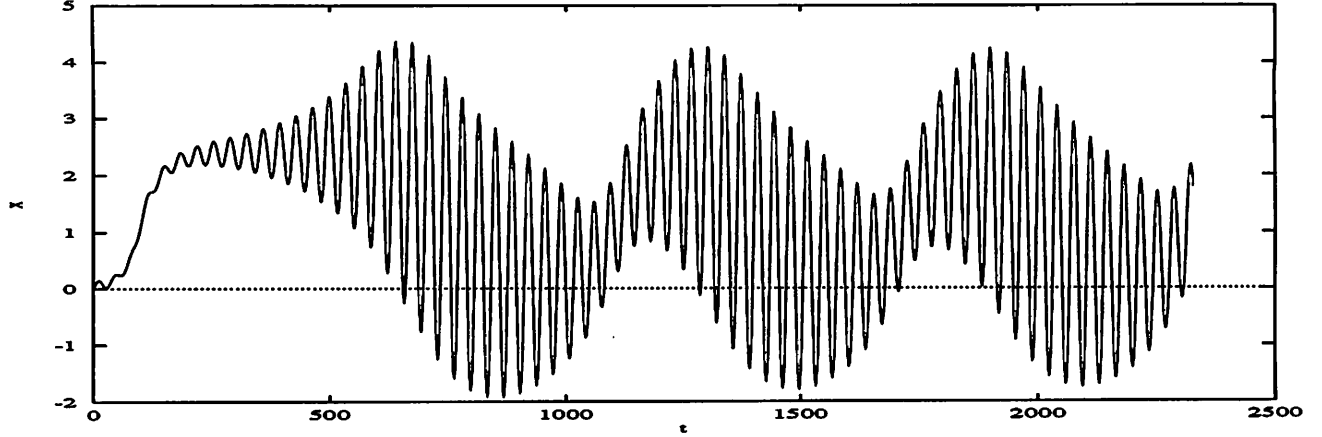


Figure 14: Time series of a quasi-periodic torus obtained from  $\Sigma_d$

Note that the coefficient obtained after perturbing  $p_2$  of  $10^{-6}$  would lead to a trajectory identical to that obtained in Fig.11a if we were using better precision. The question is : how much can we perturb the eigenvalues and still obtain the same trajectory ? There is no general answer to this question, as it depends on the attractor <sup>10</sup>. We know that in theory, if the perturbation is small enough, we shall find a system that has the same qualitative behavior. In practice, in section 4, we have found without any difficulty the coefficients of  $\Sigma_d$ , that give the expected trajectory with our program. As we shall see in this section, one must identify where the singularity comes from ( $K_3 = 0$  in our case) and slightly modify the eigenvalue pattern to avoid the singularity. Note that in our case, by changing one of the eigenvalues we shall exit from  $S_d$ , if we change several eigenvalues we should verify that we do not stay in  $S_d$ .

---

<sup>10</sup>see 5.2 for more details

### 3.3.2 A folded torus

For  $\tilde{\alpha} = 15$ ;  $\tilde{\beta} = 1$ ;  $\tilde{m}_0 = 0.1$ ;  $\tilde{m}_1 = -0.07$ , (47) leads to an attractor [13] shown in Fig 12-a,. It corresponds to the following set of eigenvalues :

$$\begin{cases} \mu_1 = 1.408 & \mu_2 = -0.0161 + j1.006 & \mu_3 = -0.0161 - j1.006 \\ \nu_1 = -0.997 & \nu_2 = 0.01695 + j & \nu_3 = 0.01695 + j \end{cases} \quad (50)$$

Which is equivalent to :

$$\begin{cases} p_1 = 1.376 & p_2 = 0.9634 & p_3 = 1.425 \\ q_1 = -0.9634 & q_2 = 0.9664 & q_3 = -0.9976 \end{cases} \quad (51)$$

With (11) we can determine the parameters of Chua's canonical circuit :  $C_1 = 1$  ;  $C_2 = -0.06666$  ;  $G = 0$  ;  $G_a = -0.09958$  ;  $G_b = 0.06970$  ;  $L = -1.008$  ;  $R = 0$

As above, and as for any eigenvalue pattern obtained from Chua's torus circuit, we have found  $R = 0$ . We apply the same perturbation as above, by adding 0.01 to  $\mu_1$ . This leads to the following values of dimensionless parameters :

$\alpha = 0.07068$  ;  $\beta = -15.992$  ;  $\gamma = -0.07512$  ;  $m_0 = -1.474$  ;  $m_1 = 1.0398$  ;  $\theta = 1$  and to the trajectory shown in Fig. 15-b which is identical to that of Fig. 15-a.

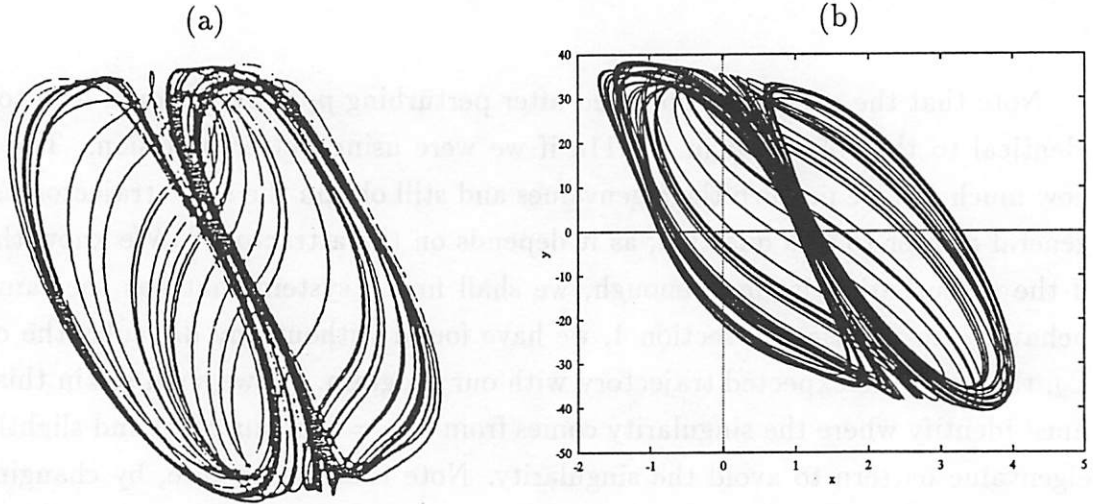


Figure 15: Folded torus obtained from the original Chua's torus system and from  $\Sigma_d$ .

### 3.4 Ogorzalek's example

In order to simplify the equations of his ladder circuit, Ogorzalek assumes in [14] that  $R_1 = R_2 = R_3 = 1\Omega$  and  $C_1 = C_2 = C_3 = 1F$ . The state equation becomes :

$$\begin{pmatrix} \dot{x}_1 \\ \dot{x}_1 \\ \dot{x}_1 \end{pmatrix} = \begin{pmatrix} -2 & 1 & 0 \\ 1 & -2 & 1 \\ 0 & 1 & -1 \end{pmatrix} \begin{pmatrix} x_1 \\ x_1 \\ x_1 \end{pmatrix} + \begin{pmatrix} 1 \\ 0 \\ 0 \end{pmatrix} \tilde{f}(x_3) \quad (52)$$

For  $m_0 = -33.03$  and  $m_1 = 400$ , Ogorzalek obtains the trajectory shown in Fig.13-a . The eigenvalue pattern of this system is :

$$\begin{cases} \mu_1 = -0.809 & \mu_{2-3} = 0.00753 & \pm j0.4045 \\ \nu_1 = 0.9234 & \sigma_1 = -0.8588 & \omega_1 = 1 \end{cases} \quad (53)$$

which is equivalent to :

$$\begin{cases} p_1 = -.7944 & p_2 = 0.151 & p_3 = -0.132 \\ q_1 = -0.794 & q_2 = 0.151 & q_3 = 1.604 \end{cases} \quad (54)$$

One can note that  $p_1 = q_1$  therefore we have to perturb the eigenvalue pattern in order to be able to determine the parameters of Chua's canonical circuit and Chua's canonical equations. If we modify one of the eigenvalues, it will have an effect on  $p_1$  or  $q_1$  and therefore we shall be able to calculate the canonical parameters. In the case of the torus we have seen that if the perturbation is too small the parameters exist but in practice for numerical reasons the integration of the system does not lead to the expected trajectory. On one hand, we want to avoid a singularity of the type  $\frac{1}{p_1 - q_1}$ . On the other hand we do not want to change the eigenvalues too much because then it is very likely that we shall not find the same qualitative behavior. The best way to do so is to modify  $(p; q)$  directly instead of  $(\mu; \nu)$ . By proceeding this way we are sure that we eliminate the singularity as efficiently as possible for a minimum perturbation of the eigenvalues. In our case, let us add 0.1 to  $p_1$  and subtract 0.1 from  $q_1$ , in order to maximize  $p_1 - q_1$ . This leads to the following eigenvalue pattern :

$$\begin{cases} p_1 = -.6944 & p_2 = 0.151 & p_3 = -0.132 \\ q_1 = -0.894 & q_2 = 0.151 & q_3 = 1.604 \end{cases} \quad (55)$$

which is equivalent to :

$$\begin{cases} \mu_1 = -0.746 & \mu_{2-3} = -0.913 & \pm j0.431 \\ \nu_1 = 0.918 & \sigma_1 = - - 0.913 & \omega_1 = 1 \end{cases} \quad (56)$$

and to the following parameters for chua's canonical circuit (resp  $\Sigma_d$ )  
 $C_1 = 1$  ;  $C_2 = -1.077$  ;  $G = -0.764$  ;  $G_a = 0.706$  ;  $G_b = 0.909$  ;  $L = 0.109$  ;  $R = -0.0776$   
 (resp.  $\alpha = 0.0551$  ;  $\beta = 0.928$  ;  $\gamma = -0.0551$  ;  $m_0 = 0.0548$  ;  $m_1 = 0.0706$  ;  $\theta = -1$  )

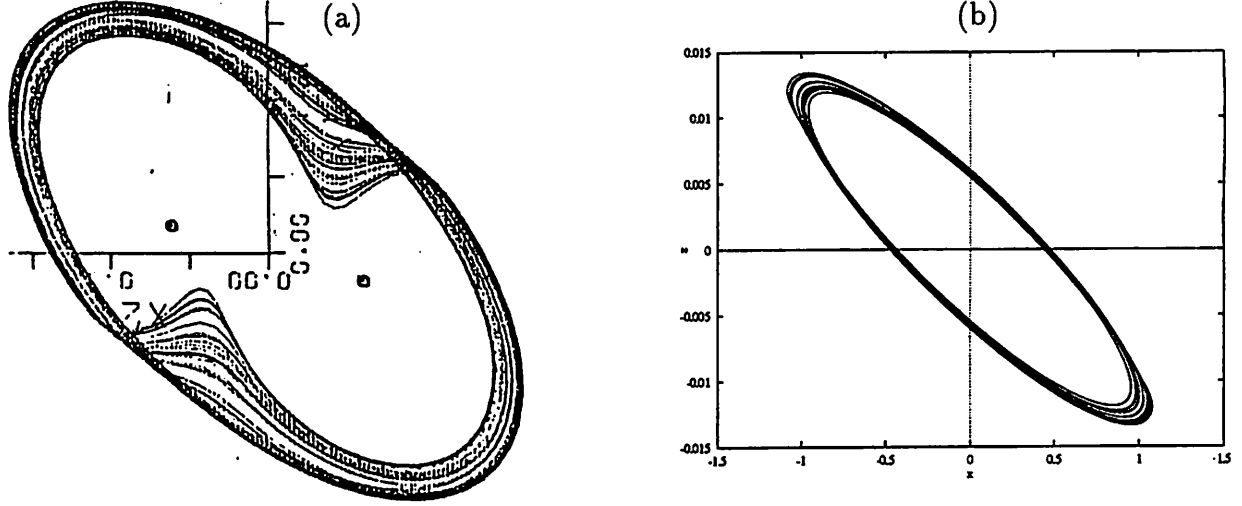


Figure 16: Attractor from Ogorzalec's example obtained from the original system and from  $\Sigma_d$ .

The trajectories on Fig. 16a and Fig. 16b do not look quite the same. As shown in Fig. 16c, the problem is that the trajectory is flattened onto a plane P that does not correspond to any of the planes  $x = 0$ ,  $y = 0$  or  $z = 0$ . Therefore there is no way of expanding the trajectory along one of the axes. As shown in Fig. 16d-e, we rotate the attractor around the axis x through an angle of 45.4 degrees to expose the third dimension of the attractor in greater details. We eventually obtain the attractor shown in Fig. 16f that looks identical to the original one in Fig. 16a.

### 3.5 Brockett's example

In [15], Brockett studies the following single loop feedback system:

$$\begin{pmatrix} \dot{x}_1 \\ \dot{x}_1 \\ \dot{x}_1 \end{pmatrix} = \begin{pmatrix} 0 & 1 & 0 \\ 0 & 0 & 1 \\ -1 & -1.25 & 0 \end{pmatrix} \begin{pmatrix} x_1 \\ x_1 \\ x_1 \end{pmatrix} + \begin{pmatrix} 0 \\ 0 \\ 1 \end{pmatrix} \tilde{g}(x_1) \quad (57)$$

where :

$$\tilde{g}(y) = \begin{cases} -\tilde{k}y & \text{if } |y| < 1 \\ 2\tilde{k}y - \tilde{3}k & \text{if } 1 < |y| < 3 \\ -3\tilde{k} \operatorname{sgn}(y) & \text{if } |y| > 3 \end{cases} \quad (58)$$

The only interest of the region  $|y| > 3$  is to claim that all solutions of (57) are bounded when  $t$  goes to infinity [16]. This region does not play any role in the dynamics of the system, therefore we replace the function  $\tilde{g}$  by  $f$  defined by  $m_0 = -\tilde{k}$  and  $m_1 = -3\tilde{k}$ .

The phase portrait obtained in [15] from (57) is shown in Fig. 17-a. As in the previous case, we find  $p_1 = q_1$ , after adding 0.05 to  $p_1$  and subtracting 0.05 from  $q_1$  we obtain :

$$\begin{cases} p_1 = -0.95 & p_2 = 1.25 & p_3 = 1.8 \\ q_1 = -1.05 & q_2 = 1.25 & q_3 = -3.6 \end{cases} \quad (59)$$

which is equivalent to :

$$\begin{cases} \mu_1 = 0.500 & \mu_{2-3} = -0.576 & \pm j0.913 \\ \nu_1 = -1.12 & \sigma_1 = -0.201 & \omega_1 = 1 \end{cases} \quad (60)$$

and to the following parameters for Chua's canonical circuit (resp  $\Sigma_d$ )

$C_1 = 1$  ;  $C_2 = -0.959$  ;  $G = -0.663$  ;  $G_a = 0.652$  ;  $G_b = 0.721$  ;  $L = -0.0402$  ;  $R = 0.0277$

(resp.  $\alpha = 0.0192$  ;  $\beta = -1.042$  ;  $\gamma = -0.0192$  ;  $m_0 = 0.0181$  ;  $m_1 = 0.02004$  ;  $\theta = 1$  )

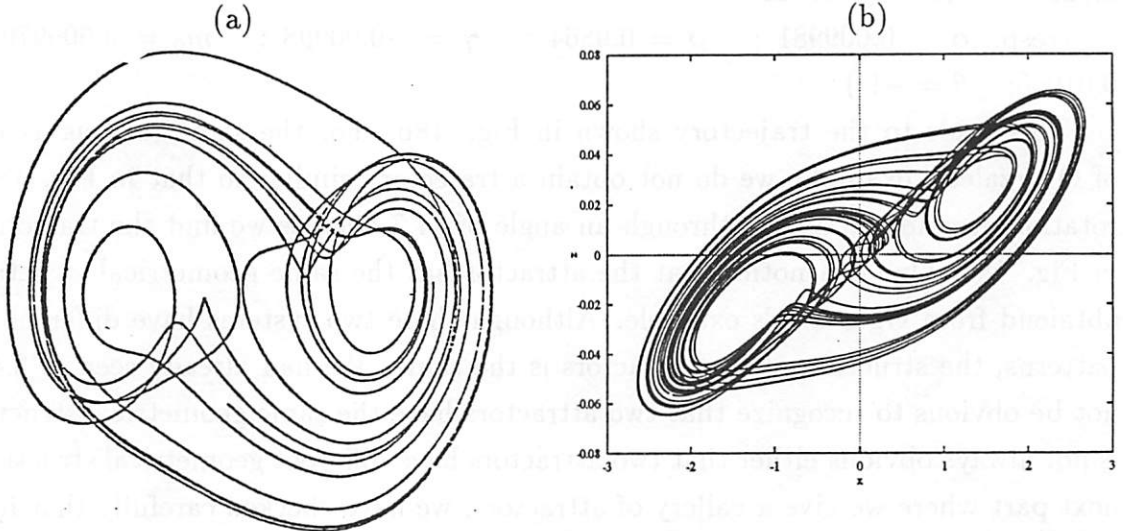


Figure 17: Attractor from Brockett's example obtained from the original system and from  $\Sigma_d$ .

### 3.6 Sparrow's example

Sparrow studies in [17] the following system of single-loop feedback system :

$$\begin{cases} \dot{x} = \tilde{g}(z) - x \\ \dot{y} = x - y \\ \dot{z} = y - z \end{cases} \quad (61)$$

where:

$$\tilde{g}(z) = \begin{cases} = -8.14z + 3.35 & \text{if } z \leq \frac{3}{7} \\ = 8.14rz - 0.25 - 3.6r & \text{if } z > \frac{3}{7} \end{cases} \quad (62)$$

This system does not directly belong to  $\mathcal{C}$  but after making the system symmetrical with respect to the origin, Sparrow obtained the double sided attractor shown in Fig. 18a. The only thing that changes in the vector field is the nonlinear function that becomes  $\tilde{f}$  given in (35) with  $m_0 = -8.4$  and  $m_1 = 8.4r$ . After adding 0.1 to  $p_1$  and subtracting 0.1 from  $q_1$  we obtained the following eigenvalue pattern:

$$\begin{cases} \mu_1 = -0.6316 & \mu_2 = 0.006352 + j0.3802 & \mu_3 = 0.006352 - j0.3802 \\ \nu_1 = 0.9395 & \nu_2 = -0.8005 + j & \nu_3 = -0.8005 - j \end{cases}$$

and the following parameters for Chua's canonical circuit (resp. Chua's canonical equations):

$$C_1 = 1 ; \quad C_2 = -1.0137 ; \quad G = -0.6275 ; \quad G_a = 0.61890 ; \quad G_b = 0.6615 ; \quad L = 0.02604 ; \quad R = -0.01612$$

$$(\text{resp. } \alpha = 0.009981 ; \quad \beta = 0.9864 ; \quad \gamma = -0.00998 ; \quad m_0 = 0.009979 ; \quad m_1 = 0.01066 ; \quad \theta = -1)$$

This leads to the trajectory shown in Fig. 18b. For the same reasons as in the case of Ogorzalec's example, we do not obtain a trajectory similar to that in Fig. 18a. After a rotation around the axis  $x$  through an angle of 44.7 degrees we find the trajectory shown in Fig. 18c. One can notice that the attractor has the same geometrical structure as that obtained from Ogorzalec's example. Although these two systems have different eigenvalue patterns, the structure of the attractors is the same. We had already seen in 3.4 that it is not obvious to recognize that two attractors have the same geometrical structure, but it is not always obvious either that two attractors have different geometrical structures. In the next part where we give a gallery of attractors, we have checked carefully that it is not the case.



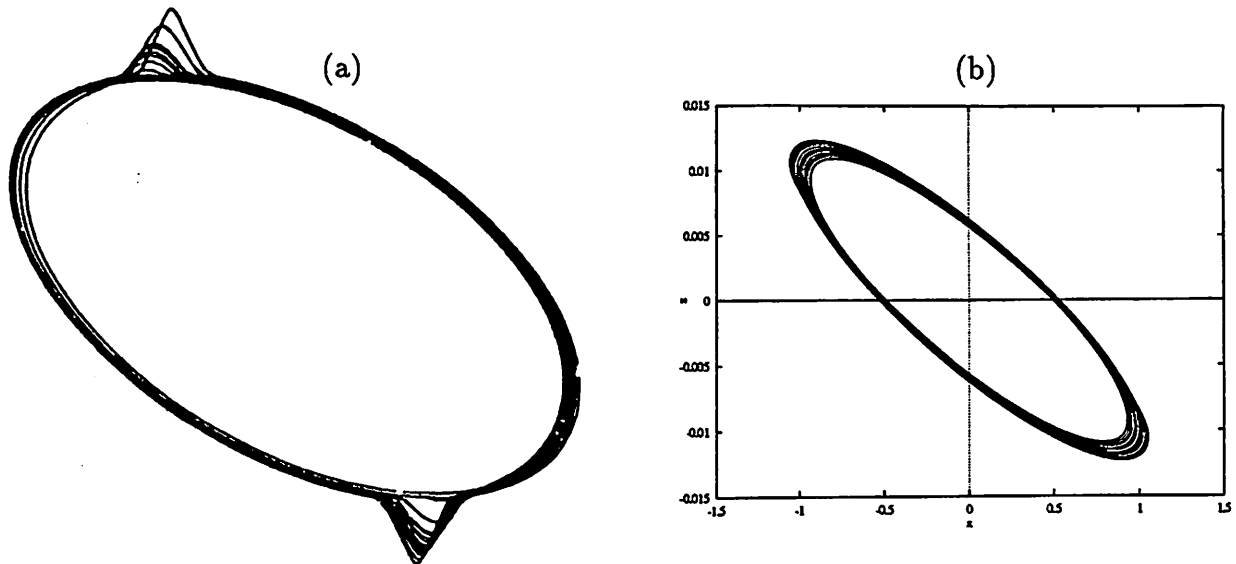


Figure 18: Attractor from Sparrow's example obtained from the original system and from  $\Sigma_d$ .

### 3.7 Conclusion

For each example considered in this section, it has been possible to find easily the parameters for both Chua's canonical circuit and Chua's canonical equations that lead to the same behavior. Through these examples, we have also presented a method to perturb the eigenvalues when needed. This method can be used to find the dynamics of any system of  $\mathcal{C}$  in that of  $\Sigma_c$  or  $\Sigma_d$ , as soon as we know its eigenvalue pattern. As far as the existing elements of  $\mathcal{C}$ <sup>11</sup> are concerned, it has been possible to find formulas that give the parameters of Chua's canonical equations directly as a function of the parameters of the original systems. With the formulas given in appendix A, the reader can directly use the program provided with this article, or use (5) to find the parameters of Chua's canonical circuit to study the dynamics of any element of  $\mathcal{C}$  studied so far. In the next section, we shall give a list of all the attractors found in  $\mathcal{C}$ .

## 4 A gallery of attractors

In this section, we present a zoo of attractors obtained from elements of Chua's canonical family. As it has already been explained earlier, all these attractors lie in the dynamics of Chua's canonical circuit and in that of its associated dimensionless form. We shall use this last system  $\Sigma_d$  to generate the trajectories of each of them. For each attractor, we shall also

---

<sup>11</sup>Chua's circuit, Chua's torus circuit, Ogorzalec ladder circuit, Sparrow and Brockett's examples

provide the eigenvalue pattern, the parameters of Chua's canonical equation  $\Sigma_d$  and Chua's canonical circuit  $\sigma_c$  as well as the Lyapunov dimension <sup>12 13</sup>. All these informations are gathered in two tables given in appendix D.

Among this zoo of attractors, we first find those studied in the previous section : Rossler's attractor, the double scroll, the double hook, the quasi-periodic and folded tori, Ogorzalec, Brockett and Sparrow's examples. In the case of Chua's circuit we present six new attractors. In addition to the attractors originally discovered from one of the system presented in the previous section, we add 12 other attractors reported in Chua's canonical circuits.

## 4.1 Attractors obtained from Chua's circuit

In addition to the Rossler's attractor, the double scroll, and the double hook, we add six other attractors obtained from Chua's circuit :

- a torus obtained for large values of  $\tilde{\alpha}$  and  $\tilde{\beta}$ .<sup>14</sup> :  $\tilde{\alpha} = 1800.0; \tilde{\beta} = 10000.0; \tilde{m}_0 = -0.026; \tilde{m}_1 = 0.018$

$\alpha = 0$  ;  $\beta = -11.111$  ;  $\gamma = -0.001111$  ;  $m_0 = 0.052$  ;  $m_1 = -0.036$  ;  $\theta = -1$

- three attractors obtained for the following values of parameters for the dimensionless form of Chua's circuit :

$\tilde{\alpha} = -4.087; \tilde{\beta} = -2.0; \tilde{m}_0 = -0.1429; \tilde{m}_1 = 0.2858$  (Fig. 19b)

$\tilde{\alpha} = -6.691; \tilde{\beta} = -1.520; \tilde{m}_0 = -0.1429; \tilde{m}_1 = 0.2858$  (Fig. 19c)

$\tilde{\alpha} = 8.342; \tilde{\beta} = 11.925; \tilde{m}_0 = 0.2952; \tilde{m}_1 = 0.1467$  (Fig. 19d)

- Two attractors obtained for the same values of parameters but different initial conditions. One of them is not symmetrical with respect to the origin, therefore we can consider its symmetric image as a third attractor. These attractors are obtained for :  $\tilde{\alpha} = 15.6; \tilde{\beta} = 28.58; \tilde{m}_0 = -1/7; \tilde{m}_1 = 2/7$  which is equivalent to :  $\alpha = 0$  ;  $\beta = 1.832$  ;  $\gamma = 0.0641$  ;  $m_0 = -1/7$  ;  $m_1 = 2/7$  ;  $\theta = -1$  and the following initial conditions (for  $\Sigma_d$ ):

$x = 1.27790; y = -1.83719; z = 0.190468$ ; (Fig. 19e)

$x = 1.34501; y = -0.32641; z = -0.256188$ ; (Fig. 19f)

$x = -1.34501; y = 0.32641; z = 0.256188$ ; ( the symmetric of the previous one )

The theory of confinors [18] [19] made possible to prove rigorously that these three attractors are different. As we shall see in the next section, this is a non-trivial problem that will

---

<sup>12</sup>see 5.4

<sup>13</sup>obtained with the software package INSITE

<sup>14</sup>Note that it is the first torus obtained in Chua's circuit

not be tackled in this paper. Let us say that all the geometrical structure of the attractors discovered so far in  $\mathcal{C}$  is close to that of one of the attractors presented in our gallery.

## 4.2 Concluding remarks

As explained earlier in this paper, all the dynamics of  $\mathcal{C}$  lies in a five parameter family of dynamical system :  $\Sigma_d$ . The corresponding five dimensional parameter space  $P_d$  is huge and a systematic scanning of  $P_d$  is almost impossible. So far, only a tiny portion of  $P_d$  has been explored, many more new attractors are expected. The aim of this gallery is mainly to give an idea of the wealth of the complicated dynamics in  $\mathcal{C}$  and to encourage the reader to look for new attractors with programs like that proposed with this article of that in [20].

Figure 19: Attractors originally obtained from Chua's circuit

## 5 Elements of dynamics in $\mathcal{C}$

### 5.1 Comparison of the original system and the corresponding Chua's canonical systems $\Sigma_c$ and $\Sigma_d$

Let us first recall the exact relation between the original dynamical system and that obtained from Chua's canonical circuit  $\Sigma_c$  or from its associated canonical system  $\Sigma_d$ . Let us denote by  $F_o, F_c$  and  $F_d$  the vector field of the original circuit, that of  $\Sigma_c$  and  $\Sigma_d$ , respectively. As it is proven in section 6, there exists two invertible matrices  $J_c$  and  $J_d$ , and a positive non-zero constant  $S_d$ , such that<sup>15</sup>:

---

<sup>15</sup> $J$  and  $J_c$  are said to be linearly conjugate, while  $J$  and  $J_d$  are said to be linearly equivalent

Figure 20: Some other attractors obtained from Chua's canonical circuit

$$\begin{cases} F_c = J_c^{-1} F_o J_c \\ F_d = S_d J_d^{-1} F_o J_d \end{cases} \quad (63)$$

If  $X(t, x_0)$  where  $t$  is the time and  $x_0$  the initial condition, (i.e. the value of  $X$  at  $t = 0$ ) is a solution of the original equation :

$$\dot{X}(t) = F(X) \quad (64)$$

then

$$\overline{J_c \dot{X}(t)} = J_c \dot{X} = J_c F_c(x) = F_c(J_c X(t)) \quad (65)$$

and

$$\overline{J_d \dot{X}} = J_d \dot{X} = S_d J_d F_d(x) = S_d F_d(J_d X(t)) \quad (66)$$

(65) implies that  $J_c X(t)$  is a solution of  $\Sigma_c$ , and (66) implies that  $J_d X(S_d t)$  is a solution of  $\Sigma_d$ . Concretely, this means that the trajectory obtained from Chua's canonical circuit is the same as  $X(t)$ , but in a different basis. The trajectory obtained from Chua's canonical equation is also the same as  $X(t)$  in a different basis, but after a time rescaling<sup>16</sup>. Therefore, we have to compare two trajectories which are not in the same basis. If there exists a relation of the type (63) between two vector fields (after a small perturbation if needed) the two systems are said to have the same qualitative behavior. In section 3, we did not insist on this point. By choosing the appropriate view point, we were able to verify that the trajectories obtained from the original system and from  $\Sigma_d$  look the same. Regardless of this, strictly speaking,

---

<sup>16</sup>Note that we cannot see this time rescaling in a phase portrait

we had not the same trajectory in two different basis, but two different trajectories. Indeed, we should not think in term of trajectory but in term of attractor as we explain below.

## 5.2 steady-state behavior and attracting sets

Let us first give some definitions:

A steady state refers to the asymptotic behavior as  $t \rightarrow \infty$ .

A point  $y$  is a limit point of  $x$  if, for every open neighborhood  $U$  of  $y$ ,  $X(t, x)$  repeatedly enters  $U$  as  $t \rightarrow \infty$ .

The set of all limit points of  $x$  is called the limit set of  $X(t, x)$ .

A limit set  $L$  is said *attracting* if there exists an open neighborhood of  $L$  such that the steady-state of  $X(t, x)$  is  $L$  for any  $x$  of  $U$ .

The *basin of attraction* of an attracting set  $L$  is  $B(L)$  such that every trajectory starting from  $B(L)$  tends toward  $L$  as  $t \rightarrow \infty$ .

Attracting limit sets are the only set that can be observed in physical system. This does not mean that a nonattracting set cannot have an influence on the transient (before the steady-state is reached). The definition of limit sets that we gave is in fact too simple for complex steady-state behaviors such as those existing in chaotic systems. The term *strange attractor* has been introduced as the set on which the trajectory accumulates. For us we shall use interchangeably attracting limit set and attractor. Note that in a stable linear system there is only *one* limit set but in a nonlinear system there are typically several attracting sets with their own basins of attraction. The initial conditions determine in which limit set the system settles.

## 5.3 Equilibrium points, periodic orbits, quasi-periodic orbits and chaos

$X_{eq}$  is an *equilibrium point* if for all  $t$ :  $X(t, X_{eq}) = X_{eq}$ .

$X(t, X_0)$  is a *periodic solution* if there exists a minimal period  $T$  such that  $X(t, X_0) = X(t + T, X_0)$  for all  $t$ .

$X(t, X_0)$  is a *quasi-periodic* solution if it can be written as the sum of periodic functions :  $X(t) = \sum_i h_i(t)$  where  $h_i$  has a minimal period  $T_i$  and a frequency  $f_i$ . In addition to this, there exists a finite set of base frequencies  $(\hat{f}_1, \dots, \hat{f}_p)$  such that

- there does not exist a nonzero set of integers  $(\hat{k}_1, \dots, \hat{k}_p)$  such that  $\hat{k}_1 \hat{f}_1 + \dots + \hat{k}_p \hat{f}_p = 0$
- it forms a finite integral basis for any  $f_i$ .

The base frequency is not unique but  $p$  is. A quasi-periodic solution with  $p$  base frequencies is called *p-periodic*.

From a practical point of view, *chaos* can be defined as none of the above; that is, a bounded steady-state behavior that is not an equilibrium point, periodic and not quasi-periodic. The limit set for chaotic behavior is not a simple set like a circle or a torus but it is related to fractals and cantor sets [21].

Another property of chaotic system is its *sensitive dependence on initial conditions* already mentioned in 3.2.2. Consider two different initial conditions arbitrarily close to each other, the corresponding trajectories to these two points diverge at a rate characteristic of the system before becoming uncorrelated for all practical purposes. Even if two different initial conditions are very close to each other, so that they cannot be distinguished, the corresponding trajectories will diverge and become uncorrelated after a finite amount of time. Therefore, no matter how precisely the initial conditions are known, the long term behavior of a chaotic system cannot be predicted. That is why chaotic systems, although deterministic are said to exhibit a “random behavior”. This is the reason why it is impossible to reproduce with Chua’s canonical system exactly the same trajectory as with the original system. In the previous section, we in fact verified that the attractors obtained from the original system from  $\Sigma_d$  look the same. The reader can easily imagine that to prove that two chaotic attractors are identical, or different, is a non trivial task [19]. When we do not have to perturb the parameters, the dynamical systems  $\Sigma_o$ ,  $\Sigma_c$  and  $\Sigma_d$  are equivalent. Therefore the same attractors should be present in the three systems. In fact this is not obvious either. Indeed the vector fields are not defined with infinite precision. Fortunately, except in some pathological cases, attractors are said to be structurally stable which means that they are preserved under perturbations of the system (otherwise we could not see them). This is equivalent to the continuity properties of the ODE with respect to parameters. One can also refer to a real circuit where the components are not defined with an infinite precision, fluctuate but still give birth to the “same” attractor. Assuming that an attractor is stable, it has an open basin of attraction. On one hand, we cannot reproduce the same initial conditions in Chua’s canonical systems ( $\Sigma_c$  and  $\Sigma_d$ ) as in the original system. On the other hand, it is possible to start in the same basin of attraction and therefore obtain the same attractor. That is what we did in the previous section. Also note that if the notion of attractor is a non-trivial one and it is not obvious either to determine whether or not two attractors are distinct, if their basins of attraction are distinct. In this paper we shall not tackle this problem. In the previous section, we do not pretend to have given an exhaustive list of all the existing attractors in Chua’s canonical circuit but much more that all the attractors discovered so far in

$\mathcal{C}$  have a geometrical structure close to that of one presented in the gallery. There are in fact many attractors present, thinking for example of a bifurcation sequence where the attractors evolve, merge ... [9] [22] We have also seen in 3.4 that it is not always easy to recognize that two attractors are similar (almost if there is no way to predict it from the eigen pattern). To build a complete list of attractors, it would be at the same time difficult to be exhaustive but also to make sure not to mention the same attractor twice. In addition to the phase portrait, one of the criteria to characterize an attractor is its Lyapunov exponents.

## 5.4 Lyapunov exponents

After this brief presentation of what chaos is, we introduce a generalization of the eigenvalues at the equilibrium points. The Lyapunov exponents are used to determine the stability of any steady-state behavior (behavior when  $t \rightarrow \infty$ ) including chaotic and quasi-periodic solution for which they provide valuable information. They are defined in terms of solutions of the variational equation as follows: let  $\{m_i(t)\}_{i=1}^3$  be the eigenvalues of  $X(t, x_0)$ . The Lyapunov exponents are defined by :

$$\lambda_i = \lim_{t \rightarrow \infty} \frac{1}{t} \ln |m_i(t)| \quad (67)$$

if the limit exists <sup>17</sup>. To have a better understanding of what these Lyapunov exponents are, let us for example find them at the equilibrium point  $P_+$ . The eigenvalues of the Jacobian matrix  $M_1$  are  $\mu_i(t)_{i=1}^3 = e^{\mu_i(t)}$ . Therefore :

$$\begin{aligned} \lambda_i &= \lim_{t \rightarrow \infty} \frac{1}{t} \ln |m_i(t)| \\ &= \lim_{t \rightarrow \infty} \frac{1}{t} \operatorname{Re}[\mu_i] t = \operatorname{Re}[\mu_i] \end{aligned} \quad (68)$$

Hence, in this special case, the Lyapunov exponents are equal to the real part of the eigenvalues at the equilibrium point; they indicate the rate of contraction ( $\lambda_i < 0$ ) or expansion ( $\lambda_i > 0$ ) near the equilibrium point.

Suppose that  $x_0 \neq P_+$  but  $X(t, x_0) \rightarrow P_+$  as  $t \rightarrow \infty$ , which means that  $x_0$  is in the basin of attraction of  $P_+$ . Since the Lyapunov exponents are defined as the limit as  $t \rightarrow \infty$ , the Lyapunov exponents of  $x_0$  and  $P_+$  are identical. In general, every point of an attractor has the same Lyapunov exponents as the attractor <sup>18</sup>; therefore we can refer to the lyapunov exponents of an attractor. It is proven in dimension  $n$  that at least one of the Lypunov

---

<sup>17</sup>*lim* can be replaced by *lim sup* to guarantee existence of the lyapunov exponents. Our short presentation is only true when the limit exists.

<sup>18</sup>We should say for almost every point in some cases of strange (or chaotic) attractors, but it is always true for non-strange attractors

exponents must be equal to zero. In addition to this , note that for an attractor, the contraction must outweigh expansion so :

$$\sum_{i=0}^n \lambda_i < 0 \quad (69)$$

From these Lyapunov exponents :

$$\lambda_1 \geq \lambda_2 \geq \dots \lambda_n \quad (70)$$

Kaplan and Yorke defined the Lyapunov dimension as :

$$D_L = j + \frac{\lambda_1 + \lambda_2 + \lambda_j}{\lambda_{j+1}} \quad (71)$$

where  $j$  is the largest integer such that  $\lambda_1 + \lambda_2 + \lambda_j \geq 0$ .

## 5.5 Classification of Attracting sets

Having now a better idea of what attractors are, let us classify them. One of the features of chaos is its sensitive dependence on initial conditions. This occurs only in an expanding flow. Hence, what distinguishes a chaotic (or strange) attractor from the other types of attractor is the presence of at least one positive Lyapunov exponent. In the three-dimensional case, we can only have one positive Lyapunov <sup>19</sup> but in systems of higher dimension, it is possible to have more than one positive Lyapunov exponent; the system is then termed *hyper chaotic*. Among the attracting set, it is possible to operate a classification of attracting sets as follows:

Classification of attracting sets			
Steady-state	Attracting set	Lyapunov exponents	Lyapunov dimension
Equilibrium point	point	$0 > \lambda_1 \geq \dots \lambda_n$	0
Periodic	closed curve	$\lambda_1 = 0; 0 > \lambda_2 \geq \dots \lambda_n$	1
K-periodic	K-torus	$\lambda_1 = 0 = \dots = \lambda_K = 0; 0 > \lambda_{K+1} \geq \dots \lambda_n$	K
Chaotic	Cantor-like	$\lambda_1 > 0; \sum \lambda_i < 0$	noninteger

---

<sup>19</sup>one is equal to zero, and their sum has to be negative



## 6 Linear conjugacy of two systems having the same eigenvalue pattern

Our aim in this section is to prove the following proposition :

- Two elements of  $\mathcal{C}$ , whose vector fields  $F$  and  $F'$  have the same eigenvalue pattern  $(\mu; \nu)$  or  $(p; q)$  <sup>20</sup> are linearly conjugate, i.e. : there exists a non-singular matrix  $H$  such that:

$$H \circ F = F' \circ H \quad (72)$$

(72) immediately implies that the two dynamical systems associated with  $F$  and  $F'$  have the same qualitative behavior. If  $X$  is a solution of the dynamical system

$$\dot{X} = F(X) \quad (73)$$

in the basis  $B$ , then:

$$H\dot{X} = H \circ F(X) = F'(HX) \quad (74)$$

therefore  $\hat{X} = HX$  is a solution of :

$$\dot{\hat{X}} = F'(\hat{X}) \quad (75)$$

This means that if (73) leads to a trajectory, (75) leads to a similar trajectory <sup>21</sup> in another basis defined from  $B$  by  $H$  (we invite the reader to verify that this is equivalent to what has been said in 5.1).

More precisely, in order to prove our proposition, we shall show that any vector field of  $\mathcal{C}$  with an eigenvalue pattern  $(p; q)$  is linearly conjugate to some function  $F_{pq}$  uniquely determined by  $(p; q)$ . By transitivity, this implies that two vector fields have the same eigenvalue pattern  $(p; q)$  are linearly conjugate. The proof is decomposed into three steps :

### 6.1 step 1

Let us first express the vector field  $F$  of any element of  $\mathcal{C}$  in a form in which it will be easier to prove our proposition. It is first possible to recast the equation of  $F$  in a basis  $\tilde{B}$  where the equations of the boundary planes are  $x = 1$  and  $x = -1$ .  $F$  can be expressed in the form <sup>22</sup>:

---

<sup>20</sup>In this section, it will more convenient to define the eigenvalue patterns by  $(p; q)$ , let us recall that there exists a bijection between  $(\mu; \nu)$  and  $(p; q)$

<sup>21</sup>with the restrictions of the previous section

<sup>22</sup> $\langle, \rangle$  denotes the vector dot product. If for exmple  $x = (x_1, x_2, x_3)^T$  and  $y = (y_1, y_2, y_3)^T$  then  $\langle x, y \rangle = x_1y_1 + x_2y_2 + x_3y_3$

$$f(X) = \begin{cases} \tilde{B}X + \tilde{c} & \text{for } \langle \tilde{W}, X \rangle < -1 \\ \tilde{A}X & \text{for } |\langle \tilde{W}, X \rangle| \leq 1 \\ \tilde{B}X - c & \text{for } \langle \tilde{W}, X \rangle > 1 \end{cases} \quad (76)$$

where:

$\tilde{A} = (a_{ij})$  is the Jacobian matrix of  $F$  in the middle region, denoted by  $M_0$  in Fig.1.

$\tilde{B} = (b_{ij})$  is the Jacobian matrix of  $F$  in the outer region, denoted by  $M_1$  in Fig.1.

$\tilde{c} = (c_1, c_2, c_3)$  is a vector of  $R^3$  that ensures the continuity of  $F$  on the boundary point.

$\tilde{W} = (1, 0, 0)^T$  is a vector of  $R^3$ .

The coordinates of a point belonging to the boundary plane  $B_1$  can be expressed by  $(1, y, z)$  where  $y$  and  $z$  are two real numbers. The assumption that  $F$  is continuous on  $B_1$  is equivalent to :

$$\forall y, z \in R, \quad \tilde{A} \begin{pmatrix} 1 \\ y \\ z \end{pmatrix} = \tilde{B} \begin{pmatrix} 1 \\ y \\ z \end{pmatrix} + \tilde{c} \quad (77)$$

which can be explicitly written as follows :

$$\forall y, z \in R, \quad \begin{cases} a_{11} - b_{11} - c_1 + (a_{12} - b_{12})y + (a_{13} - b_{13})z = 0 \\ a_{21} - b_{21} - c_2 + (a_{22} - b_{22})y + (a_{23} - b_{23})z = 0 \\ a_{31} - b_{31} - c_3 + (a_{32} - b_{32})y + (a_{33} - b_{33})z = 0 \end{cases} \quad (78)$$

Eq.(78) implies that the two last columns of the matrices  $A$  and  $B$  are identical. Thus there exists a vector

$$\tilde{P} = \begin{pmatrix} -b_{11} - c_1 \\ -b_{21} - c_2 \\ -b_{31} - c_3 \end{pmatrix} \quad (79)$$

such that

$$B = A + P(1, 0, 0)^T \quad (80)$$

Therefore  $f$  can be expressed as follows [11] [10] :

$$F(X) = \tilde{A}X + \frac{1}{2}\tilde{P} \left( |\langle \tilde{W}, X \rangle - 1| + (\langle \tilde{W}, X \rangle - 1) \right) - \left( |\langle \tilde{W}, X \rangle + 1| - (\langle \tilde{W}, X \rangle + 1) \right) \quad (81)$$

Let us now note that there exists a nonsingular matrix  $H$  such that  $A = H\tilde{A}H^{-1}$  is in

its Jordan form [23]. The equation of  $f(\cdot)$  as defined in (81) in a basis  $B$ , becomes

$$Hf(H^{-1}X) = H\tilde{A}H^{-1}X + \frac{1}{2}H\tilde{P} \left\{ \left( |\langle (H^{-1})^T\tilde{W}, X \rangle - 1| \right. \right. \\ \left. \left. + (\langle (H^{-1})^T\tilde{W}, X \rangle - 1) \right) \right. \\ \left. - \left( |\langle (H^{-1})^T\tilde{W}, X \rangle + 1| \right) \right. \\ \left. - (\langle (H^{-1})^T\tilde{W}, X \rangle + 1) \right\} \quad (82)$$

in a basis  $B$  characterized by the passage matrix  $H$  from  $\tilde{B}$  to  $B$ .  $\tilde{A}$ ,  $\tilde{P}$  and  $\tilde{W}$  are transformed into  $H\tilde{A}H^{-1}$ ,  $H\tilde{P}$  and  $(H^{-1})^T\tilde{W}$ , respectively, and denoted by  $A, P$  and  $W$ . Therefore, we can suppose, without loss of generality that  $F$   $A$  is in the form

$$F(X) = X + \frac{1}{2}P \left( |\langle W, X \rangle - 1| + (\langle W, X \rangle - 1) \right) \\ - \left( |\langle W, X \rangle + 1| - (\langle W, X \rangle + 1) \right) \quad (83)$$

where  $A$  is in its Jordan form. Note that  $W$  is *not* necessarily equal to  $(1, 0, 0)^T$ .

## 6.2 Step 2

In a second step, we shall prove that there exists a basis  $B'$  where  $A'$  is in its horizontal companion form <sup>23</sup> :

$$\begin{pmatrix} 0 & 1 & 0 \\ 0 & 0 & 1 \\ r_1 & r_2 & r_3 \end{pmatrix} \quad (84)$$

and  $W'$  is equal to  $(1, 0, 0)^T$ . We have assumed above that  $A$  is in its Jordan form, there are four possible cases :

$$\begin{aligned} (a) & \begin{pmatrix} a & 1 & 0 \\ 0 & a & 1 \\ 0 & 0 & a \end{pmatrix} & (b) & \begin{pmatrix} a & 0 & 0 \\ 0 & b & 1 \\ 0 & 0 & b \end{pmatrix} \\ (c) & \begin{pmatrix} a & 1 & 0 \\ 0 & b & 0 \\ 0 & 0 & c \end{pmatrix} & (d) & \begin{pmatrix} a & 0 & 0 \\ 0 & \sigma & -\omega \\ 0 & \omega & \sigma \end{pmatrix} \end{aligned}$$

where  $a, b$  and  $c$  are distinct and  $\omega \neq 0$ . In each case, we shall make some assumptions regarding the vector  $W$ . They correspond to the fact that, as stipulated in the introduction, there is no plane or line parallel to the boundary plane which is invariant under the action of the linear vector field  $f$  in the middle region. Let us now examine these four cases :

---

<sup>23</sup>One can easily verify that  $r_1 = p_1, r_2 = -p_2$  and  $r_3 = p_3$

### 6.2.1 Case (a)

Assume that  $W = (w_1, w_2, w_3)^T$  satisfies  $w_1 \neq 0$ .  $W$  is transformed by the matrix  $w_1 I$  into  $W = (1, y, z)^T$  which in turn is transformed by the matrix :

$$\begin{pmatrix} 1 & y & z \\ 0 & 1 & y \\ 0 & 0 & 1 \end{pmatrix} \quad (85)$$

into  $W = (1, 0, 0)^T$ .  $A$  is invariant under these transformations. Choosing

$$K = \begin{pmatrix} 1 & 0 & 0 \\ a & 1 & 0 \\ a^2 & 2a & 1 \end{pmatrix} \quad (86)$$

$A$  is transformed into :

$$A' = KAK^{-1} = \begin{pmatrix} 0 & 1 & 0 \\ 0 & 0 & 1 \\ 3a & -3a^2 & a^3 \end{pmatrix} \quad (87)$$

and  $W$  is transformed into  $W' = (K^{-1})^T W = (1, 0, 0)^T$ .

### 6.2.2 Case (b)

Assume that  $W = (w_1, w_2, w_3)^T$  satisfies  $w_1 \neq 0$  and  $w_2 \neq 0$ .  $W$  is transformed by the matrix

$$\begin{pmatrix} w_1 & 0 & 0 \\ 0 & w_2 & 0 \\ 0 & 0 & w_3 \end{pmatrix} \quad (88)$$

into  $W = (1, 1, z)^T$  which in turn is transformed by the matrix

$$\begin{pmatrix} 1 & 0 & 0 \\ 0 & 1 & z \\ 0 & 0 & 1 \end{pmatrix} \quad (89)$$

into  $W = (1, 0, 0)^T$ .  $A$  is invariant under these transformations. Choosing

$$K = \begin{pmatrix} 1 & 0 & 0 \\ a & b & 1 \\ a^2 & b^2 & 2b \end{pmatrix} \quad (90)$$

$A$  is transformed into

$$A' = KAK^{-1} = \begin{pmatrix} 0 & 1 & 0 \\ 0 & 0 & 1 \\ ab^2 & -(2a+b)b & a+2b \end{pmatrix} \quad (91)$$

and  $W$  is transformed into  $W' = (K^{-1})^T W = (1, 0, 0)^T$ .

### 6.2.3 Case(c)

Assume that  $W = (w_1, w_2, w_3)^T$  satisfies  $w_1 \neq 0$ ,  $w_2 \neq 0$  and  $w_3 \neq 0$ .  $W$  is transformed by the matrix

$$\begin{pmatrix} w_1 & 0 & 0 \\ 0 & w_2 & 0 \\ 0 & 0 & w_3 \end{pmatrix} \quad (92)$$

into  $W = (1, 1, 1)^T$ .  $A$  is invariant under these transformations. Choosing

$$K = \begin{pmatrix} 1 & 0 & 1 \\ a & b & c \\ a^2 & b^2 & c^2 \end{pmatrix} \quad (93)$$

$A$  is transformed into

$$A' = KAK^{-1} = \begin{pmatrix} 0 & 1 & 0 \\ 0 & 0 & 1 \\ abc & -(ab+bc+ca) & a+b+c \end{pmatrix} \quad (94)$$

and  $W$  is transformed into  $W' = (K^{-1})^T W = (1, 0, 0)^T$ .

### 6.2.4 Case(d)

Assume that  $W = (w_1, w_2, w_3)^T$  satisfies  $w_1 \neq 0$  and  $w_2^2 + w_3^2 \neq 0$ .  $W$  is transformed by the matrix

$$\begin{pmatrix} w_1 & 0 & 0 \\ 0 & w_2 & w_3 \\ 0 & -w_3 & w_2 \end{pmatrix} \quad (95)$$

into  $W = (1, 1, 1)^T$ .  $A$  is invariant under these transformations. Choosing

$$K = \begin{pmatrix} 1 & 1 & 0 \\ a & \sigma & -\omega \\ a^2 & \sigma^2 + \omega^2 & -2\omega^2 \end{pmatrix} \quad (96)$$

$A$  is transformed into

$$A' = KAK^{-1} = \begin{pmatrix} 0 & 1 & 0 \\ 0 & 0 & 1 \\ a + 2\sigma & -(2a\sigma + \sigma^2 + \omega^2) & a(\sigma^2 + \omega^2) \end{pmatrix} \quad (97)$$

and  $W$  is transformed into  $W' = (K^{-1})^T W = (1, 0, 0)^T$ .

### 6.2.5 Conclusion

In each case, it exists a matrix  $K$  such that :

$$A' = KAK^{-1} = \begin{pmatrix} 0 & 1 & 0 \\ 0 & 0 & 1 \\ -p_3 & -p_2 & -p_1 \end{pmatrix} \quad (98)$$

$$W' = (K^{-1})^T W = (1, 0, 0) \quad (99)$$

### 6.3 Step 3

The vector field expressed in (70) is defined by  $A, W$  and  $P$ . We have proven that there exists a basis  $B'$  defined by  $K$  from  $\tilde{B}$  where *simultaneously*  $A'$  is in its companion form (completely defined by  $p_1, p_2$  and  $p_3$ ) and  $W' = (1, 0, 0)^T$ . The last unknown is

$$p' = Kp = (e_1, e_2, e_3)^T \quad (100)$$

We are now going to prove that it is also uniquely defined by  $(p; q)$ . Indeed, from (80), the Jacobian matrix of the vector field in the outer regions is the matrix :

$$B' = p'w'^T + A' = \begin{pmatrix} e_1 & 1 & 0 \\ e_2 & 0 & 1 \\ e_3 - p'_3 & p'_2 & -p'_1 \end{pmatrix} \quad (101)$$

Its characteristic polynomial is :

$$\begin{aligned} P(\lambda) &= |\lambda I - B| = \lambda^3 - \lambda^2(p_1 + e_1) \\ &\quad + \lambda(e_1 p_1 - p_2 - e_2) \\ &\quad + (e_3 + p_3 - p_2 e_1 - p_1 e_2) = 0 \end{aligned} \quad (102)$$

but it is also, by definition of  $q_1, q_2$  and  $q_3$ ,

$$P(\lambda) = \lambda^3 - q_1\lambda^2 + q_2\lambda - q_3 \quad (103)$$

This leads to the following set of equations

$$\begin{cases} e_1 &= q_1 - p_1 \\ e_2 &= q_2 - p_2 - p_1 e_1 \\ e_3 &= q_3 - p_3 + p_2 q_1 + p_1 q_2 \end{cases} \quad (104)$$

that uniquely defines  $p'$ . We have exhibited a function  $F_{pq}$  uniquely determined by  $p_1, p_2, p_3, q_1, q_2$  and  $q_3$  that is linearly conjugate to any element  $f$  of  $L$  with the same eigenvalue pattern.

## 7 Conclusion

In this paper, we have shown how rich the dynamics of a huge family of dynamical systems  $\mathcal{C}$  are, but also how all these dynamics can be subsumed within that of a simple circuit or of its associated dimensionless form driven by only five parameters. The fact that the only nonlinearity in the system is three-region piecewise linear and therefore that in each of the three regions the system is linear makes the study of the dynamics easier. With some examples, it has been possible to give some intuitions about the evolution of the trajectory, mainly in terms of eigen spaces and to introduce the notion of sensitive dependence to initial conditions. The program available with this article constitutes a complement for the study of attractors in a more lively way and allows a better understanding of the structure of an attractors. This paper is aimed for the non-specialist. We tried to make full use of the simplicity of the structure of the vector fields in  $\mathcal{C}$ . However, the theory of chaotic dynamics is much more complex than it appears in this paper. The simplicity of the elements of  $\mathcal{C}$  provides a vehicle for finding an answer to many questions still opened about *chaos*. Reference [21] constitutes a good introduction to chaotic dynamics, [24] will provide the necessary algorithms to study these systems. To close this paper we shall remember that the elements of Chua's circuit family can be built with standard components, thereby providing a useful real-time complement to their study.

## Acknowledgements :

This work is supported in part by the National Science Foundation under grant MIP 89-12639 and by the Office of Naval research under Grant N00014-89-J-1402

## List of Figures

1	A three-region piecewise-linear system . . . . .	2
2	(a) Chua's circuit (b) characteristic of Chua's diode . . . . .	3
3	Three-region characteristic of Chua diode . . . . .	3
4	Chua's canonical circuit . . . . .	5
5	dc operating points of the Chua diode . . . . .	11
6	Comparison of a Rossler-type attractor and its odd-symmetric twin obtained from $\Sigma_d$ with the attractor obtained from the original Chua's system . . . .	15
7	Phase portrait of the double scroll obtained from Chua's original system and from $\Sigma_d$ . . . . .	16
8	Typical trajectories and eigen spaces for the double scroll . . . . .	17
9	Four types of trajectory in an affine system with one real and two complex conjugate eigenvalues . . . . .	18
10	Time series of the double scroll obtained from $\Sigma_d$ , starting from two different but close initial conditions . . . . .	19
11	Phase portrait of the double hook obtained from Chua's original system in and from $\Sigma_d$ . . . . .	20
12	Two-dimensionnal quasi-periodic torus obtained from the original Chua's torus system and from $\Sigma_d$ . . . . .	22
13	Typical trajectories and eigenspaces for the 2-torus . . . . .	22
14	Time series of a quasi-periodic torus obtained from $\Sigma_d$ . . . . .	23
15	Folded torus obtained from the original Chua's torus system and from $\Sigma_d$ . .	24
16	Attractor from Ogorzalec's example obtained from the original system and from $\Sigma_d$ . . . . .	26
17	Attractor from Brockett's example obtained from the original system and from $\Sigma_d$ . . . . .	27
18	Attractor from Sparrow's example obtained from the original system and from $\Sigma_d$ . . . . .	28
19	Attractors originally obtained from Chua's circuit . . . . .	30
20	Some other attractors obtained from Chua's canonical circuit . . . . .	31



## References

- [1] L.O. Chua, M. Komuro and T. Matsumoto. The double scroll family. *IEEE Trans Circuits Syst*, 33:1073–1118, 1986.
- [2] L.O. Chua. The genesis of chua's circuit. *Arkiv fur elektronik and Ubertragungstechnik*, 46(4):250–257, 1992.
- [3] G.-Q. Zhong and F. Ayrom. Experimental confirmation of chaos from chua's circuit. *Int. J. Circuit Theory and Applications*, 15(2), 1985.
- [4] M. P. Kennedy. Robust op amp realization of chua's circuit. *Frequenz*, 46:66–80, 1992.
- [5] L.O. Chua, G.N. Lin. Canonical realization of chua's circuit family. *IEEE Trans Circuits and Syst*, 37(7):885–902, 1990.
- [6] C.M. Blazquez and E. Tuma. Dynamics of the double scroll circuit. *IEEE Trans. Circuits and Systems*, 37(5):589–593, 1987.
- [7] T.S. Parker and L.O. Chua. The dual double scroll. *IEEE Trans. Circuits and Systems*, 34(9):1059–1073, 1987.
- [8] T. Matsumoto, L.O. Chua and M. Kumoro. Birth and death of the double scroll. *Physica D*, 24:97–124, 1987.
- [9] T. Matsumoto, L.O. Chua and M. Kumoro. the double scroll bifurcations. *Int. J. Circuit Theory Appl.*, 14(1):117–146, 1986.
- [10] T. Matsumoto, L.O. Chua and M. Kumoro. the double scroll. *IEEE Trans. Circuits and Systems*, 32(8):589–593, 1985.
- [11] T. Matsumoto. A chaotic attractor from chua's circuit. *IEEE Trans. Circuits and Systems*, 21(12):1055–1058, 1984.
- [12] P. Bartissol and L.O. Chua. The double hook. *IEEE Trans. Circuits and Systems*, 35(12):1512–1522, 1988.
- [13] T. Matsumoto, L.O. Chua and R. Tokunaga. Chaos via torus breakdown'. *IEEE Trans. Circuits and Systems*, 34(3):240–253, 1987.
- [14] M.J. Ogorzalec. Order and chaos in a third order rc ladder network with nonlinear feedback. *IEEE Trans. Circuits and Systems*, 36(9):1221–1230, 1989.

- [15] R. W. Brocket. On conditions leading to chaos in feedback systems. *IEEE Trans. Circuits and Systems*, 1982.
- [16] R. W. Brockett and J.L. Willems. Frequency domain stability criteria, part. i and ii. *IEEE trans. on Automatic control*, 10:407–413, 1965.
- [17] C. T. Sparrow. Chaos in a three-dimensional single loop feedback system with a piecewise linear feedback function. *J. of mathematical analysis and applications*, 83(1):275–291, 1981.
- [18] R. Lozi and S. Ushiki. Cofinors and bounded-time patterns in chua’s circuit and the double scroll family. *Int Journal of Bifurcation and Chaos*, 1(1):119–138, 1991.
- [19] R. Lozi and S. Ushiki. Coexisting chaotic attractors in chua’s circuit. *Int Journal of Bifurcation and Chaos*, 1(4):923–926, 1991.
- [20] M.P. Kennedy C.W. Wu S. Pau and J. Tow. Digital signal processor-based investigation of chua’s circuit family. *to appear in special issue on Chua’s circuit : a paradigm for chaos*, 1993.
- [21] J. Guckenheimer and P. J. Holmes. *Nonlinear Oscillations, Dynamical Systems and Bifurcations of Vector Fields*. Springer-Verlag, 1983.
- [22] M. Komuro. Bifurcation equations of 3-dimensional piecewise-linear vector fields. *Advanced series in dynamical systems*, 8:113–123, 1990.
- [23] G. Strang. *Linear algebra and its applications*. Harcourt Brace Janovich,publisher, 1980.
- [24] T. S. Parker and L. O. Chua. *Practical Numerical algorythms for chaotic systems*. Springer Verlag, New york, 1989.

## 8 Appendix

### 8.1 Appendix A : derivation of Chua's canonical equations

In section 6, we proved that two vector fields with the same eigenvalue pattern  $(p; q)$  lead to dynamical systems with the same behavior. We are now going to show that from (6) it is possible to reach any eigenvalue pattern. In fact we shall see that a set of eigenvalues of zero measure cannot be reached. It may happen that some attractors are not structurally stable, but the only relevant properties for the elements of  $L$  are the ones preserved under perturbation of the system. Subsequently, as it has already been explained, we consider that if we cannot reach a certain set of eigenvalues, we change the parameters slightly to obtain a topologically conjugate vector field whose eigenvalues can be reached.

In the region  $D_0$  the state equation is :  $\dot{X} = M_0 X$

Where  $M_0$  is the constant matrix:

$$M_0 = \theta \begin{pmatrix} -a & 0 & 1 \\ 0 & -\alpha & \beta \\ -\gamma & -\gamma & -\gamma \end{pmatrix} \quad (105)$$

Its characteristic polynomial is :

$$\begin{aligned} |\lambda I - M_0| &= \lambda^3 + \lambda^2 \theta(a + \alpha + \gamma) \\ &\quad + \lambda \theta^2(\alpha a + \alpha \gamma + a \gamma + \beta \gamma + \gamma) \\ &\quad + \theta^3(a \alpha \gamma + \gamma \alpha \epsilon + \beta \gamma a) = 0 \end{aligned} \quad (106)$$

Since  $\mu_1, \mu_2$  and  $\mu_3$  are the eigenvalues that we expect in Chua's canonical system, we also have:

$$(\lambda - \mu_1)(\lambda - \mu_2)(\lambda - \mu_3) = \lambda^3 - p_1 \lambda^2 + p_2 \lambda - p_3 \quad (107)$$

Comparing 106 to 107, we obtain :

$$\begin{cases} \theta(a + \alpha + \gamma) = -p_1 \\ \theta^2(\alpha a + \alpha \gamma + a \gamma + \beta \gamma + \gamma) = p_2 \\ \theta^3(a \alpha \gamma + \gamma \alpha \epsilon + \beta \gamma a) = -p_3 \end{cases} \quad (108)$$

Similarly, we would find in the region  $D_{\pm 1}$ :

$$\begin{cases} \theta(b + \alpha + \gamma) = -q_1 \\ \theta^2(\alpha b + \alpha \gamma + b \gamma + \beta \gamma + \gamma) = q_2 \\ \theta^3(b \alpha \gamma + \beta \gamma + \gamma \alpha) = -q_3 \end{cases} \quad (109)$$

The two sets of equations (109) and (110) constitute a system of six nonlinear equations; one can verify that in general it is impossible to find a solution with  $\theta = \pm 1$ .

Therefore, in the first step, we replace  $\theta$  by  $\delta$  on which we do not impose any condition. This leads us to a system  $\xi$  which has the eigenvalue pattern required.

In the second step, we divide  $\xi$  by  $|\delta| \neq 0$  and obtain a system  $\xi$  of the form (6) which is linearly conjugate to  $\xi$  and therefore has the same behavior. Physically, the coefficient  $\delta$  represents a time rescaling. The dimensionless forms are governed by five parameters; therefore, there cannot exist any bijection between this five parameter space and the 6 dimensional eigenvalue space. However, by allowing a time rescaling, it is possible to reduce this six-dimensional space, except for a zero measure family, to a five dimensional space. The zero measure set depends on the method we apply to do this "reduction". In any case, we have to normalize the system by a coefficient which may be equal to zero or infinite. In our example this normalization coefficient will be  $\delta$ .

Let us first solve, when possible, the following system of 6 nonlinear equations obtained by subtracting (110) from (109) where the six unknowns are:  $\alpha, \beta, \gamma, \delta, a$  and  $b$  :

$$\begin{cases} \delta(a - b) = q_1 - p_1 \\ \delta(a + \alpha + \gamma) = -p_1 \\ \delta^2(a - b)(\alpha + \gamma) = p_2 - q_2 \\ \delta^2(a(\alpha + \gamma) + \gamma(\alpha + \beta) + \gamma) = p_2 \\ \delta^3(a - b)\gamma(\alpha + \beta) = q_3 - p_3 \\ \delta^3(a\gamma(\alpha + \beta) + \gamma\alpha\delta) = -p_3 \end{cases} \quad (110)$$

If  $p_1 = q_1$ , from the first equation of (110), we have  $a = b$  and from the third and the fifth equations of (110), we have  $p_2 = q_2$  and  $p_3 = q_3$ , respectively. This means that if  $p_1 = q_1$ , the vector field is in fact linear, which cannot lead to any complex dynamics. From now on, let us suppose that  $p_1 \neq q_1$ . The system (110) is equivalent to :

$$\begin{cases} -p_1 - \frac{p_2 - q_2}{q_1 - p_1} = \delta a & (111) \\ -q_1 - \frac{p_2 - q_2}{p_1 - q_1} = \delta b & (112) \\ \delta(q_1 - p_1)(\alpha + \gamma) = p_2 - q_2 & (113) \\ \delta^2(a(\alpha + \gamma) + \gamma(\alpha + \beta) + \gamma) = p_2 & (114) \\ (q_1 - p_1)\delta\gamma(\alpha + \beta) = q_3 - p_3 & (115) \\ \delta^3(a\gamma(\alpha + \beta) + \gamma\alpha) = -p_3 & (116) \end{cases}$$

Substituting (114) and (116) into (115), we obtain :

$$\delta a \frac{p_2 - q_2}{q_1 - p_1} + \frac{q_3 - p_3}{q_1 - p_1} + \gamma\delta^2 = p_2 \quad (117)$$

Substituting (116) into (117), we obtain :

$$\delta\alpha \frac{p_2 - q_2}{q_1 - p_1} + \alpha(\gamma\delta^2) = -p_3 \quad (118)$$

If  $\gamma\delta^2$  given in (118) is different from zero, we can substitute its value into (47) in order to obtain  $\delta\alpha$

$$\delta\alpha = -\frac{\left(-\delta\alpha \frac{p_3 - q_3}{q_1 - p_1} - p_3\right) \left(\delta\alpha \frac{p_2 - q_2}{q_1 - p_1} + \frac{q_3 - p_3}{q_1 - p_1}\right)}{p_2} \quad (119)$$

From (114), we obtain  $\delta\gamma$  as a function of  $\delta\alpha$  given above in (120)

$$\delta\gamma = \frac{p_2 - q_2}{q_1 - p_1} - \delta\alpha \quad (120)$$

From (116) we can determine  $\delta\beta$  as a function of  $\delta\alpha$  and  $\delta\gamma$  as follows

$$\delta\beta = \frac{q_3 - p_3}{\delta\gamma(q_1 - p_1)} - \delta\alpha \quad (121)$$

The last unknown  $\delta$  can be obtain from either (115) or (117). Having found the values of  $\alpha, \beta, \gamma, \delta, a$  and  $b$  we now have to normalize these values by  $|\delta|$  when it exists and is different from zero. To avoid any confusion, from now on in this paper, we shall denote by  $\tilde{\alpha}, \tilde{\beta}, \tilde{\gamma}, \tilde{\epsilon}, \tilde{a}$  and  $\tilde{b}$  the parameters of this new system. The parameters of Chua's canonical equations are given in (17).

## 8.2 Appendix B : Presentation of the user-friendly program

The aim of this C-program available on PC is to simulate Chua's canonical equations and to display the trajectory, the eigen spaces, the boundary planes, to rotate them, and to provide the eigenvalues. In this appendix, we give a brief description of the main menu presented at the top of the screen. To have access to any of the following features, click on the corresponding rectangle with the mouse or press the first letter of the option on the keyboard <sup>24</sup>:

### Parameters

Choose the values of  $\alpha, \beta, \gamma, m_0, m_1$  and  $k$ . To set the value of a particular parameter, choose the **parameter** option in the main menu and then select the parameter to be modified by clicking on the appropriate menu button. When the parameter is chosen, a tick mark appears in the box along side the name of the parameter. Enter the parameter value by typing the desired number in the dialog box and pressing **modify** or by incrementing/decrementing

---

<sup>24</sup>except for Plot, type O

the digits of the display by clicking on the arrow keys. Note that  $k$  can only take the value 1 and -1, by clicking on the button  $k$  one sets the opposite value.

The **calculate** button initiates the circuit equations from the chosen initial conditions from the chosen initial condition.

**continue** uses the last point of the previous integration as the new initial condition and continues to solve the equations.

### **Load**

Instead of typing in a new set of parameters each time one runs the program, one may load the values from an option file by choosing the load option from the main menu. Pressing this button brings up the search path for a file. Complete the path name to the desired subdirectory and press the **return** key. A scrolling window appears which displays the content of a subdirectory. Use the arrow keys or scroll bar to move through the list of files; select a file by highlighting it and pressing the **Okay** button. Press **Cancel** to return to the main menu without menu without saving file.

### **Initial conditions**

The window for choosing the initial conditions of the simulation is similar to that for setting the parameters. Each state variable is initialized by clicking the appropriate state button ( $x, y$  or  $z$ ), and either incrementing/decrementing the current values by mean of the up and down arrows, or typing the value in the dialog box and pressing **modify**. The default values are :  $x_0 = y_0 = z_0 = 0.1$ . Note that if one uses **continue** in the menu **Parameters** to integrate the equations, he can press **initial condition** in the main menu and henceforth obtain the coordinates of a current point on the trajectory (the initial condition of the next iteration).

### **Algorithm**

In our program, the user may choose to solve chua's canonical equations by means of the forwards Euler, fourth order Runge-Kutta, or sixth order Adams-Bashforth algorith. The user specifies the value of the integration step. He also gives an upper bound on the relative local truncation error  $|T_n|/|x(t_n)|$ . The program puts out an alert if the current step size causes the LTE estimate to exceed the bound.

### **plot**

Choose what you want to display on the screen : eigenplanes and eigenvector in the **middle** region and in the **outer** regions , **boundary** planes, equilibrium points. When the button is lighted, the corresponding element is displayed. The users can also choose the **speed** option which displays the trajectory slowly so that he can have a better understanding of the evolution of the trajectory. This is particularly interesting when the eigen elements

are displayed. When the selections are done, press **Okay** and the graphic display appears.

If you click on the button of the mouse with the cursor inside the graphic screen, a menu appears that allows one to rotate the attractor, either step by step (10 degrees) or automatically by choosing the option **auto**. To exit the menu type **cancel**. **reset** sets back the attractor in its initial position (before any rotation). For convenience, it is also possible to rotate the attractor directly from the keyboard without even selecting the rotation menu : Q and A rotate the attractor around the axis  $X$  in both directions, W and S around the axis  $Y$  and E and D around the axis  $Z$ .

### **Save**

The save option prompts the user for the names of files in which to save options and/or data from a simulation. Data files include the parameters for the simulation as a header and are written in ASCII format.

### **Quit**

The **quit** button exits the program gracefully

## **8.3 Appendix C : formulas giving directly the value of $\alpha, \beta, \gamma, m_0, m_1$ and $\theta$ as a function of the parameters of other elements of $\mathcal{C}$ .**

In this appendix we provide formulas that give directly the values of the parameters of Chua's canonical equations as a function of those of the five systems presented in section 3<sup>25</sup> :

### **8.3.1 Chua's circuit**

$$\left\{ \begin{array}{l} \alpha = 0 \\ \beta = \frac{\tilde{\beta}}{\tilde{\alpha}} \\ \gamma = \frac{1}{\tilde{\alpha}} \\ a = \tilde{m}_0 \\ b = \tilde{m}_1 \\ \theta = \text{sgn}(\tilde{\alpha}) \end{array} \right. \quad (122)$$

### **8.3.2 Chua's Torus circuit**

The parameters of Chua's canonical circuit, after adding 0.01 to  $p_2$  and subtracting 0.01 to  $q_2$  are obtained by replacing  $p_1, p_2, p_3, q_1, q_2$  and  $q_3$  by :

---

<sup>25</sup>let us recall that the parameters of the original systems have a tilde

$$\begin{cases} p_1 = \tilde{m}_0(\tilde{\alpha} - 1) \\ p_2 = \tilde{\beta} + 0.01 \\ p_3 = \tilde{\beta}\tilde{\alpha}\tilde{m}_0 \\ q_1 = \tilde{m}_1(\tilde{\alpha} - 1) \\ q_2 = \tilde{\beta} - 0.01 \\ q_3 = \tilde{\beta}\tilde{\alpha}\tilde{m}_1 \end{cases} \quad (123)$$

### 8.3.3 Ogorzalek's ladder circuit

The parameters of Chua's canonical circuit, after adding 0.1 to  $p_2$  and subtracting 0.1 to  $q_2$  are :

$$\begin{cases} \alpha = -\frac{(-\tilde{m}_0 + 24.5(\tilde{m}_1 - \tilde{m}_0))^2}{(6 + 5(\tilde{m}_1 - \tilde{m}_0))^3} \\ \beta = \frac{-5(\tilde{m}_1 - \tilde{m}_0)}{(6 + 5(\tilde{m}_1 - \tilde{m}_0))} - \frac{(-\tilde{m}_0 + 24.5(\tilde{m}_1 - \tilde{m}_0))^2}{(6 + 5(\tilde{m}_1 - \tilde{m}_0))^3} \\ \gamma = \frac{(-\tilde{m}_0 + 24.5(\tilde{m}_1 - \tilde{m}_0))^2}{(6 + 5(\tilde{m}_1 - \tilde{m}_0))^3} \\ a = -4.9 \frac{(-\tilde{m}_0 + 24.5(\tilde{m}_1 - \tilde{m}_0))^2}{(6 + 5(\tilde{m}_1 - \tilde{m}_0))^2} \\ b = -5.1 \frac{(-\tilde{m}_0 + 24.5(\tilde{m}_1 - \tilde{m}_0))^2}{(6 + 5(\tilde{m}_1 - \tilde{m}_0))^2} \\ \theta = -\text{sgn}(-\tilde{m}_0 + 24.5(\tilde{m}_1 - \tilde{m}_0)) \end{cases} \quad (124)$$

### 8.3.4 Brockett's system

The parameters of Chua's canonical circuit, after adding 0.1 to  $p_2$  and subtracting 0.1 to  $q_2$  are :

$$\begin{cases} \alpha = -\frac{(29.5\tilde{k})^2}{(30\tilde{k} - 1.25)^3} \\ \beta = \frac{30\tilde{k}}{30\tilde{k} - 1.25} + \frac{(29.5\tilde{k})^2}{(30\tilde{k} - 1.25)^3} \\ \gamma = \frac{(29.5\tilde{k})^2}{(30\tilde{k} - 1.25)^3} \\ a = \frac{27.075\tilde{k}}{(30\tilde{k} - 1.25)^2} \\ b = \frac{30.975\tilde{k}}{(30\tilde{k} - 1.25)^2} \\ \theta = \text{sgn}(30\tilde{k} - 1.25) \end{cases} \quad (125)$$

### 8.3.5 Sparrow's system

After adding 0.1 to  $p_2$  and subtracting 0.1 from  $q_2$  we obtain :



$$\left\{ \begin{array}{l} \alpha = \frac{(9.4+121.8(\tilde{r}+1))^2}{(45+42\tilde{r})^3} \\ \beta = \frac{42(\tilde{r}+1)}{45+42\tilde{r}} - \frac{(9.4+121.8(\tilde{r}+1))^2}{(45+42\tilde{r})^3} \\ \gamma = \frac{(9.4+121.8(\tilde{r}+1))^2}{(45+42\tilde{r})^3} \\ a = -2.9 \frac{9.4+121.8(\tilde{r}+1)}{(45+42\tilde{r})^2} \\ b = -3.1 - \frac{9.4+121.8(\tilde{r}+1)}{(45+42\tilde{r})^2} \\ \theta = \text{sgn}(45 + 42\tilde{r}) \end{array} \right. \quad (126)$$

#### 8.4 Appendix D : eigenvalues, canonical parameters, circuit parameters and Lyapunov dimension for the gallery of attractors

In this last appendix we have gathered all the data relative to the gallery of attractors. For each of them, in a first table we give the number of the figure where it is displayed, its lyapunov dimension, the eigenvalue pattern and the parameters of Chua's canonical equations, and in a second table the value of Chua's canonical circuit.

A gallery of attractors

Fig	dim	Eigenvalues					Canonical parameters						
		$\mu_1$	$\mu_2$	$\mu_3$	$\gamma_1$	$\sigma_2$	$\alpha$	$\beta$	$\gamma$	$a$	$b$	$\theta$	
6	2.14	0.667	-0.304	$\pm j$ 0.901	-1.22	-0.304	0	1.641	.1149	-1.429	.2857	-1	
7	2.11	0.728	-0.317	$\pm j$ 0.889	-1.29	0.061	0	1.58	0.111	-0.143	0.286	-1	
11	2.09	1.15	-2.98	-5.70	-0.892	0.150	0	-0.741	0.2029	1.492	4.928	1	
19a	2	0.634	-0.0479	$\pm j$ 1.013	-.419	0.0275	0	-5.555	-0.000555	0.028	-0.018	-1	
19b	2.09	0.2574	-0.7129	$\pm j$ 1.145	-0.7792	0.45159	0	-0.4893	0.244689	0.1428	-0.2858	1	
19c	2.185	0.1144	.5657	$\pm j$ 1.211	-0.3496	0.4119	0	-0.2272	0.1494	0.1428	-0.28572	1	
19d	e13	-1.615	0.08336	$\pm j$ 1.149	0.9212	-0.4122	0	-1.429	-0.1198	-0.2951	0.1479	-1	
19e	2.03	0.7545	-0.2430	$\pm j$ 0.9059	-1.322	.0651	0	-1.832	-0.0641	0.1429	-.2857	-1	
19f	2.007	0.7545	-0.2430	$\pm j$ 0.9059	-1.322	.0651	0	-1.832	-0.0641	0.1429	-.2857	-1	
12	2.0	0.2055	-0.04794	$\pm j$ 1.004	-0.1381	-0.03419	0.0211	-2.036	-0.03169	-.0007359	0.02302	1	
15	2.07	1.418	-0.0161	$\pm j$ 1.006	-0.997	0.01695	0.07068	-15.99	-0.07512	-1.474	1.0398	1	
16	2.03	-0.799	0.009276	$\pm j$ 0.406	0.9223	-0.8673	-0.01106	-0.9861	0.01106	-0.01106	-0.011514	-1	
17	2.1	0.50	-0.5764	$\pm j$ 0.9135	-1.122	0.2005	0.01921	-1.042	-0.01921	0.01812	0.02004	1	
18	2.04	-0.6316	0.00635	$\pm j$ 0.3802	0.9395	-0.8005	0.009981	0.9864	-0.00998	0.009979	0.01066	1	
20a	2.30	0.272	-0.136	$\pm j$ 0.409	-0.409	0.0454	.2259	.02066	.7001	-.9273	-.8166	-1	
20b	2.06	0.618	-0.37	$\pm j$ 3.5	-2.30	0.195	-.1014	-.1014	-.6385	.7594	.9605	-1	
20c	2.27	0.20	0.30	$\pm j$ 10.0	-3.00	0.30	-.006712	-8.859	-.9242	.9059	1.000	-1	
20d	2.39	0.30	0.0577	$\pm j$ 2.78	-1.33	0.29	-.06978	-0.05907	-.80888	.8228	.9832	-1	
20e	2.24	0.44	0.0577	$\pm j$ 2.78	-1.33	0.29	-.1003	.009521	-.7576	.7755	.9705	-1	
20f	2.27	1.474	-0.487	$\pm j$ 1.0	-1.04	0.0343	-.2313	6.494	.2685	-1.762	1.176	-1	
20g	2.032	0.527	0.0948	$\pm j$ 2.011	-20.61	0.1384	-0.04166	.4166	0.01333	-0.02	1.4	1	
20h	2.014	-10.248	0.0688	$\pm j$ 0.4971	0.2619	0.04714	-.04166	.41666	0.01333	1.4	-.02	1	
20i	2.17	-0.07620	-0.06497	$\pm j$ 0.74	-0.0762	0.005615	0.1847	0.04378	0.6213	-.8608	-0.7825	1	
20j	2.07	0.7874	-3.8089	-0.27395	-0.3618	0.1829	-0.2283	-0.06409	0.7334	-2.292	-0.5028	-1	
20k	2.17	1.032	0.1354	-0.4425	0.020	-.20	-.02279	-.01045	.7680	-1.168	-0.5231	-1	
20l	2.19	0.919	-0.541	-3.64	-3.53	0.156	.2209	.06410	-.6849	2.217	.4865	-1	
20m	2.13	6.80	4.30	2.50	-9.0	0.01	.009113	.9886	-.009113	.00911	.009482	-1	

A gallery of attractors						
Fig	Circuit parameters					
	$C_2$	$G$	$G_a$	$G_b$	$L$	$R$
6	-0.6	0.01	-0.445	0.851	-1.10	-0.409
7	-0.632	-0.0033	-0.419	-0.839	-1.02	-.33
11	-1.35	0.0014	6.63	-0.310	0.251	0.226
19a	-0.18	0	-0.510	0.353	-4.677	0.05097
19b	-2.043	0	0.43	-0.8617	0.4495	0.03316
19c	-4.40	0	0.497	-0.9944	0.5524	0.2873
19d	-0.70	-0.0015	1.034	-0.515	-0.685	-0.285
19ef	0.6995	0	1.0297	-0.516	-0.6856	-0.2866
12	-0.491	-0.0579	-0.0410	0.128	1.016	0.1794
15	-0.0652	-0.004112	-1.372	0.9675	-15.38	1.074
16	-1.014	-0.79	0.7804	0.8123	0.01815	-0.01417
17	-0.958	-0.6631	0.6527	0.7214	-0.04015	0.02775
18	-1.0137	-0.6275	0.6189	0.6615	0.02604	-0.01612
20a	48.4	31.6	-2.68	-2.36	0.171	0.346
20b	99.6	-89.4	6.72	8.50	0.020	-0.113
20c	11183	-2565	30.73	33.93	0.00094	-0.02947
20d	170.0	-86.0	5.98	7.146	0.0234	-0.1376
20e	105.0	-70.3	5.17	6.47	0.0297	-0.15
20f	-0.154	0.0285	-1.41	0.941	-5.82	-1.25
20g	2.4	-1.482	-0.2965	20.76	0.3410	0.06743
20h	2.4	-0.7371	10.319	-0.1474	1.3803	0.1356
20i	22.83	11.58	-2.363	-2.148	0.2135	0.3642
20j	22.83	11.58	-2.363	-2.148	0.2135	0.3643
20k	-95.68	3.733	-2.0	-0.895	.4448	.5845
20l	41.1	-18.5	2.36	1.93	.252	-0.381
20m	12.30	-15.64	-11.1	11.47	0.0389	-0.0473

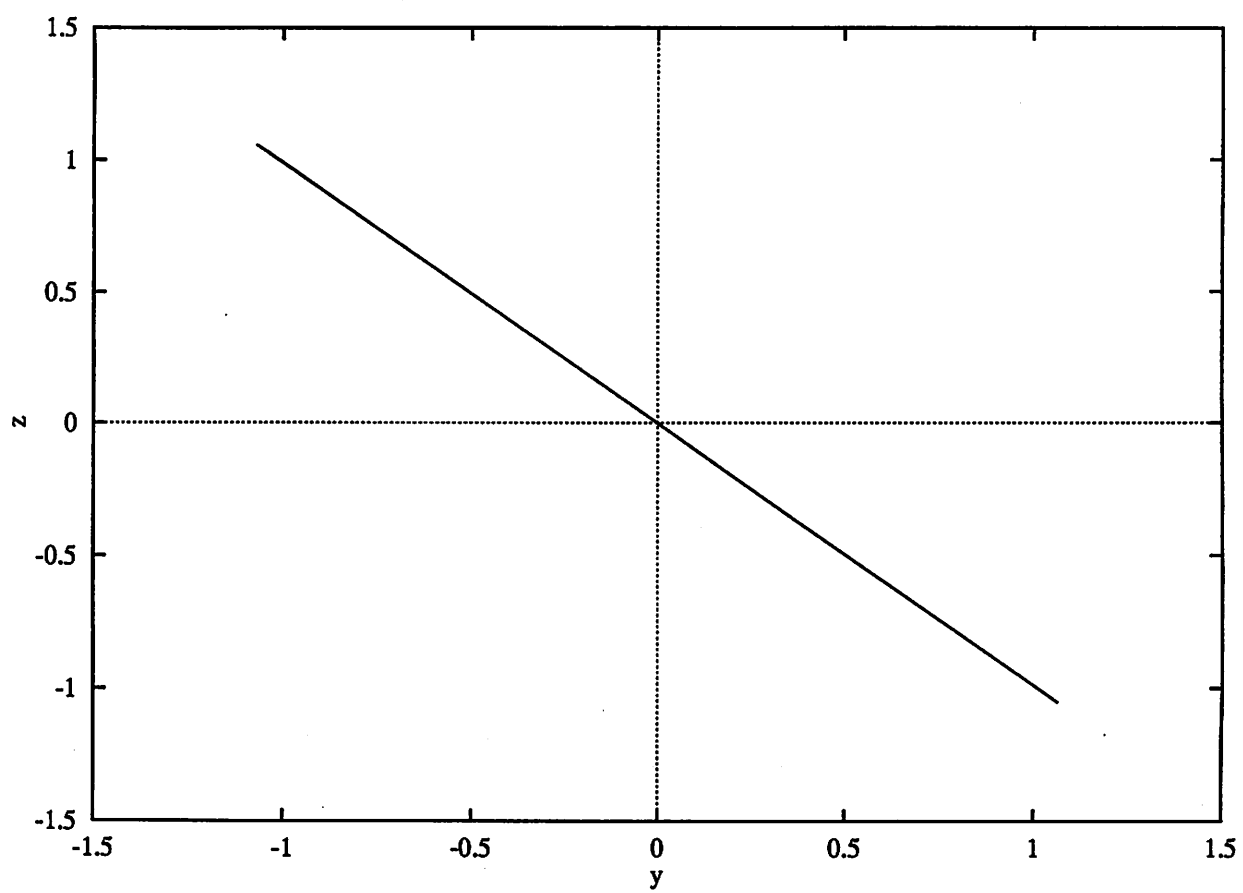


Fig. 16 c

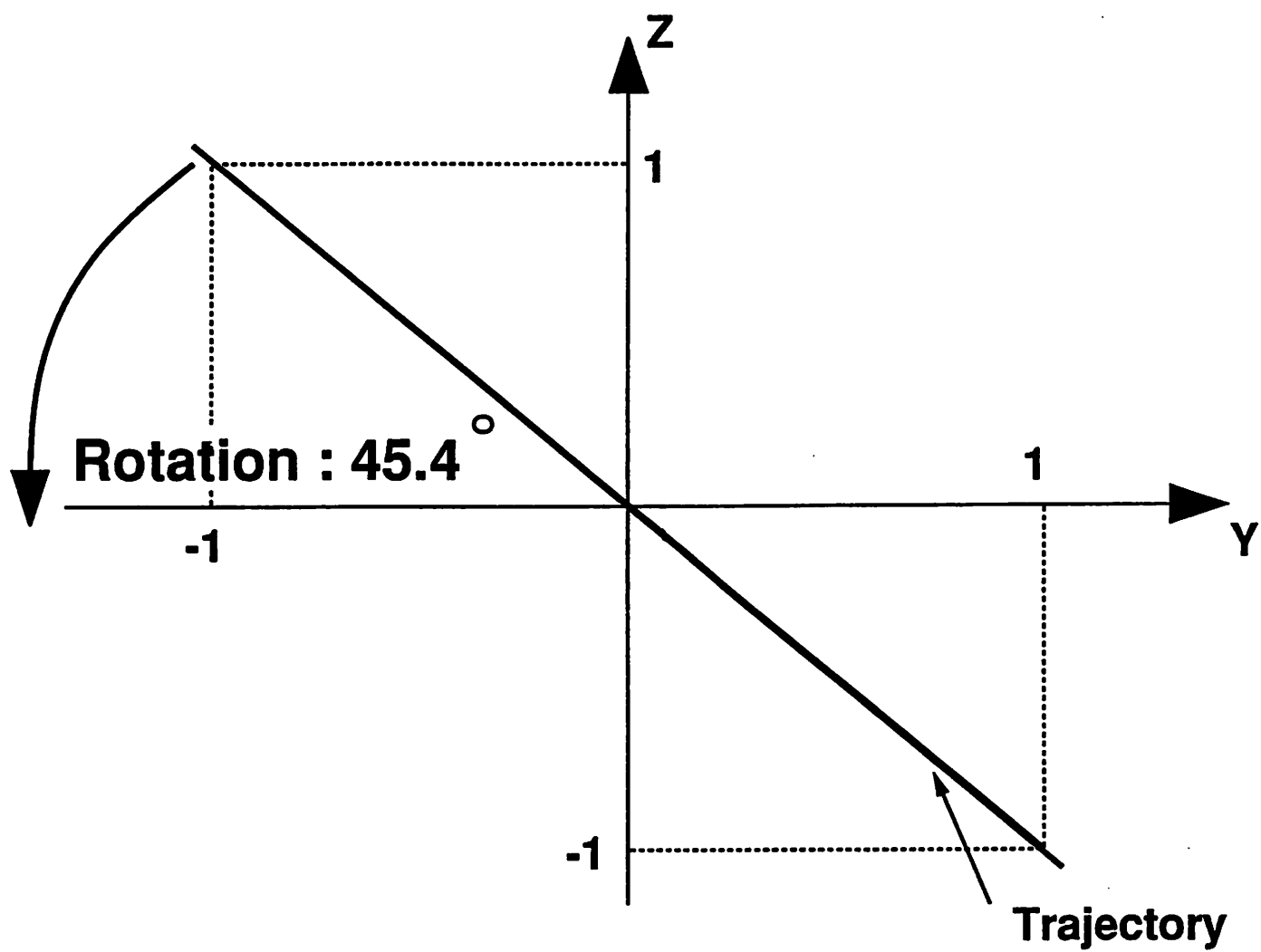


Fig. 16 d

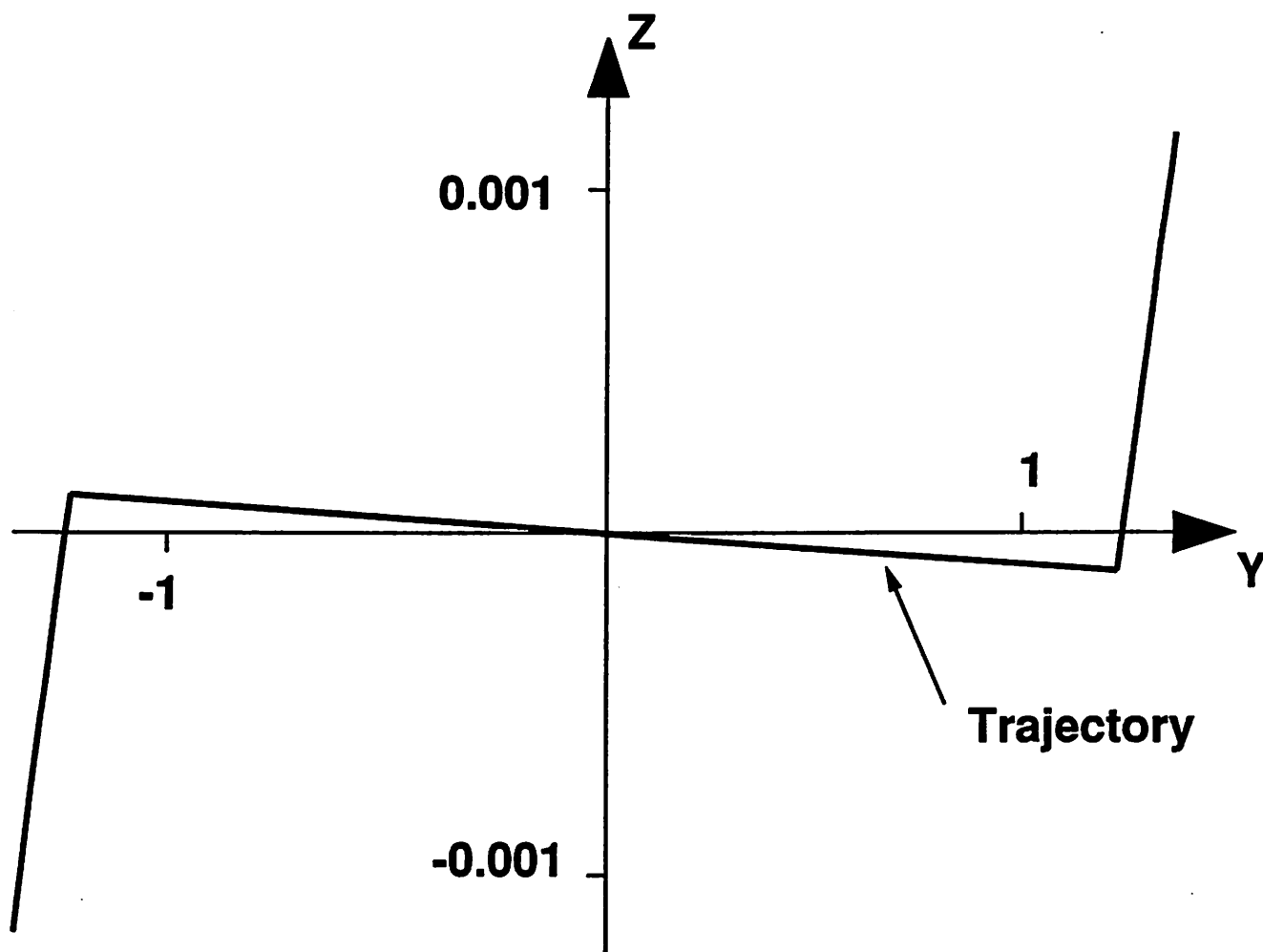


Fig. 16 e

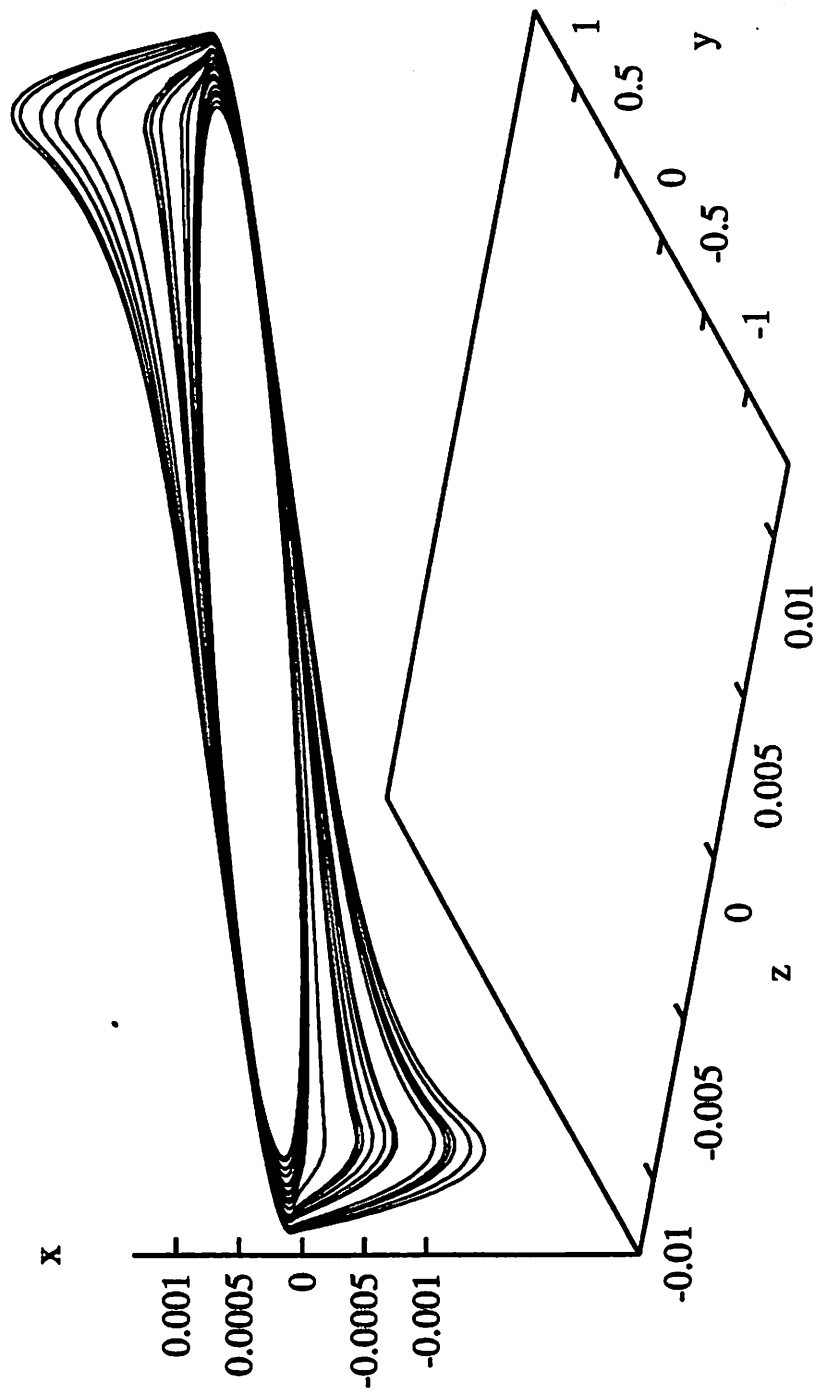
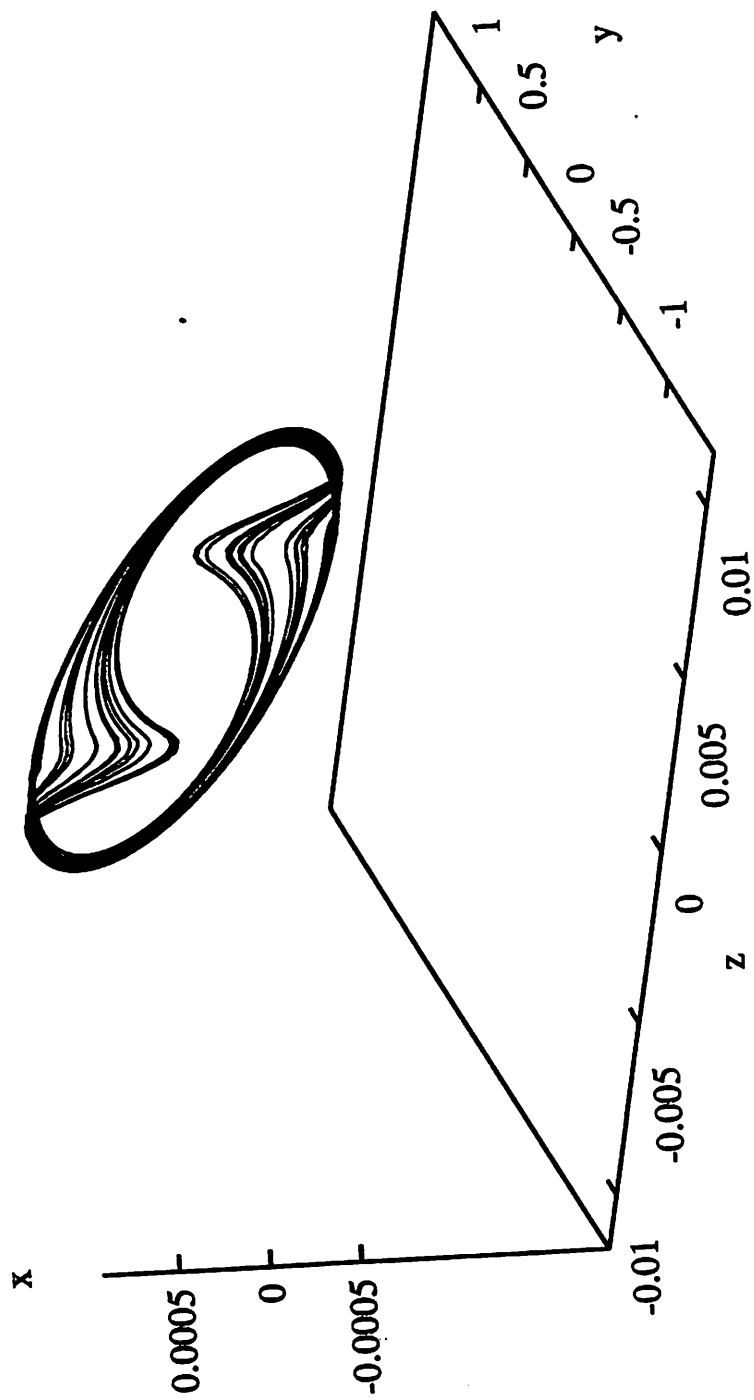


Fig. 16 f





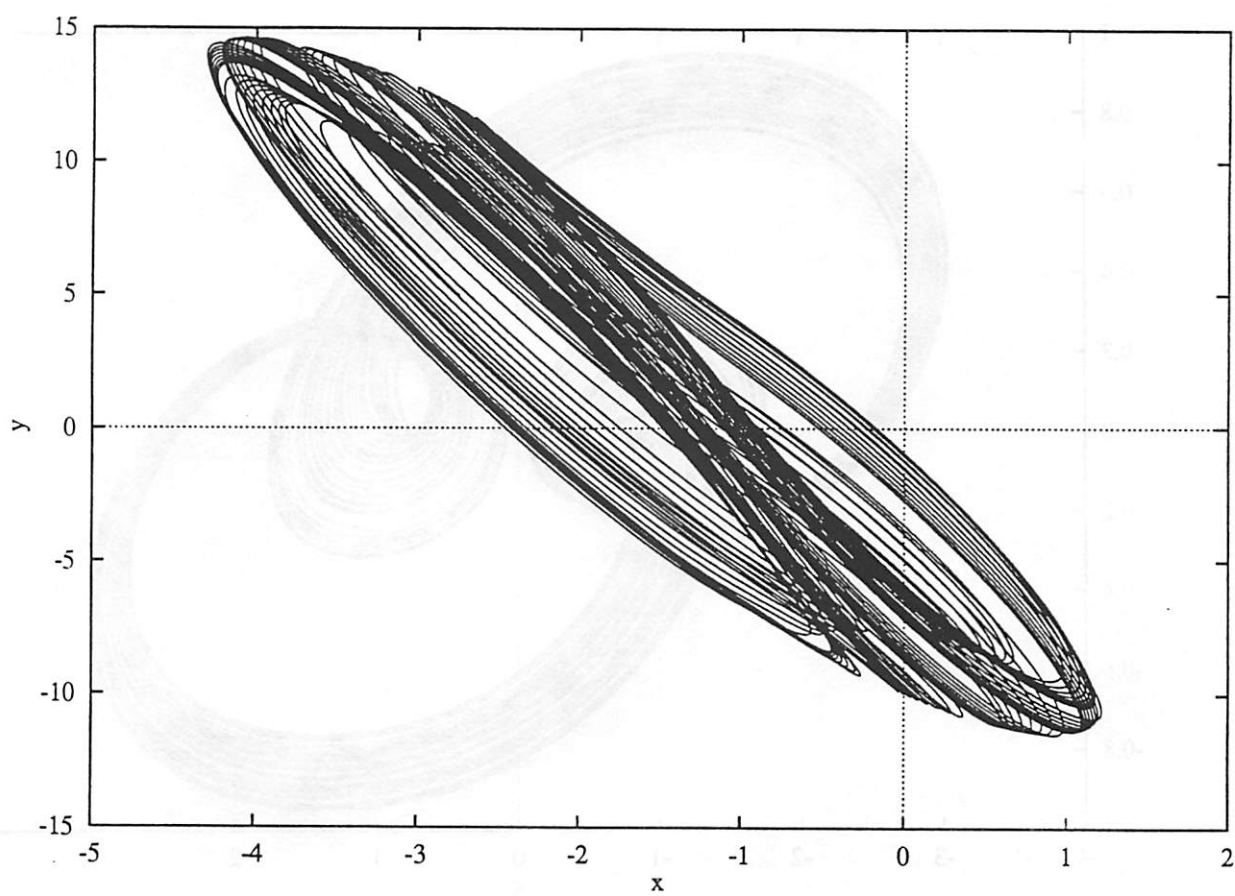


Fig. 19 a

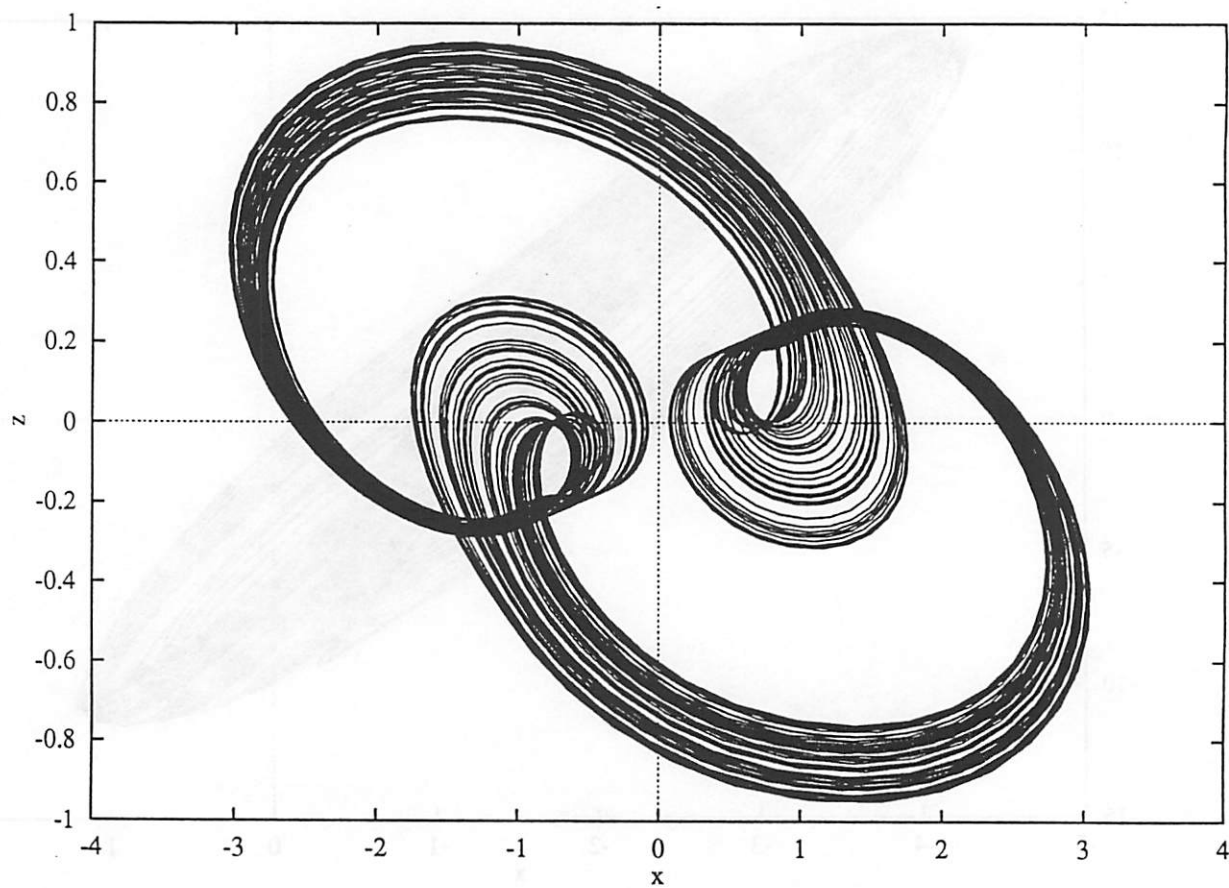


Fig. 19 b

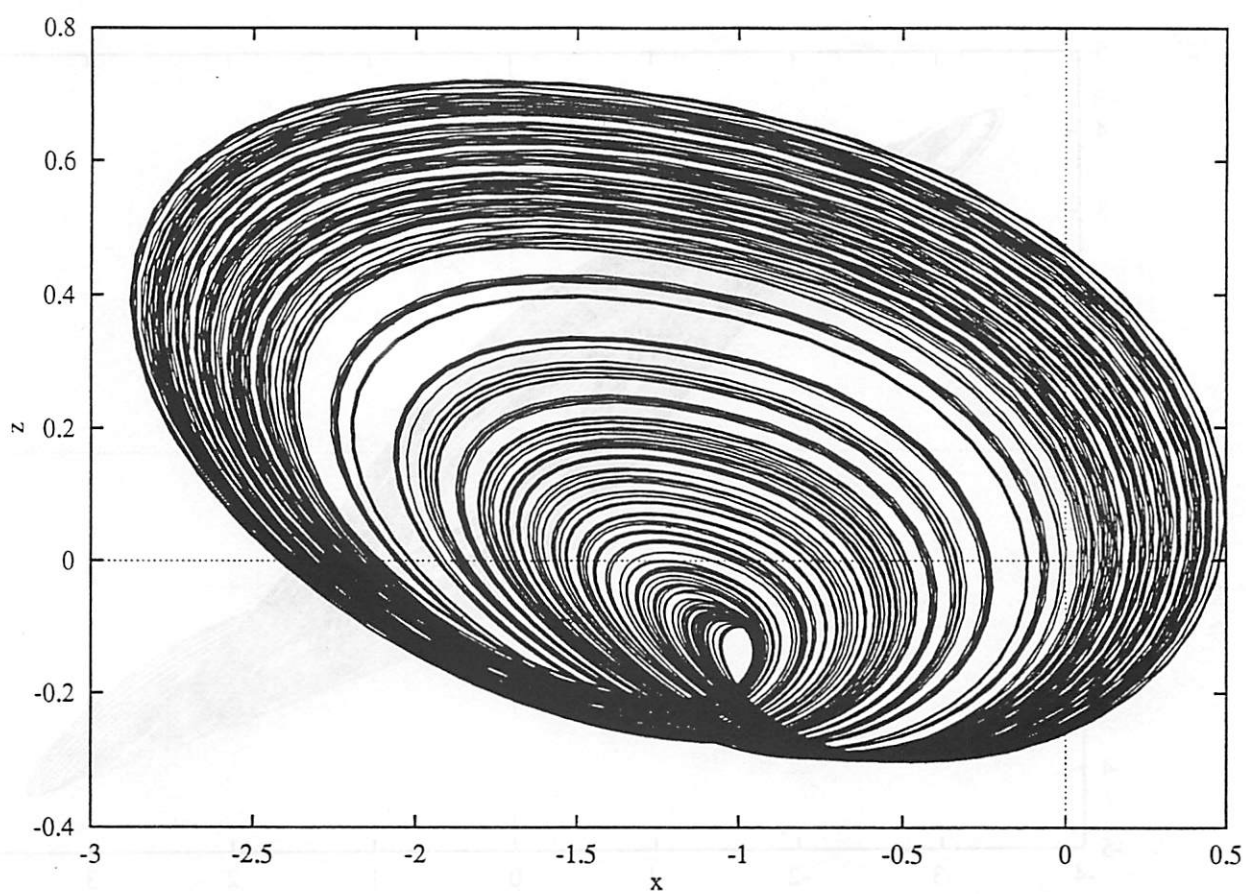


Fig. 19 c

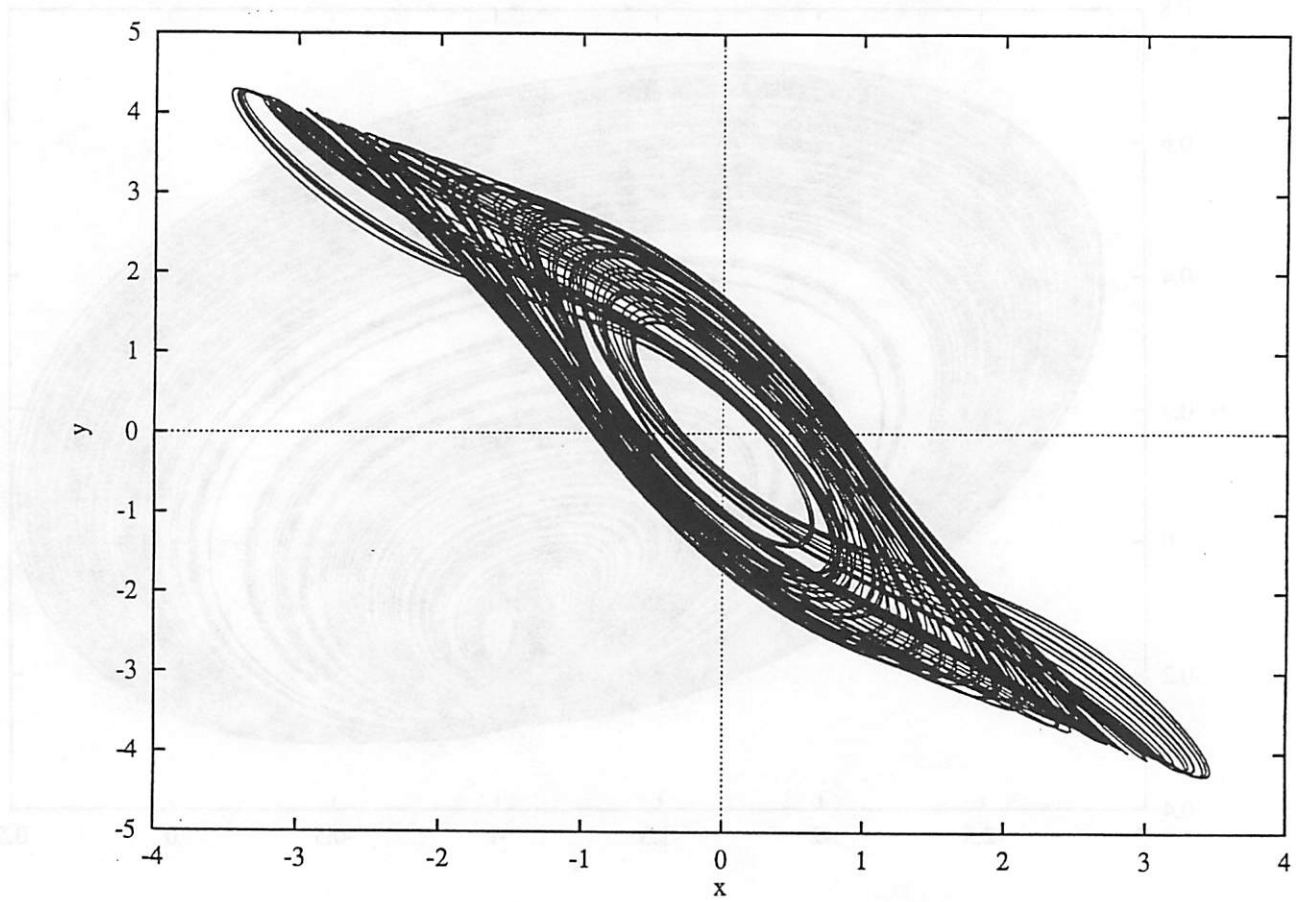


Fig. 19 d

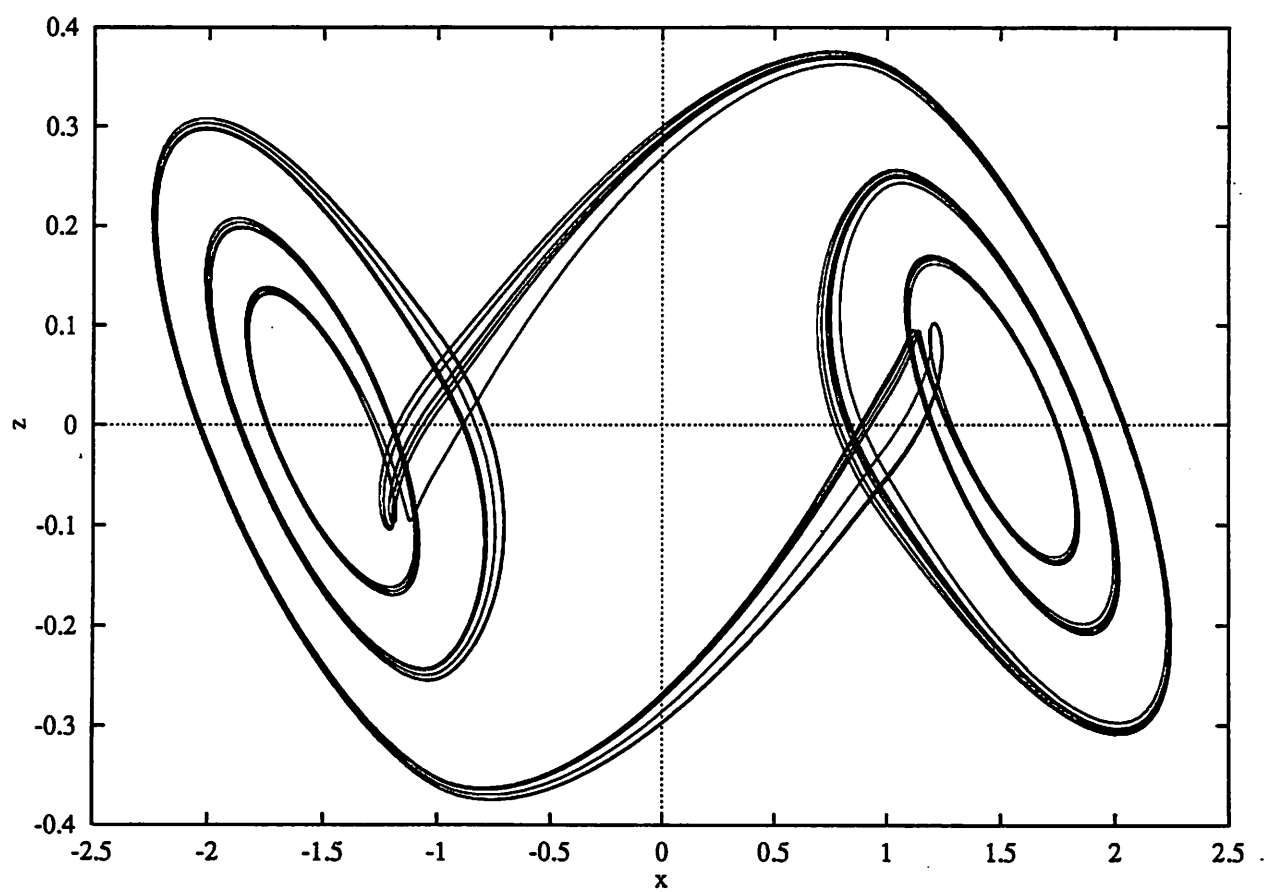


Fig. 19 e

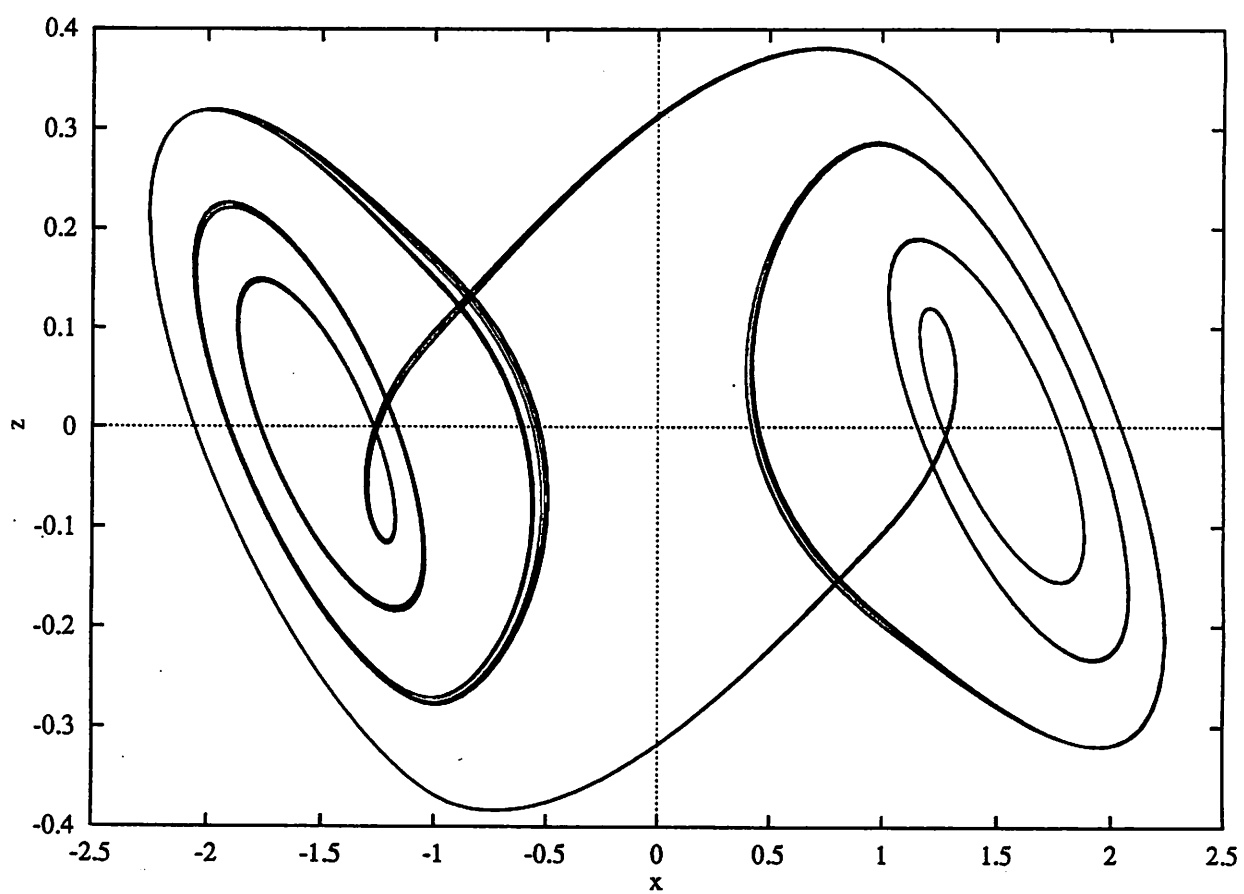


Fig. 19 f

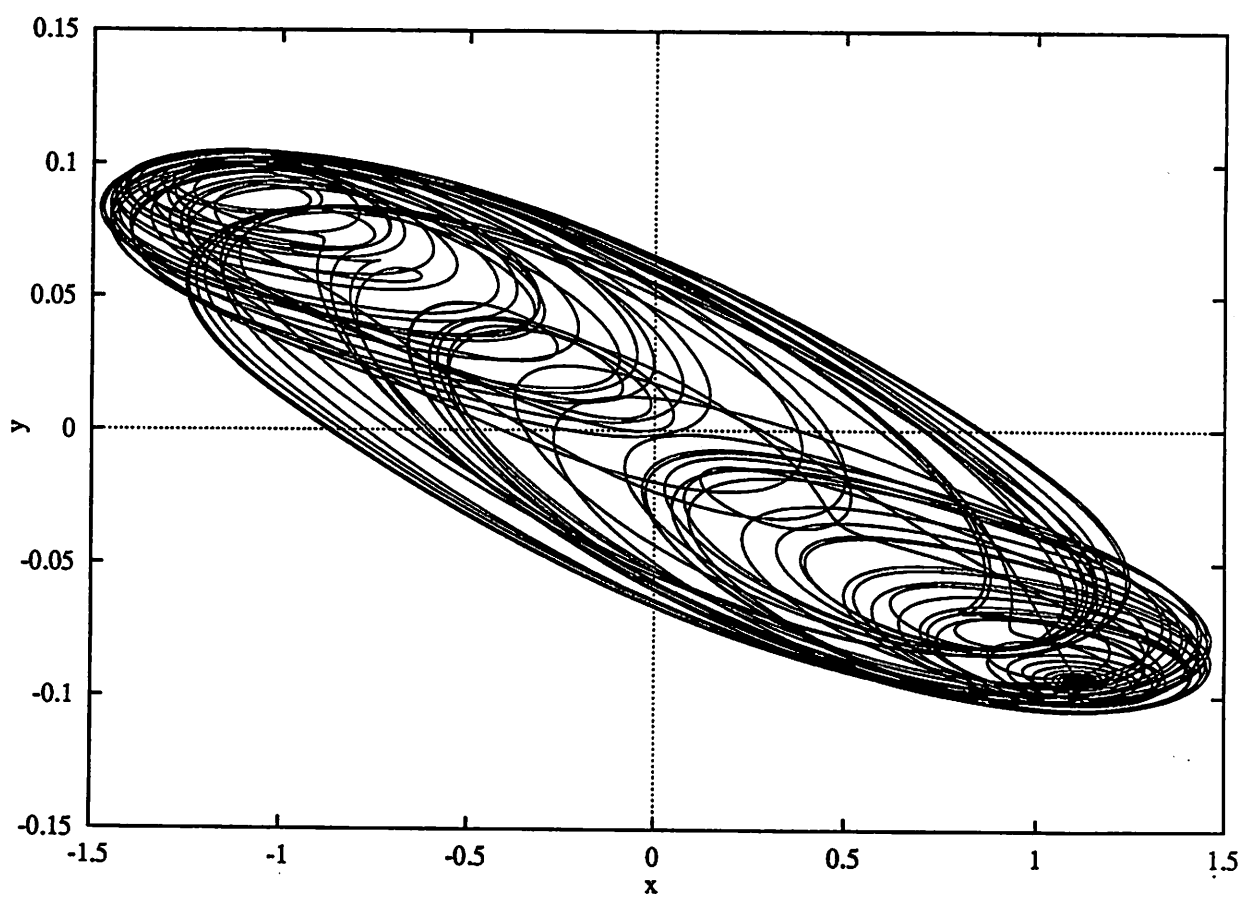


Fig. 20 a

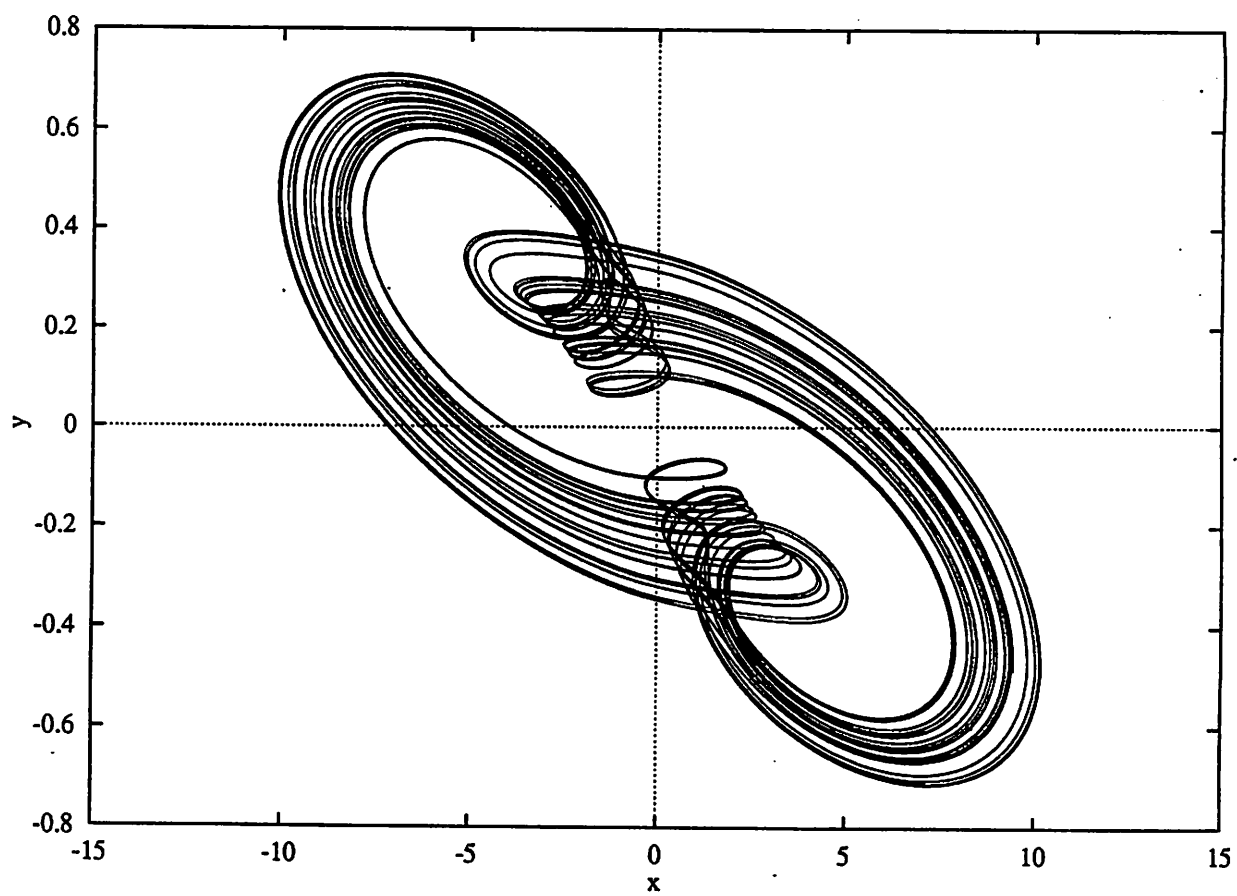


Fig. 20 b



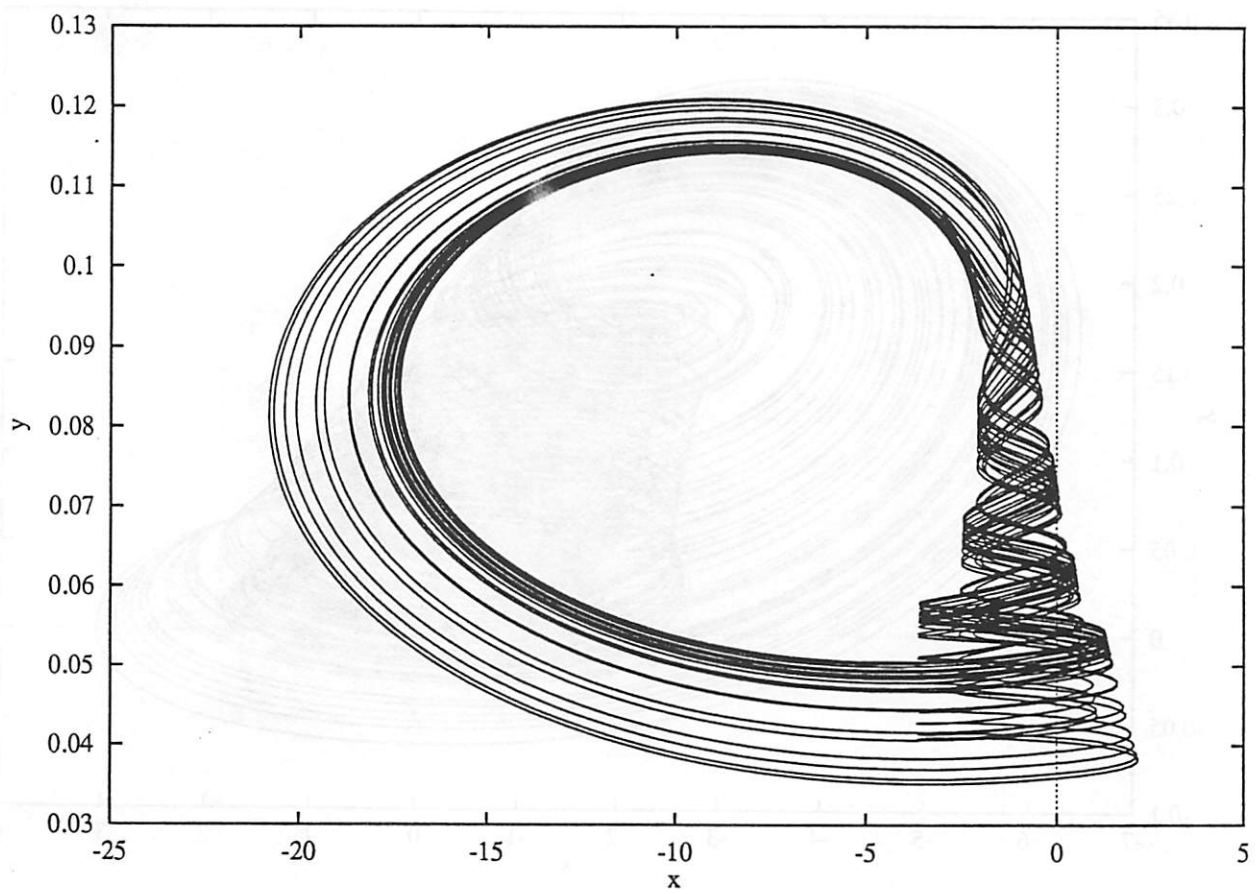


Fig. 20 c

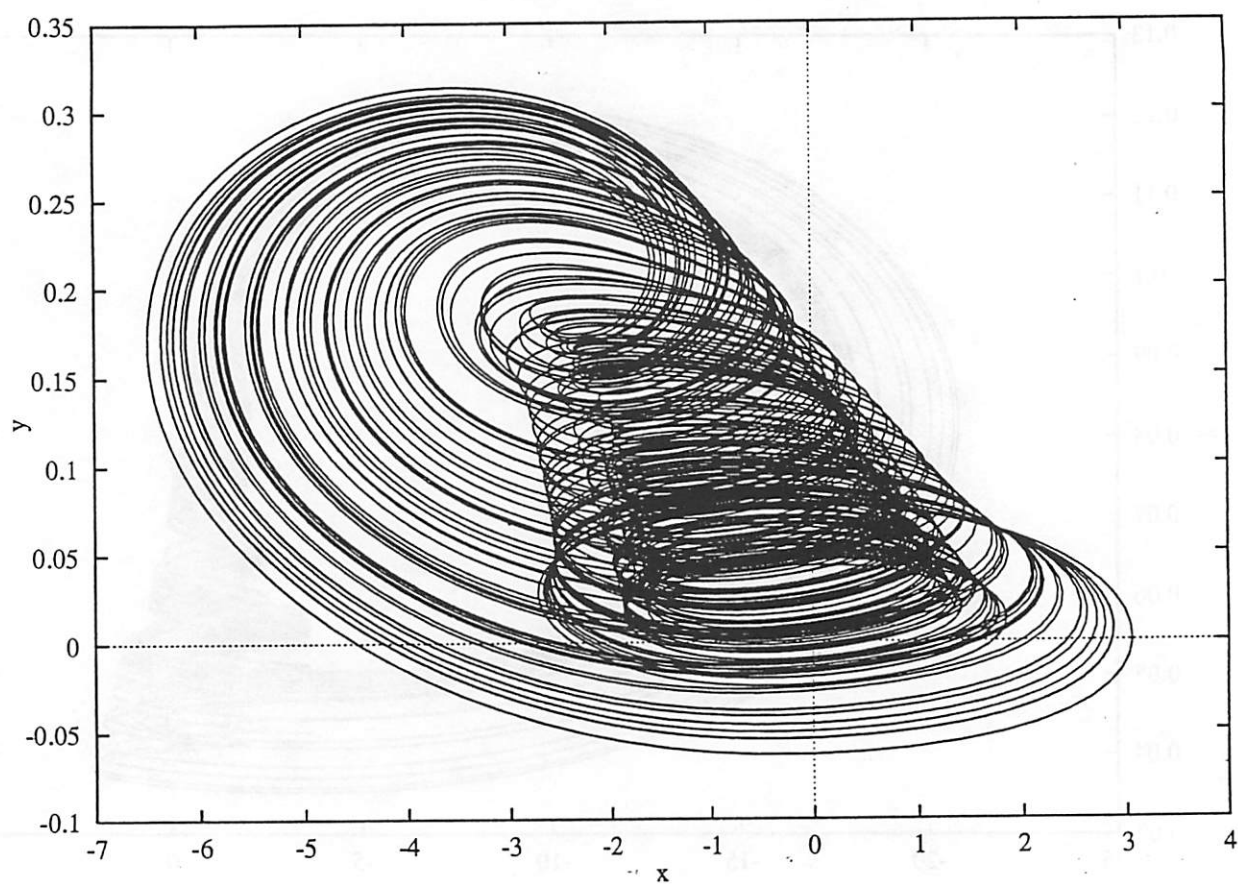


Fig. 20 d

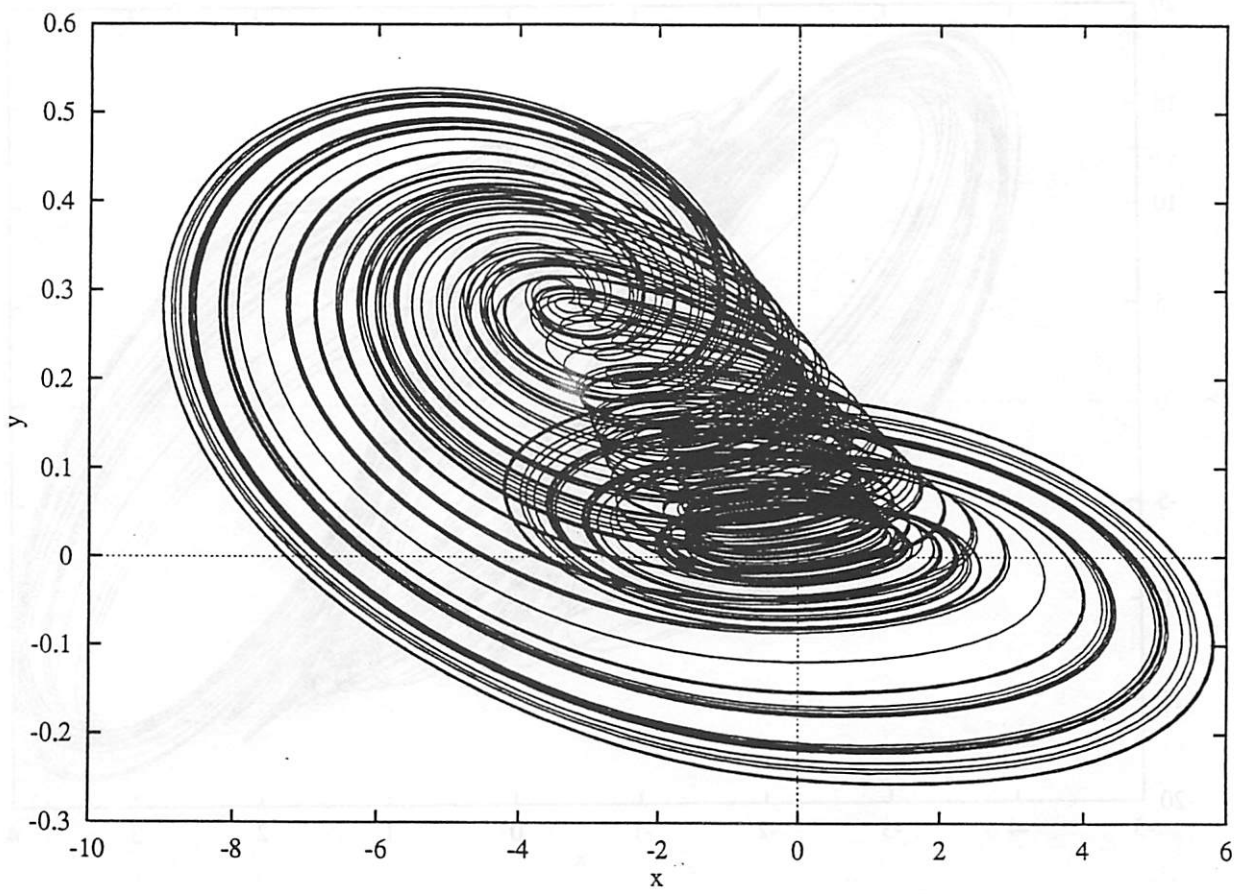


Fig. 20 e

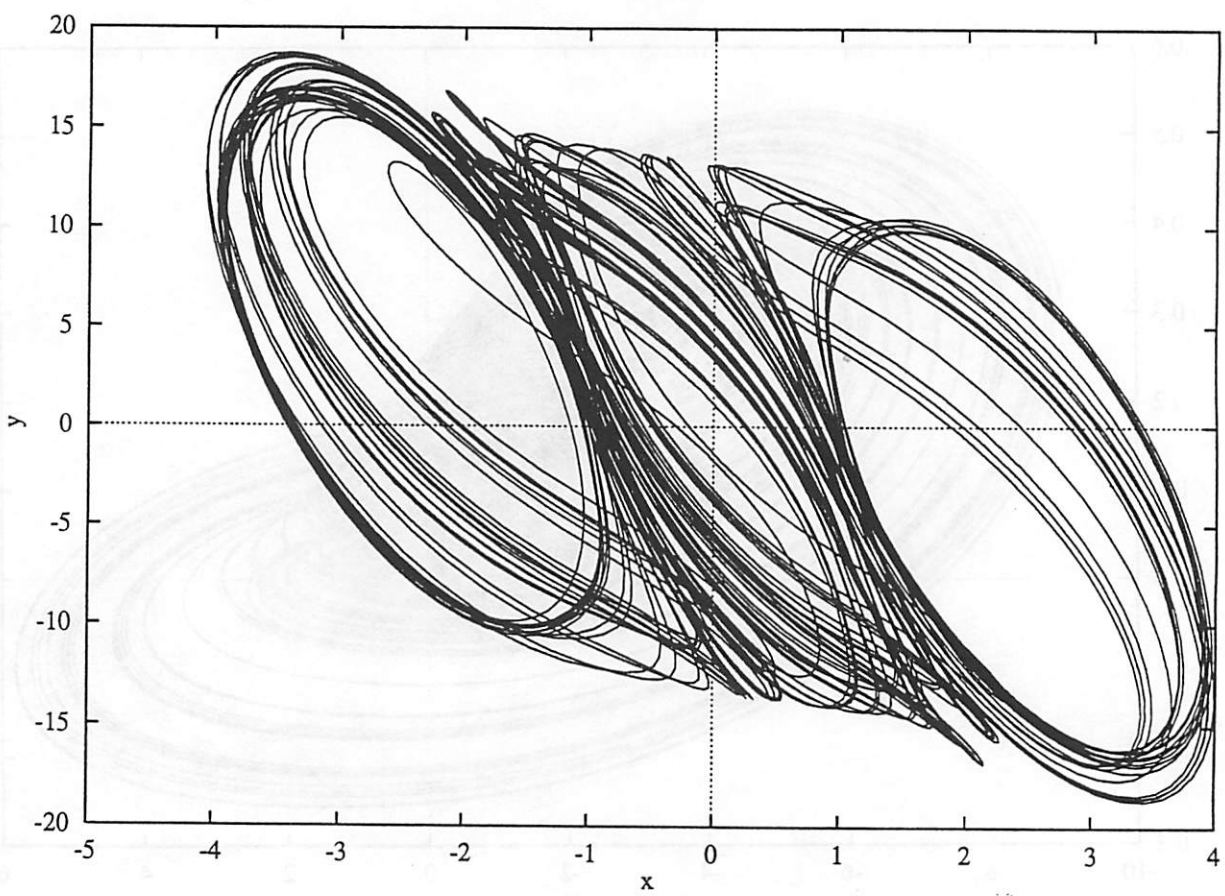


Fig. 20 f

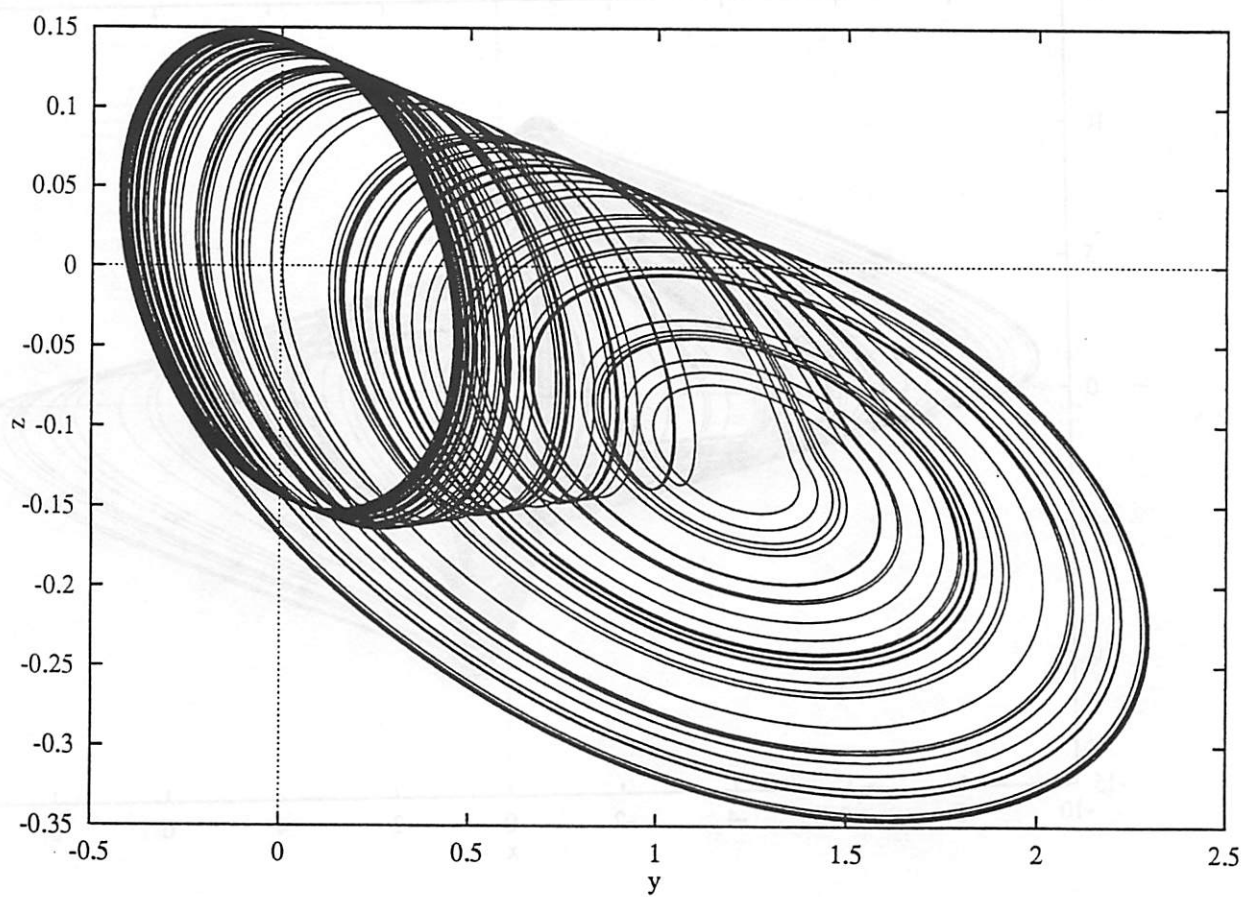


Fig. 20 g

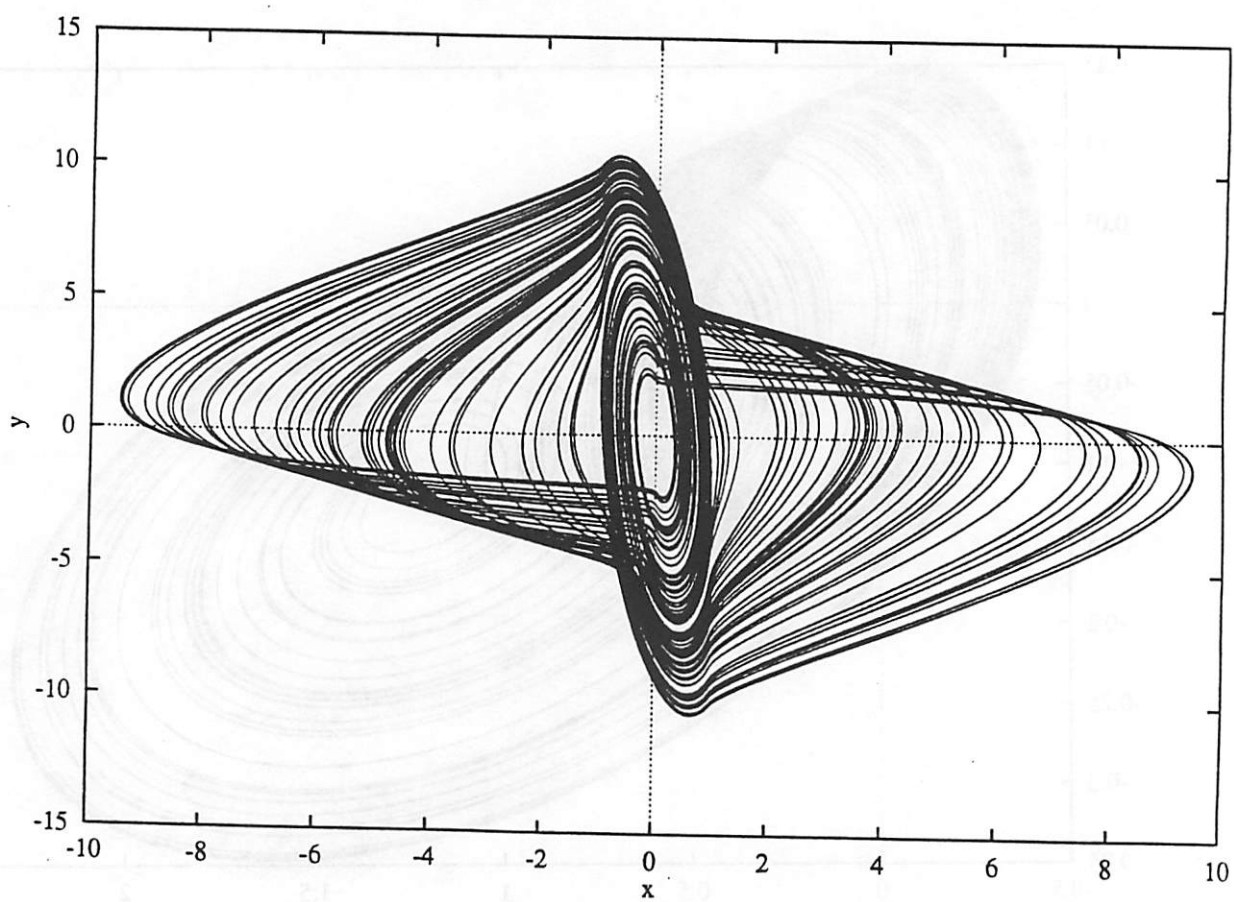


Fig. 20 h

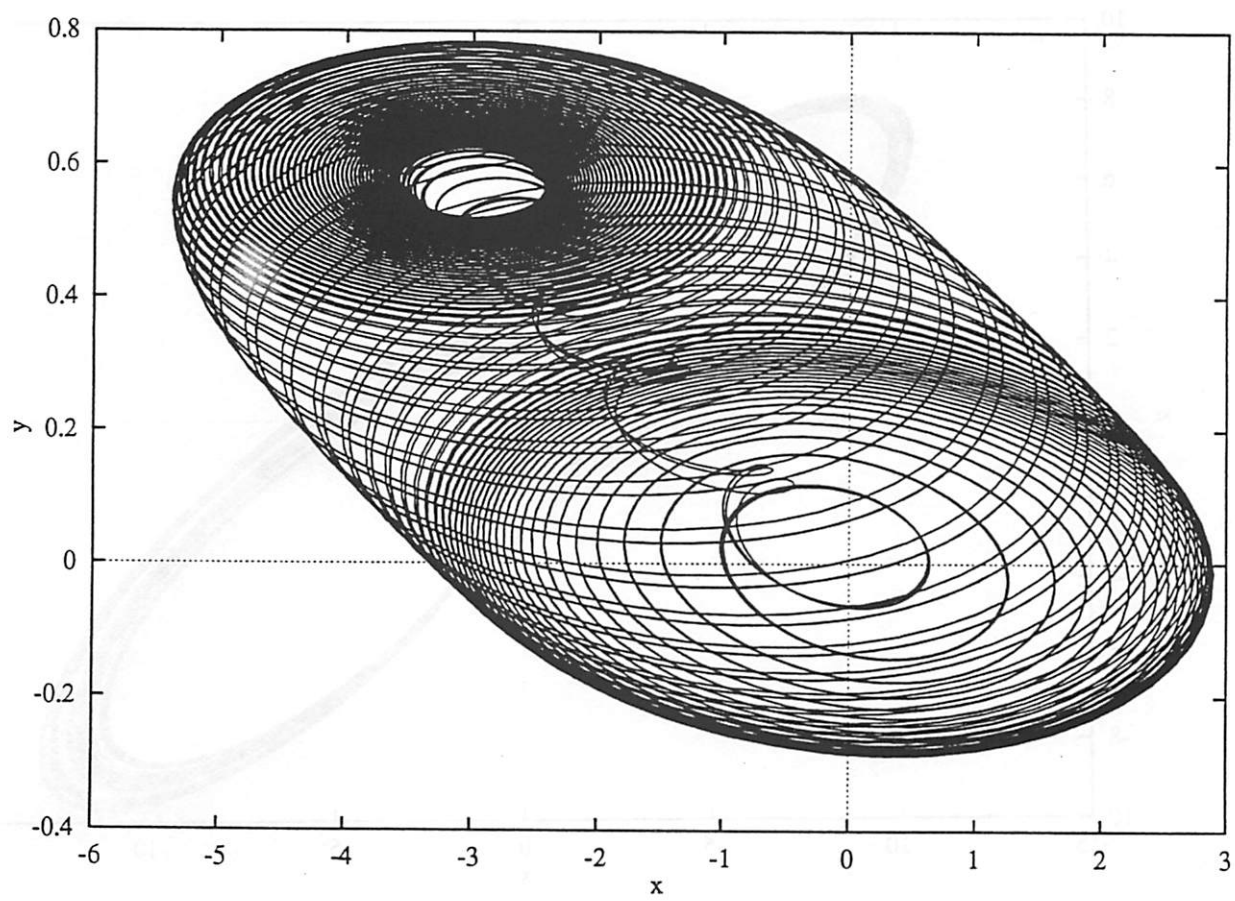


Fig. 20 i

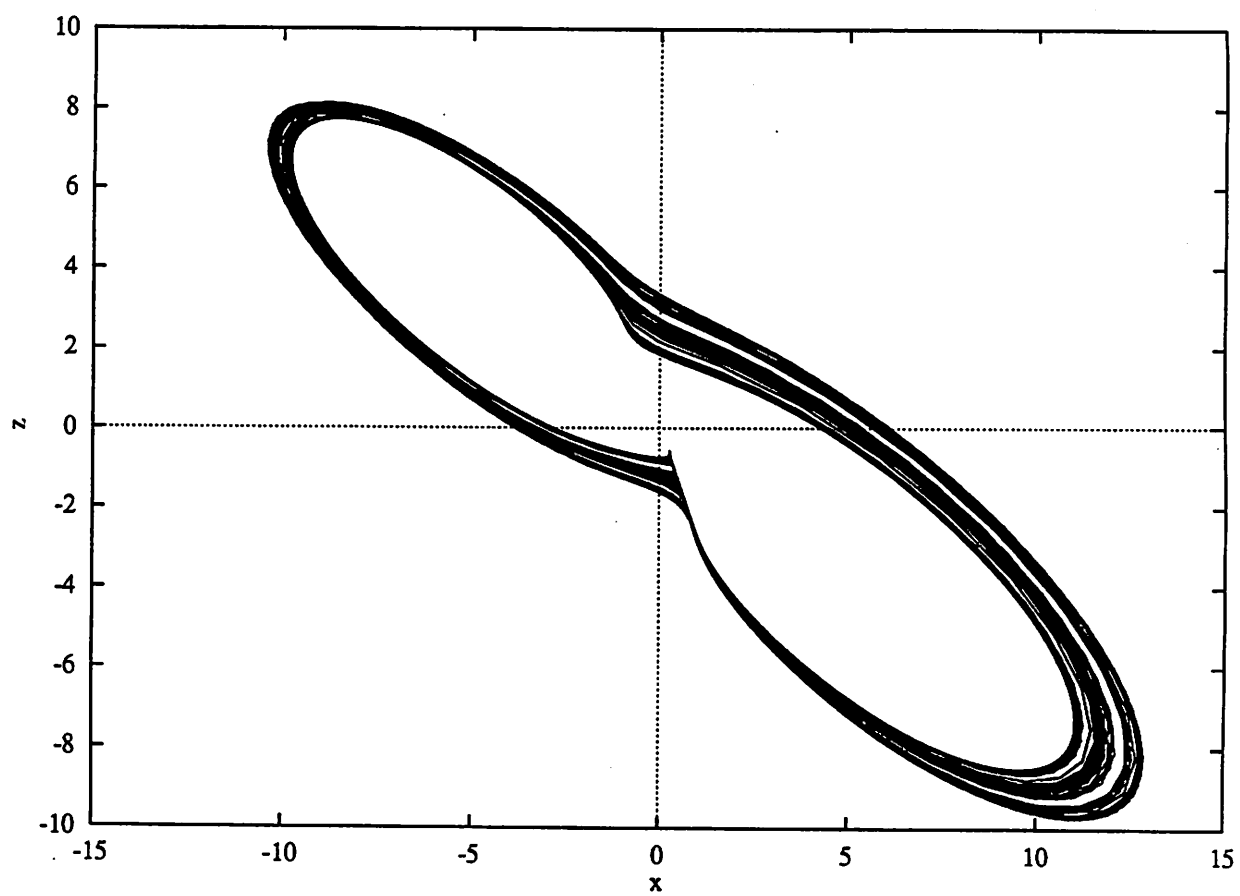


Fig. 20 j



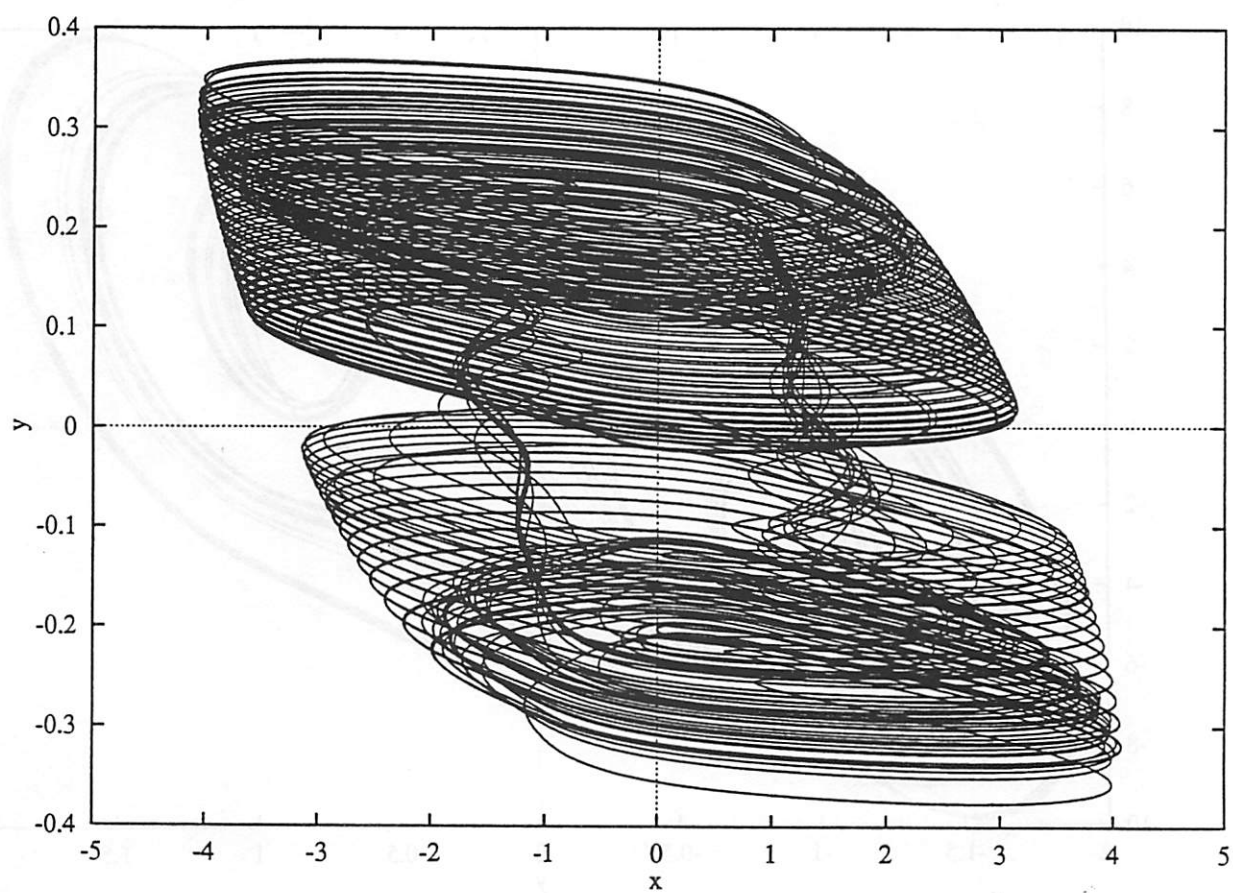


Fig. 20 k

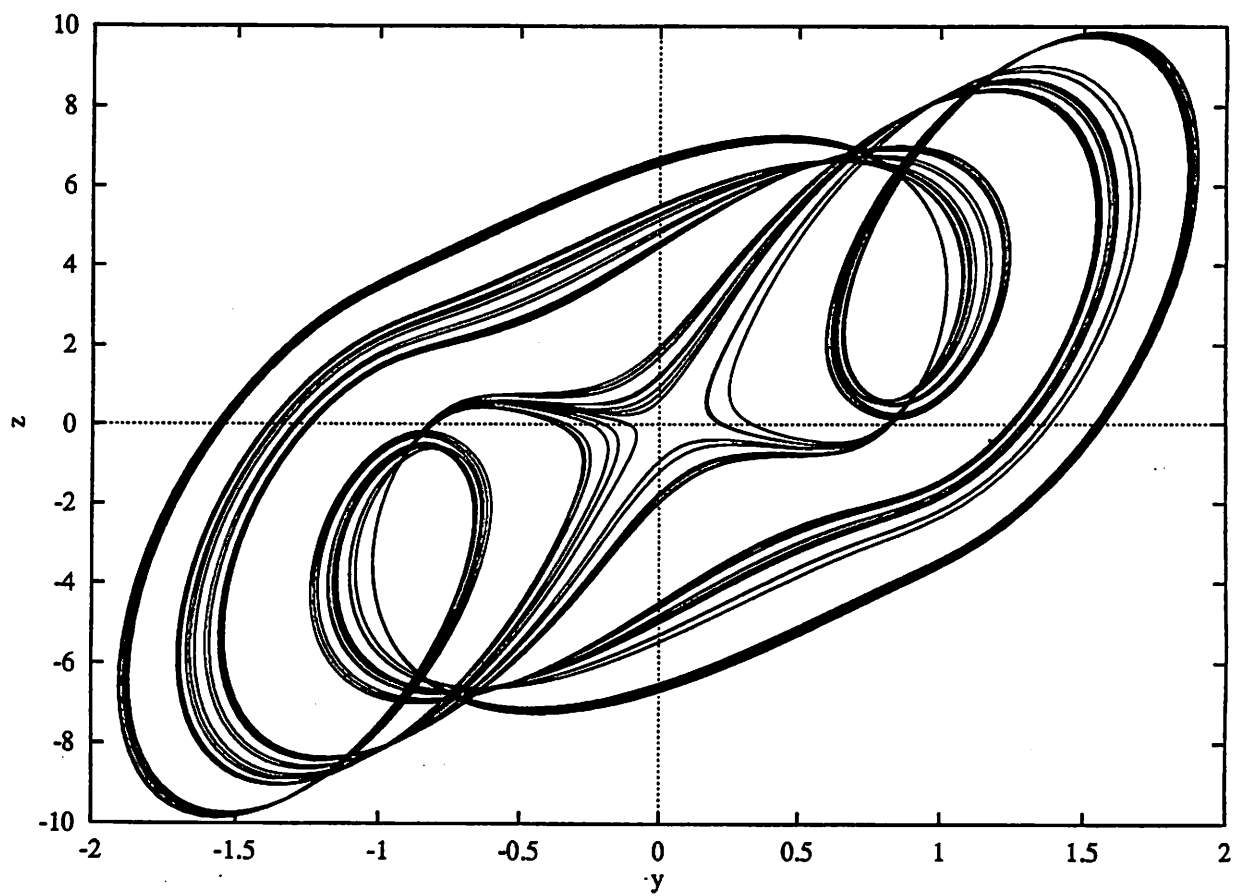


Fig. 20 1

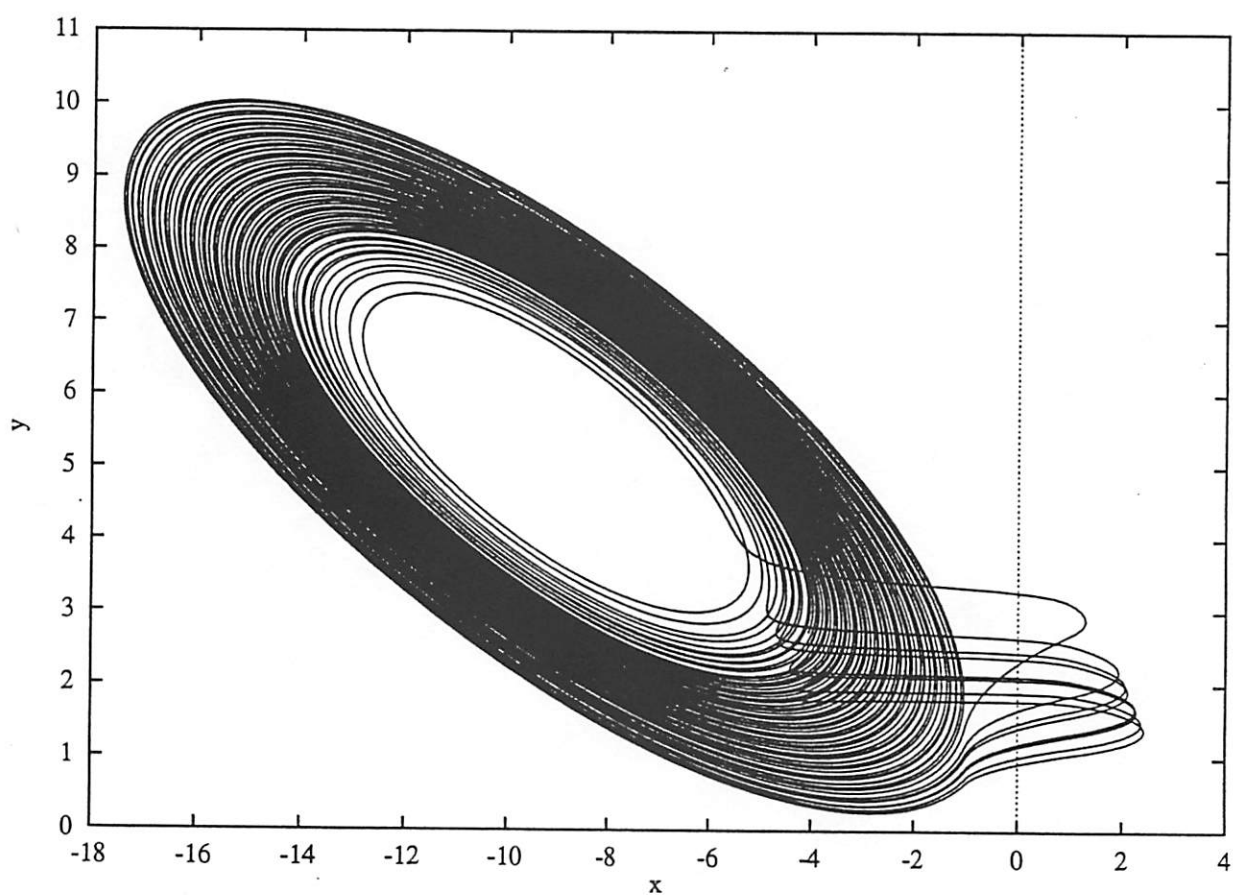


Fig. 20 m